AN ELEMENTAL AND DENDROCHRONOLOGICAL ASSESSMENT OF TREMBLING ASPEN *(POPULUS TREMULOIDES)* AND WHITE SPRUCE *(PICEA GLAUCA)* SURROUNDING THE ATHABASCA OIL SANDS REGION IN ALBERTA, CANADA

A thesis submitted to the College of Graduate Studies and Research
in Partial Fulfillment of the Requirements
for the Degree of

Master of Science

in the Department of Soil Science
University of Saskatchewan
Saskatoon, Saskatchewan, Canada

By
Nicole Rene Marleau

PERMISSION TO USE

In presenting this thesis for the partial fulfillment of the requirements for a Postgraduate degree from the University of Saskatchewan, I agree that the Libraries of this University may make it freely available for inspection. I further agree that permission for copying this thesis in any manner, in whole or in part, for scholarly purposes may be granted by the professor or professors who supervised this thesis' work or, in his/her absence, by the Head of the Department of Soil Science or the Dean of the College of Agriculture and Bioresources. It is understood that any copying or publication or use of this thesis, or parts thereof, for financial gain shall not be allowed without my written permission. It is also understood that due recognition shall be given to me and to the University of Saskatchewan in any scholarly use that may be made of any material in this thesis. Requests for permission to copy or to make other uses of materials in this thesis, in whole or part, should be addressed to:

Head of the Department of Soil Science
University of Saskatchewan
51 Campus Drive
Saskatoon, Saskatchewan, Canada
S7N 5A8

DISCLAIMER

This thesis was prepared by the author to meet thesis requirements for the degree of Master of Science at the University of Saskatchewan. Reference in this thesis to any specific commercial products, processes, or service by trade name, trademark, manufacturer, or otherwise, does not constitute or imply its endorsement, recommendation, or favoring by the University of Saskatchewan. The views and opinions of the author expressed herein do not state or reflect those of the University of Saskatchewan, and shall not be used for advertising or product endorsement purposes.

ABSTRACT

The Athabasca Oil Sands Region (AOSR) is a renowned source of air pollution in Alberta, Canada. Oil sands activities within the AOSR release a diverse set of contaminants into the atmosphere, which deposit onto surrounding boreal forest ecosystem components. Previous research has illustrated that airborne pollutant enrichment is occurring within a 50 km radius of the AOSR. Concentrations of these pollutants increase at areas in closer proximity to the AOSR. Boreal forest vegetation that lives within this 50 km zone of pollutant enrichment may be susceptible to alteration or adverse influences by these pollutants. To date, the impact of AOSR emissions on surrounding boreal forest species is largely unknown.

Therefore, the objective of this study was to assess the impact of AOSR aerial deposition on two endemic tree species: trembling aspen (*Populus tremuloides*) and white spruce (*Picea glauca*). The radial growth and elemental composition of white spruce and trembling aspen stands, and associated soils, were compared at three study sites: a Control site upwind from the AOSR, to represent baseline radial growth and tree/soil elemental composition within the region, and two downwind sites, one at the edge of the AOSR and the second approximately 50 km from the oil sand facilities. At each site plant and soil samples and tree ring cores were collected and analyzed for radial growth and elemental composition using dendrochronology, soil science, dendrochemistry, X-Ray Fluorescence (XRF), and X-ray Absorbance Near Edge Structure (XANES) spectroscopy. These methods were utilized to assess whether trembling aspen and white spruce radial growth and tree chemistry were altered at sites downwind from the AOSR, and to determine if soil characteristics were similar and comparable across sites.

White spruce stands from the two downwind sites showed a decline in radial growth compared to the Control site. A gradual and persistent decline in radial growth occurred for the last decade of growth at both downwind sites in white spruce, illustrating at threshold point in time of adverse impacts on the trees. More severe radial-growth declines occurred at the site closest to the AOSR. Radial growth did not change per site for trembling aspen, illustrating a different radial-growth response per species.

Greater Mn fluorescence, using XRF, occurred in the majority of trembling aspen and white spruce tree components (leaves, trees, roots, cores) and topsoil at the downwind sites compared to the Control site. Topsoil Mn enrichment increased at sites in closer proximity to the

AOSR, where radial-growth declines were most severe and aerial deposition from the AOSR is most concentrated. Excess Mn is known to be toxic to trees, suggesting that Mn enrichment may be causing a decline in radial growth in white spruce at the downwind sites. Manganese was elevated in the majority of trembling aspen tree media compared to white spruce potentially explaining different radial-growth responses per tree species at the downwind sites. XANES revealed the speciation of Mn to be the same in all white spruce tree materials (Mn(II)) but different in the leaf litter (Mn-oxides) at Site 0 km. Other elements observed did not show a distinct pattern, as seen with Mn.

These results suggest that Mn may be a potential contaminant of concern to white spruce downwind and at a minimum of a 50 km radius from the AOSR. Aerial deposition from the AOSR may be adversely impacting nearby white spruce trees, which could lead to losses of resources to local forestry companies. Trembling aspen appears to be more resilient to Mn deposition as it did not illustrate the same radial-growth declines as white spruce. It is recommended that the AOSR monitor boreal forest ecosystem components downwind and, especially within a 50 km zone of their facilities to better understand aerial-fallout accumulations and any further adverse impacts from ongoing emission releases.

ACKNOWLEDGEMENTS

Colin, where do I even begin? You have been my main source of encouragement throughout this whole process and words cannot express how grateful I am to have you as my supervisor. Your dedication to my thesis was invaluable. I sincerely think you're an inspirational teacher and leader and your efforts have helped me develop not only professionally but also as an individual. I've truly enjoyed my time spent with you, from field work to celebratory gatherings. Things I hold dear to me that I learned from you throughout my Master's are: a sense of light-heartedness and humor at work, ambition in the face of adversity, planning A, B, C, D, E options, always lending a helping hand to co-workers, having an abundance of snacks on field trips to avoid the h*a*ngries, how to network, and how to make more interesting presentations. Being a part of the MAD lab "family" is something I hold dear to my heart with great pride and gratitude thanks to the many incredible people who made my Master's a positive experience.

I would like to acknowledge my brilliant and friendly committee members, Ken Van Rees and Derek Peak. I appreciate the time and energy you've put into editing my thesis, asking me challenging but relevant questions, answering my questions, providing me with advice, lending me field/lab equipment, and encouraging my efforts.

Mom and dad, I would not have had the opportunity to pursue a Master's without you! No amount of words can express how grateful I am to have you as parents. I love you both very much. Your support has been detrimental to my success.

I would also like to send a HUGE thank you to my field crew! Megan and Jay, I appreciate your diligence and hard-work in the field, as well as the emotional support and friendship you have provided me throughout this whole Master's process. Preston, thanks for volunteering to help me with my field work, you saved my crew and I from doing a lot of additional work. I love you for being the remarkable guy you are!

I relied on the expertise of Chithra, David, and their associates to learn and collect my synchrotron data. Thank you all for your efforts regarding my project. It has been a learning experience I will never forget.

Finally, I would like to thank all Soil Science students and staff for their guidance, and the Natural Sciences and Engineering Research Council of Canada (NSERC), Government of Saskatchewan, and Department of Soil Science for their financial support.

TABLE OF CONTENTS

LIST OF TABLES

LIST OF FIGURES

LIST OF ABBREVIATIONS

AOSR	Athabasca Oil Sands Region
XRF	X-Ray Fluorescence
XANES	X-ray Absorbance Near Edge Structure
VOC	Volatile Organic Compounds
PAH	Polycyclic Aromatic Hydrocarbons
Al-Pac	Alberta-Pacific Forest Industries Incorporated
GCOS	Great Canadian Oil Sands
FMA	Forest Management Agreement
CLS	Canadian Light Source
PCA	Principle Component Analysis
MSI	Mean Series Intercorrelation
MS	Mean Sensitivity
MTA	Mean Tree Age
bpd	Barrels per day
rpm	Rotations per minute
g	Gram
mg	Milligram
cm	Centimeter
m	Meters
µm	Micrometer
km	Kilometers
km^2	Kilometers squared
mm	Millimeters
s	Seconds

µs	Microseconds
min	Minute
eV	Electronvolt
keV	Kiloelectronvolt
mV/keV	Millivolt per kiloelectronvolt
nA/V	Nanoampere per volt
pA/V	Petaampere per volt
$CaCl_2$	Calcium Chloride
K	Potassium
Ca	Calcium
Ti	Titanium
Zn	Zinc
Ni	Nickel
Mn	Manganese
Cr	Chromium
Fe	Iron
Cu	Copper
Pb	Lead
As	Arsenic
Cd	Cadmium

1. INTRODUCTION

Northern Alberta, Canada, is home to the third largest oil sand repository in the world (Canadian Association of Petroleum Producers, 2015; Government of Alberta, 2015a). Commercial oil sands production in Alberta has been ongoing since 1967, which has since expanded to encompass multiple large-scale oil sand companies and facilities. Oil sands operations in Alberta are projected to grow from producing 2.3 million barrels per day (bpd) of oil to four million bpd by 2024 (Canadian Association of Petroleum Producers, 2015; Government of Alberta, 2015a). Alberta's oil sands region is split into three zones; Peace Lake, Athabasca, and Cold Lake, collectively covering an area of 142, 000 km^2 (Gosselin et al., 2010; Canadian Association of Petroleum Producers, 2015; Government of Alberta, 2015a). The Athabasca Oils Sands Region (AOSR) is the largest and most commercially developed region (Gosselin et al., 2010). AOSR operations are energy and water intensive processes that discharge by-products or wastes. Wastes released from oil sands operations are acute and ongoing. Acute pollutant expulsions and environmental destruction include on-site explosions or equipment malfunction, spills, and mining operations (deforestation from surface mining and *in situ* techniques) (Weinhold, 2011). Ongoing pollutant releases include discharge of ore waste into tailings ponds and atmospheric emissions from fossil fuel use and upgrading facilities. Wastes emitted from oil sands operations are destructive to the surrounding environment and are a renowned source of pollution (Testa, 2008; Gosselin et al., 2010; Schindler, 2010; Simpson et al., 2010; Schindler, 2014; Liggio et al., 2016).

Atmospheric emissions released from the AOSR are particularly concerning because of their unpredictable fate and undetermined influence on surrounding ecosystem components. Vast and diverse amounts of contaminants are released into the atmosphere on a daily basis inclusive to various chemical speciation's of volatile organic compounds (VOC)'s, polycyclic aromatic hydrocarbons (PAH)'s, particulate matter, ozone, carbon, nitrogen, sulfur, and metals (Gosselin et al., 2010; Kelly et al., 2010; Schindler, 2010; Simpson et al., 2010; Bari et al., 2014; Lynam et al., 2015; Huang et al., 2016; Liggio et al., 2016). Airborne pollutants are released into the atmosphere and carried great distances beyond AOSR boundaries by prevailing winds in the region, and are deposited onto the surrounding ecosystem through wet (rain, snowfall, fog) and dry (gravitational settling) deposition events, a phenomenon identified as aerial fallout (Bari et

al., 2014). Evidence suggests air-pollutant enrichment is occurring within a 50 km radius of AOSR facilities (Kelly et al., 2010; Simpson et al., 2010; Proemse et al., 2012; Proemse et al., 2013; Hodson, 2013; Bari et al., 2014; Schindler, 2014; Fenn et al., 2015; Lynam et al., 2015; Huang et al., 2016). The impact of AOSR emissions on the surrounding ecosystem is largely unknown but is an important and relevant topic to scientists, locals, governments, and stakeholders alike (Schindler, 2010).

The boreal forest provides many essential ecological and economical services including forestry operations (the production of paper products and timber for building homes, and employment), supplying oxygen to all living species, providing habitat and food, contributing to global nutrient and water cycling and carbon storage, and providing aesthetic value. Currently, forest around the AOSR is leased to one of Alberta's largest forest companies: Alberta-Pacific Forestry Industries Incorporated (Al-Pac) (Government of Alberta, 2015b).

The impact of Alberta's ongoing atmospheric emissions on biotic forest ecosystems components surrounding the AOSR has only been assessed for a few organisms inclusive to soil microbe communities (Hu et al., 2013); *sphagnum fucsum* moss (Weider et al., 2010), diatom assemblages (Hazewinkel et al., 2008) and several endemic fish species (Schindler, 2014). Surprisingly, the impact of Alberta's emissions on endemic forest species has yet to be published in the literature. A previous M.Sc. student identified a decline in radial growth occurring in white spruce (*Picea glauca*) trees downwind from AOSR facilities, which was attributed to air pollution (Kershaw, 2013). Previous studies used trees as mediums to describe depositional patterns within the region (Laxton et al., 2012; Jung et al., 2013; Savard et al., 2014), but the actual health of trees surrounding the AOSR was never assessed in these studies. Globally, aerial deposition from industrial facilities onto surrounding forests is known to hinder tree physiology and growth (Thompson, 1981; Smith, 1974; Roberts, 1984; Oleksyn et al., 1987; Helmisaari et al., 1995; Kurczynska et al., 1997; Juknys et al.; 2003; Watmough and Hutchinson, 2003; Shparyk and Parpan, 2004; Wilczynski, 2006; Cheng et al., 2007; Lageard et al., 2008; Aznar et al., 2009; Siwik et al., 2010; Hojdova et al., 2011; Malik et al., 2012)

This aim of this study is to assess the impact of AOSR aerial fallout on surrounding trembling aspen (*Populus tremuloides*) and white spruce trees. These two species were chosen because they are endemic boreal forest species that surround the AOSR within its 50 km zone of airborne contaminant enrichment, are vital constitutes to Al-Pac's forest production, and allow

for species comparisons of aerial fallout to be assessed (Brassard and Chen, 2006; Smith and D'eon, 2006; Gosselin et al., 2010). Trembling aspen and white spruce were assessed through dendrochronology, dendrochemistry, a broken-stick model, X-Ray Fluorescence (XRF), and X-ray Absorbance Near Edge Structure (XANES) spectroscopy. Soil parameters, including pH, texture, bulk density, and organic carbon content were also assessed at each forest site. Three upland sites, comprised of mature trembling aspen and white spruce stands, were selected for this study; one upwind Control site and two downwind sites (Site 0 km and Site 50 km). The Control site represents baseline growth within the region. The downwind sites were suspected to receive aerial fallout from the AOSR. The before-mentioned chemical, physical, and dendrochronological parameters were compared between sites.

My thesis is separated into two manuscripts. The first manuscript (Chapter three) discusses the dendrochronological assessment of trembling aspen and white spruce stands at each site, as well as the physical soil properties at each location. Specific objectives of manuscript one are:

- to use dendrochronology and a broken-stick model to determine if AOSR emissions are adversely impacting the radial growth of trembling aspen and white spruce at the downwind sites
- determine if radial-growth responses differ between tree species
- determine if soil properties are similar at each site

The second manuscript (Chapter four) discusses the chemical assessment of trembling aspen and white spruce tree components and their soils at each site, using synchrotron XRF and XANES from a beamline at the Canadian Light Source. Specific objectives of manuscript two are:

- to use XRF and XANES to assess if elemental compositions are altered in trembling aspen and white spruce tree components at the downwind sites
- determine if elemental compositions differ between tree species
- determine if soil chemistry varies per site

1.2 References

Aznar, J., M. Richer-Lafleche, C. Begin, and Y. Begin. 2009. Lead exclusion and copper translocation in black spruce needles. Water Air Soil Pollut. 203: 139-145.

Bari, M., W. Kindzierski, and S. Cho. 2014. A wintertime investigation of atmospheric deposition of metals and polycyclic aromatic hydrocarbons in the Athabasca Oils Sands Region, Canada. Sci. Tot. Environ. 485-486: 180-192.

Brassard, B.W., and H. Y. H. Chen. 2006. Stand Structural Dynamics of North American Boreal Forests. Crit. Rev. in Plant Sci. 25: 115-137

Canadian Association of Petroleum Producers. 2015. Canadian Oil and Natural Gas [Online]. Available at http://www.capp.ca/canadian-oil-and-natural-gas/oil (accessed April 2015).

Cheng, Z., B. Buckley, B. Katz, W. Wright, R. Bailey, K. Smith, J. Li, A. Curtis, and A. van Green. 2007. Arsenic in tree rings at a highly contaminated site. Sci. Tot. Environ. 376: 324-334.

Fenn, M.E., A. Bytnerowicz, S.L. Schilling, and C.S. Ross. 2015. Atmospheric deposition of nitrogen, sulfur and base cation sin jack pine stands in the Athabasca Oil Sands Region, Alberta, Canada. Environ. Pollut.196: 497-510.

Gosselin, P., S. Hrudey, A. Naeth, A. Plourde, R. Therrien, G. Van Der Kraak, and Z. Xu. 2010. Environmental and health impacts of Canada's oil industry. The Royal Society of Canada. Ottawa, Ontario.

Government of Alberta. 2015a. Oil sands [Online]. Available at http://www.energy.alberta.ca/OurBusiness/oilsands.asp.asp (accessed April 2016)

Government of Alberta. 2015b. Forest Management [Online]. Available at http://esrd.alberta.ca/lands-forests/forest-management/forest-management-agreements/default.aspx (accessed April 2015).

Hazewinkel, R., A. Wolfe, S. Pla, C. Curtis, and K. Hadley. 2008. Have atmospheric emissions from the Athabasca oil sands impacted lakes in northestern Alberta*?* Can. J. Fish. Aquat. Sci. 65: 1554-1567.

Helmisaari, H-S., J. Derome, H. Fritze, T. Nieminem, K. Palmgren, M. Salemaa, and I. Vanha-majamaa. 1995. Copper in Scots pine forests around a heavy-metal smelter in south-western Finland. Water Air Soil Pollut. 85: 1727-1732.

Hodson, P.V. 2013. History of environmental contamination by oil sands extraction. Proc. Natl. Acad. Sci. 110: 1569-1570.

Hojdova, M., T. Navratil, J. Rohovec, K. Zak, A. Vanek, V. Chrastny, R. Bace, and M. Svoboda. 2011. Changes in mercury deposition in mining and smelting region as recorded in tree rings. Water Air Soil Pollut. 216: 73-82.

Hu, Y., K. Jung, D. Zeng, and S. Chang. 2013. Nitrogen-and-sulphur-deposition-altered soil microbial community functions and enzyme activities in a boreal mixedwood forest in western Canada. Can. J. For. Res. 43: 777-784.

Huang, R., K.N. McPhedran, L. Yang, and M.G. El-Din. 2016. Characterization and distribution of metal and nonmetal elements in the Alberta oil sands region of Canada. Chemosphere 147: 218-229.

Juknys, R., J. Vencloviene, V. Stravinskiene, A. Augustaitis, and E. Bartkevicius. 2003. Scots pine (Pinus sylvestris L.) growth and condition in a polluted environment: from decline to recovery. Environ. Pollut. 125: 205-212.

Jung, K., W-J. Choi, S.X. Chang, and M.A. Arshad. 2013. Soil and tree ring chemistry of *Pinus banksiana* and *Populus tremuloides* stands as indicators of changes in atmospheric environments in the oil sands region of Alberta, Canada. Ecol. Indi. 25: 256-265.

Kelly, E., D. Schindler, P. Hodson, J. Short, R. Radmanovich, and C. Nielson. 2010. Oil sands development contributes elements toxic at low concentrations to the Athabasca River and its tributaries. Proc. Natl. Acad. Sci. 107: 16178-16183.

Kershaw, G. 2013. Talking to trees: A dendrochronological assessment of the atmospheric pollution effects of Athabasca bitumen mining downwind from the industry. MS Thesis. University of Dalhousie. Halifax, Nova Scotia.

Kurczynska, E., W. Dmuchowski, W. Wloch, and A. Bytnerowicz. 1997. The influence of air pollutants on needles and stems of scots pine (*Pinus sylvestris L.*) trees. Environ. Pollut. 98: 325-334.

Lageard, J., J. Howell, J. Rothwell, and I. Drew. 2008. The utility of *Pinus sylvestris* L. in dendrochemical investigations: pollution impact of lead mining and smelting in Darley Dale, Derbyshire, UK. Environ. Pollut. 153: 284-294.

Laxton, D., S. Watmough, and J. Aherne. 2012. Nitrogen cycling in *Pinus banksiana* and *Populous tremuloides* stands in the Athabasca oil sands region, Alberta, Canada. Water Air Soil Pollut. 223: 1-13.

Liggio, J., S-M. Li, K. Hayden, Y. M. Taha, C. Stroud, A. Darlington, B. D. Drollette, M. Gordon, P. Lee, P. Liu, A. Leithead, S. G. Moussa, D. Wang, J. O'Brien, R. L. Mittermeier, J. R. Brook, G. Lu, R. M. Staebler, Y. Han, T. W. Tokarek, H. D. Osthoff, P. A. Makar, J. Zhang, D. L. Plata, and D. R. Gentner. 2016. Oil sands operations as a large source of secondary organic aerosols. Nature 534: 91 – 94.

Lynam, M.M., J.T. Dvonch, J.A. Barres, M. Morishita, A. Legge, and K. Percy. 2015. Oil sands development and its impact on atmospheric wet deposition of air pollutants to the Athabasca Oil Sands Region, Alberta, Canada. Environ. Poll. 206: 469-478.

Malik, I., M. Danek, E. Marchwinska- Wyrwal, T. Danek, M. Wistuba, and M. Krapiec. 2012. Scots Pine (*Pinus sylvestris L*.) Growth suppression and adverse effects on human health due to air pollution in the upper silesian industrial district (USID), Southern Poland. Water Air & Soil Pollut. 223: 3345-3364.

Oleksyn, J., K. Oleksynowa, E. Kozlowska, and L. Rachwal. 1987. Mineral content and sensitivity of black pine (*Pinus nigra*) of various provenances to industrial air pollution. For. Ecol. Manage. 21: 237-247.

Proemse, B., B. Mayer, and M. Fenn. 2012. Tracing industrial sulfur contributions to atmospheric sulfate deposition in the Athabasca oil sands region, Alberta, Canada. Appl. Geochem. 27: 2425-2434.

Proemse, B., B. Mayer, M. Fenn, and C. Ross. 2013. A multi-isotope approach for estimating industrial contributions to atmospheric nitrogen deposition in the Athabasca oil sands region in Alberta, Canada. Atmos. Environ. 60: 555-563.

Roberts, T. 1984. Effects of air pollution on agriculture and forestry. Atmos. Environ. 18: 629-652.

Savard, M.M., C. Begin, and J. Marion. 2014. Modelling carbon isotopes in spruce trees reproduces air quality changes due to oil sands operations. Ecol. Indic. 45: 1-8

Schindler, D. 2010. Tar sands needs solid science. Nature 468: 499-501.

Schindler, D.W. 2014. Unravelling the complexity of pollution by the oil sands industry. Proc. Nat. Acad. Sci. 111: 3209-3210.

Simpson, I., N. Blake, B. Barletta, D. Diskin, H. Fuelberg, K. Gorham, L. Huey, S. Meinardi, F. Rowland, S. Vay, A. Weinheimer, M. Yang, and D. Blake. 2010. Characterization of trace gases measured over Alberta oil sands mining operations: 76 speciated C2 – C10 volatile organic compounds (VOCs), CO_2, CH_4, CO, NO, NO_2, NO_Y, and SO_2. Atmos. Chem. Phys. 10: 11931-11954.

Shparyk, P., and V. Parpan. 2004. Heavy metal pollution and forest health in the Ukrainian Carpathians. Environ. Pollut. 130: 55-63.

Siwik, E., L. Campbell, and G. Mierle. 2010. Distributions and trends of mercury in deciduous tree cores. Environ. Pollut. 158: 2067-2073.

Smith, W. 1974. Air pollution- effects on the structure and function of the temperate forest ecosystem. Environ. Pollut. 6: 111-129.

Smith, M.L. and R.G. D'Eon. 2006. Pre-Industrial Forest Condition Report for The Alberta-Pacific Forest Industries Inc. Forest management Agreement Area Alberta-Pacific Forest Industries Inc, Boyle, AB.

Testa, M. Bridget. 2008. Tar on Tap. Mech. Eng.12: 30-34.

Thompson, M.A. 1981. Tree rings and air pollution: a case study of Pinus monophylla growing in east-central Nevada. Environ. Pollut. 26: 251-266.

Watmough, S., and T. Hutchinson. 2003. A comparison of temporal patterns in trace metal concentration in tree rings of four common European tree species adjacent to a Cu-Cd refinery. Water Air Soil Pollut. 146: 225-241.

Weinhold, B. 2011. Alberta's oil sands: hard evidence, missing data, new promises. Environ. Health Perspec. 119: A126-A131.

Wieder, K., D. Vitt, M. Burke-Scoll, K. Scott, M. House, and M. Vile. 2010. Nitrogen and sulphur deposition and the growth of *sphagnum fuscum* in bogs of the Athabasca oil sands region, Alberta. J. Limnol. 69: 161-170.

Wilczynski, S. 2006. The variation of tree-ring widths of Scots pine (*Pinus sylvestris L.*) affected by air pollution. Eur. J. For. Res. 125: 213-21

2. LITERATURE REVIEW

2.1 Understanding the Canadian Oil Industry and the Athabasca Oil Sands Region

Oil is a commonly used energy source and commodity across the globe. Canada is the sixth largest oil producer in the world and oil is responsible for approximately 40% of Canada's local energy needs (Canadian Association of Petroleum Producers, 2015a). Oil products include gasoline fuels, diesel fuel, heavy and light fuel oils, jet fuels and are part of other manufactured products such as asphalt, lubricants, greases, waxes, polishes, synthetic rubbers, plastics and other petrochemicals (Canadian Association of Petroleum Producers, 2015a; Government of Alberta, 2015a). Practically speaking, oil fuels vehicles for transportation purposes, heats homes, generates electricity, and is an essential component in paved roads, household products, and many industrial products used in our daily home and work lives (Canadian Association of Petroleum Producers, 2015a; Government of Alberta, 2015a) Economically, oil production provides 550,000 Canadians with jobs and 18 billion dollars in taxes and royalties to Canadian governments per year (Canadian Association of Petroleum Producers, 2015a).

Oil is a natural substance that exists underground, and is produced on a geological time scale making it non-renewable. According to the Government of Alberta (2015a), "crude oil" is defined as the naturally occurring unrefined hydrocarbon mixture that exists in underground reservoirs as a liquid at atmospheric temperature and pressure. Oil reservoirs were created millions of years ago by the remains of ancient marine life and vegetation. Sediment burials, over time, applied intense heat and pressure to ancient marine and vegetation life which led to their transformation into petroleum products, such as oil. Crude oil varies in hydrocarbon content (size and number), viscosity, and color. Typically, oil containing a large number and size of hydrocarbons, has a high viscosity, and is more black in color, sometimes referred to as "heavy oil". "Light oil" contains a smaller number and size of hydrocarbons, has a lower viscosity, and is more amber in color. The varying physical properties of oil distinguish the extraction methods used to obtain it from underground. Extraction techniques used to obtain oil from underground are defined as "conventional" or "unconventional". Conventional oil is extracted through oil wells and naturally flows through pipelines without further intervention, typically associated with lighter oils. Unconventional oil is too thick to flow through pipelines naturally, therefore requires the use of other techniques to improve flow and bring it to the surface, typically

associated with heavy oil and bitumen (Government of Alberta, 2015a). Both conventional and unconventional oil must be refined, through a series of large-scale operations and processes, to produce products that can be sold in Canadian markets and exported to other countries.

The largest oil sand deposit in Canada, and third largest oil reserve in the world, occurs in Alberta, contributing to 78% of Canada's oil needs (Canadian Association of Petroleum Producers, 2015a; Government of Alberta, 2015a). Alberta's oil sand deposits are split into three zones: Athabasca, Cold River, and Peace Lake collectively covering an area of 142,000 km^2. Of these three zones, the AOSR is the largest and most commercially developed (Gosselin et al., 2010; Canadian Association of Petroleum Producers, 2015a). Alberta's oil sand deposits are a mixture of crude bitumen, silica sand, clay minerals, and water (Government of Alberta, 2015a; Canadian Association of Petroleum Producers, 2015a). Bitumen is an extremely viscous, heavy, unconventional oil. Bitumen must be refined further or "upgraded" into synthetic crude oil and other oil products (Government of Alberta, 2015a). Bitumen naturally contains higher amounts of impurities, such as sulfur, nitrogen, and metals, embedded into its chemical structures, compared to other conventional crude oils (Gosselin et al. 2010).

2.2 Summary of AOSR Production and Refinery Processes

Bitumen can be extracted from its natural environment through surface mining or *in situ* methods. Surface mining is utilized when deposits occur within 75 m of the surface, whereas *in situ* techniques are utilized when deposits occur deeper than 75 m (Government of Alberta, 2015a). Surface mining is very destructive and encompasses clearing all overlying forest, vegetation, and soil. Once the overlying environment is removed, barren and exposed ore is shoveled into large trucks and transported to nearby processing facilities that separate bitumen from its sand mixture (Testa, 2008; Government of Alberta, 2015a). The waste (clay, water, sand, and chemical diluents) generated from this separation process are piped to, and deposited into tailing ponds (Testa, 2008; Government of Alberta, 2015a). *In situ* techniques typically include cyclic steam stimulation (CSS) and steam-assisted gravity drainage (SAGD), although *in situ* technology is continually being modified and developed (Government of Alberta, 2015a). These *in situ* methods drill deep into the geological interface, where bitumen resides. Drilled wells are aligned with special piping that has the ability to heat surrounding bitumen through hot steam injections, which decreases bitumen's viscosity and improves its flow (Testa, 2008). The

heated bitumen flows downward, following the force of gravity, into the piping where it can be pumped to the surface, without generating any tailings waste (Testa, 2008). Once bitumen is extracted and separated, it must be further refined or upgraded to produce the final oil products needed in markets. In summary, upgrading requires three stages: 1) distillation, 2) coking, hydro-conversion, de-asphalting, and 3) hydrotreating (Government of Alberta, 2015a). Upgrading reduces the viscosity and molecular weight of bitumen, increases its hydrogen-to-carbon ratio, and removes impurities (Gosselin et al., 2010; Government of Alberta, 2015a). Approximately 50% of extracted oil is upgraded locally (Canadian Association of Petroleum Producers, 2015a). The end product of upgrading is a higher grade oil, or synthetic crude oil. Synthetic crude oil is then shipped to refineries that transform it into a diverse range of oil products.

2.3 A Brief History of Production in the AOSR

The dawn of commercial oil sand extraction and production in the AOSR began in 1967. Production has expanded dramatically since 1967, to encompass a conglomeration of multiple large-scale companies. In the AOSR, three major peaks of production occurred throughout history. In 1967, the Great Canadian Oil Sands (GCOS), now referred to as Suncor Energy Incorporated, was a monopoly within the region producing approximately 32,000 bpd (Canadian Association of Petroleum Producers, 2015b). Syncrude contributed its own facilities, alongside GCOS, in 1979 producing 109,000 bpd (Gosselin et al., 2010; Canadian Association of Petroleum Producers, 2015b). In 2003, Shell Canada built its own production facilities, alongside GCOS and Syncrude, within the AOSR (Jung et al., 2013a; Savard et al., 2014). In the 2000s, commercial oil sands production expanded east and west of the AOSR, to Peace Lake and the Cold River zones, because the price of oil increased making profits more attainable to oil sands businesses (The Earth Observatory, 2011). The economic upturn in 2000, led to Syncrude and Suncor's expansion within the region and the development of many new companies, including Williams Energy Inc., Albain Sands, Fort Hills, Petro-Canada and Canadian Natural Resource Limited, and China National Offshore Oil Corporation (Kershaw, 2013). From 2005 to 2006, production increased from 760,000 bpd to 1.3 million bpd (Schindler, 2010), outlining the industries explosive growth over a relatively short period of time. In 2014, Canada produced 2.3 million bpd which is projected to increase to four million bpd by 2024 (Government of Alberta, 2015a).

2.4 AOSR Pollutant Releases: A Focus on Air Pollution

Bitumen extraction and upgrading methods are energy and water intensive processes that produce by-products or wastes that can be harmful to the environment (Testa, 2008; Gosselin et al., 2010; Schindler, 2010; Simpson et al., 2010; Schindler, 2014; Liggio et al., 2016). Wastes generated from the industry are both acute and ongoing. Acute pollutant releases occur during accidents, including spills, explosions, and malfunctions at production sites, and during extraction times (surface mining and *in situ* techniques) (Weinhold, 2011). Ongoing pollutants are released into tailing ponds and into the surrounding atmosphere, through flare stacks and dusts from mining operations. Both acute and ongoing pollutant releases deposit, integrate, and accumulate materials into surrounding air, water, and soil environments over time and have the potential to harm or permanently alter wildlife, vegetation, and human health, costing the oil industry billions of dollars in revenue in lost profits, compensation, and reclamation.

With the industries projected growth (Schindler, 2010), the fate (extent and influence) of ongoing airborne-contaminant release into the surrounding environment is particularly concerning because of its unpredictability. Many airborne pollutants are transferred great distances away from their source, especially after entry into flowing wind and water (surface and below-ground systems), where they become part of regional, national, and global atmospheric and water circulation patterns. Emissions from the AOSR are comprised of a diverse set of pollutants including various chemical speciation's of polycyclic aromatic hydrocarbons (PAH)'s, volatile organic compounds (VOC)'s, metals, carbon, nitrogen, and sulfur (Gosselin et al., 2010; Kelly et al., 2010; Schindler, 2010; Simpson et al., 2010; Lynam et al., 2015; Huang et al., 2016; Liggio et al., 2016). The fate of airborne contaminants is relatively complex and depends on a variety of factors including topography, meteorological conditions (wind speed and direction, climate, cloud cover, etc.), distance from the source of pollution, as well as chemical (charge/speciation, concentration, etc.) and physical properties (volatility, solubility) of the pollutants in question (Bari et al., 2014). Emissions from the AOSR are carried by prevailing winds and deposited into surrounding environments through wet and dry deposition (Kelly et al., 2010; Kershaw, 2013; Bari et al., 2014; Lynam et al., 2016). Wet deposition occurs when airborne contaminants become incorporated into water droplets in the atmosphere and deposit onto environmental media through fog, rain, and snowfall. Dry deposition involves settling of aerosols and particulate matter onto environmental components through gravitational force.

Collectively, the movement of atmospheric pollutants and subsequent deposition onto the surrounding environment is referred to as atmospheric or aerial fallout (Bari et al., 2014). Evidence suggests that aerial fallout is most concentrated in regions within a 50 km radius of AOSR facilities, with concentrations gradually, and dramatically decreasing beyond this 50 km boundary (Kelly et al., 2010, Proemse et al., 2012b; Proemse et al., 2013; Bari et al., 2014; Fenn et al., 2015; Lynam et al., 2015; Huang et al., 2016).

2.5 Natural Ecosystems Surrounding the AOSR and their Importance

The AOSR is surrounded by boreal forest within the Taiga biome of Canada. Brassard and Chen (2006) and Gosselin et al. (2010) state that boreal forests in northern Alberta are comprised dominantly of cold-tolerant tree species including balsam fir (*Abies balsamea*), tamarack (*Larix laricina*), black spruce (*Picea mariana*), white spruce, lodgepole pine (*Pinus contorta*), jack pine (*Pinus banksiana*), balsam poplar (*Populus balsamifera*), trembling aspen, and white birch (*Betula papyrifera*). Typically, upland regions have mixed-wood stands of trembling aspen and white spruce, whereas lowland areas are comprised of muskeg with black spruce and tamarack. The boreal forest is dominantly covered by coniferous trees species which is broken up by water bodies such as fens, muskegs, rivers and streams. Mountains, valleys, plains, and exposed bedrock are scattered throughout the land as is a multitude of mammals, birds, insects, aquatic wildlife, and human settlements (Brassard and Chen, 2006; Gosselin et al., 2010). Soils in the AOSR are dominantly comprised of a mix of Luvisols, Brunisols, and Organic soil orders, with zones of Gleysols and Regosols (Crown and Twardy, 1975; Soil Classification Working Group, 1998). The climate is characterized as subarctic with short, warm, and humid summers and long, cold winters (Gosselin et al. 2010). Summer typically lasts four months, from May to August, with one month of spring and fall in April and September, and winter conditions prevailing from October to March. Average summer and winter temperatures range from +14.3ºC to -12.1 ºC, respectively (Government of Canada, 2010). Average-annual precipitation is relatively low, and most prevalent in the summer months at 418.6 mm (Government of Canada, 2010). Prevailing winds in the region follow westerly wind patterns, blowing from the west to the east/southeast of the province (Kershaw, 2013). The boreal forest is owned by the Canadian government as Crown land, but managed by each Province. Forested land can be leased out to companies for production and service purposes, through Forest

Management Agreements (FMAs). Currently, Alberta-Pacific Forest Industries Incorporated (Al-Pac) leases the majority of forest surrounding the AOSR, until 2032 (Government of Alberta, 2015b). Other companies operate within Al-Pac's FMA boundaries, and include West Fraser Mills Ltd., Ed Bobocel Lumber (1993) Ltd., Millar Western Forest Products Ltd., Northland Forest Ltd., Seehta Forest Products Ltd., Spruceland Millworks Inc., St.Jean Lumber (1994) Ltd., and Vanderwall Contractors (1971) Ltd. (Government of Alberta, 2015b). Ecologically, the boreal forest provides essential ecosystem services to humans and wildlife, such as supplying oxygen, purifying air, providing aesthetic value, cycling nutrients and water, carbon storage, and providing food and habitat. Economically, forests provide domestic lumber, paper, and food products that generate billions of dollars in revenue, as well as directly employ a significant portion of Canada's population (Government of Canada, Natural Resources Canada, 2016).

2.6 Boreal Forest Ecosystems Components Studied within the AOSR

Boreal forest ecosystems are diverse and interconnected, comprised of a variety of wildlife, understory plant species, forest species, and insects. Aerial fallout has the potential to alter these boreal forest ecosystem components, especially those circumambient to the AOSR. The impact of AOSR aerial fallout has been studied in several biotic and abiotic ecosystem components. Biotic components studied in the AOSR thus far include: isotope analyses of cores from several tree species (*Pinus banksiana*, *Populus tremuloides*, *Picea mariana,* and *Picea glauca*) (Jung et al., 2013a; Savard et al., 2014), *Pinus banksiana,* and *Populus tremuloides* leaves and branches (Laxton et al. 2012), soil microbe communities (Hu et al., 2013), *sphagnum fucsum* moss (Weider et al., 2010), diatom assemblages (Hazewinkel et al., 2008), and several endemic fish species (Schindler, 2014). Abiotic elements studied in this region include soil chemical parameters (Jung et al., 2013a; Jung et al., 2013b), the Athabasca river (Kelly et al., 2010; Gueguen et al., 2011; Schindler, 2014), snowpack (Kelly et al., 2010; Bari et al., 2014), land changes (Rooney et al., 2011), and measurements of airborne-contaminant deposition through direct and passive catchment and isotopic tracer methods (Kelly et al., 2010; Simpson et al. 2010; Proemse et al. 2012a; Proemse et al., 2012b; Jung et al., 2013a; Jung et al., 2013b; Proemse et al., 2013; Bari et al., 2014; Fenn et al., 2015; Lynam et al., 2015; Liggio et al., 2016).

Research regarding the impact and extent of AOSR aerial fallout on boreal forest ecosystem components is incomplete. Very few studies have assessed the impact of AOSR aerial

fallout on the health of surrounding tree species. Previous chemical studies that have assessed aerial fallout on tree species near the AOSR, have limited themselves to only studying specific chemicals (carbon, nitrogen and sulfur), with conflicting results depicting pollutant enrichment from aerial fallout (Savard et al., 2013) or no enrichment occurring at all (Jung et al., 2013a; Laxton et al., 2012). These studies used surrounding trees only as mediums to collect depositional information within the AOSR, meaning the actual impact of AOSR aerial fallout on the health of these trees has yet to be assessed. What is worrisome, is that globally, industrial-sourced aerial fallout has been widely studied and is known to significantly hinder tree-physiological processes and growth by causing phytotoxicity leading to symptoms of chlorosis, reduced water and nutrient uptake, reduced photosynthesis, disrupted plant metabolism and functioning, reduced root and shoot biomass, and disrupted nitrogen fixation processes (Thompson, 1981; Smith, 1974; Roberts, 1984; Oleksyn et al., 1987; Helmisaari et al., 1995; Kurczynska et al., 1997; Juknys et al.; 2003; Watmough and Hutchinson, 2003; Shparyk and Parpan, 2004; Wilczynski, 2006; Cheng et al., 2007; Lageard et al., 2008; Aznar et al., 2009; Yadav, 2010; Siwik et al., 2010; Hojdova et al., 2011).

2.7 Key Factors Controlling Tree Growth

It is important to understand the basic factors that influence tree growth to better understand the potential impact of AOSR aerial deposition on trees. Factors that influence tree growth are interconnected and vary geographically because trees are stationary and depend solely on their environment for survival. In summary, tree growth depends on sunlight exposure, climate conditions (precipitation, temperature, wind, etc.), nutrient uptake, soil properties (texture, organic matter contents, moisture, etc.), canopy characteristics, and the frequency and severity of disturbance (competition between tree and understory species, pests (pathogen/insect infestations), fires, pollution, etc.) (Kittredge, 1973). Too much sunlight dehydrates trees and not enough sunlight prevents photosynthesis. Climate dictates overall moisture and temperature conditions, including the occurrence of floods and droughts, potentially detrimental to tree growth. As well, primary tree functions, such as respiration and photosynthesis, require optimal temperature and moisture conditions. Wind has the ability to adversely impact tree structure, breaking limbs or blowing over mature trees. Trees require appropriate amounts of macro- and micronutrients to develop; with nutrient deficiencies and toxicities capable of hindering tree

growth. Soil properties dictate the uptake of nutrients into trees through their roots. Canopy structure can modify the distribution of sunlight to developing seedlings or competing plants, potentially hindering adjacent tree growth. Lastly, disturbances, such as fires, competing vegetation, insect infestations, and pathogen infestations have the ability to severely deplete entire regions of forests depending on their severity and frequency.

2.8 Mechanisms of Air-borne Pollutant Uptake into Trees (A Cellular Perspective)

White spruce and trembling aspen trees have the capability to take up pollutants through multiple pathways; stomata on their leaves, atmospherically-exposed plant surfaces (leaves, protruding roots, stem barks, branches) and especially through their root and soil systems. Tree parts are comprised of unique cell layers and types, leading to varying pollutant-deposition responses. In general, pollutants enter into trees through their cells in three ways: the apoplastic pathway via cell walls, the symplastic pathway via cell protoplasm, or the transcellular pathway via vacuoles (Rost et al., 2009).

Rost et al. (2009) states that tree leaves are comprised of different cell layers: the epidermis, mesophyll and veins. The epidermis is usually a single layer of cells. Cell types in the epidermis include subsidiary cells, guard cells, trichomes, stomata, and a cuticle. The cuticle is a hydrophobic waxy outer covering on the leaf that blocks any chemical from entering or leaving the leaf. Stomata are pore openings in the leaf that allow gas exchanges to occur. Veins are comprised of xylem and phloem which carry water and nutrients throughout the plant. The mesophyll layer is comprised of parenchyma cells with chloroplasts that capture sunlight and provide plants with food (photosynthates). The mesophyll is located below the epidermis. A variety of pollutants can enter through stomata or diffuse through the surface (cuticle) of leaves. Pollutants can migrate into the xylem and phloem where they can be transferred to and impact multiple parts of a tree.

In mature trees, the stem bark (or cork) is comprised of dead and cracked phellem cell-layers. Phellem cells are produced from a cylindrical meristem tissue layer, beneath the stem bark, called the cork cambium. The cork cambium actively produces phellem cells, which are pushed outward and shed over time, and phelloderm cells, distributed toward the trees interior. Cork protects trees from outside disturbances such as water loss, cold weather, and insect infestations. Beneath the cork cambium layer are secondary phloem cells which are produced

from another actively dividing cylindrical-cell layer called the vascular cambium. The vascular cambium distributes secondary xylem cells inward towards the center (pith) and secondary phloem cells outward towards the cork cambium, both expanding a tree's diameter.

Secondary xylem cells accumulate annually to create tree rings. The cells between the cork cambium and vascular cambium comprise sapwood and are actively transporting water and nutrients throughout a tree. The heartwood is inactive, playing a structural role, and is comprised of old, dead, secondary xylem cells deposited inward, toward the pith of trees. Tree trunks and branches are comprised of several cell types inclusive to sieve-tube members, companion cells, phloem parenchyma cells, phloem fibers, sclereids, and ray parenchyma cells. Pollutants can deposit and diffuse through stem bark (cork) cells into xylem and phloem cells. Pollutant movement, within xylem and phloem, occurs both radially and longitudinally, allowing pollutants to impact multiple tree tissues.

Root layers include the epidermis, cortex, endodermis, pericycle and vascular cylinder. The epidermis is the outermost layer of a root and is comprised of epidermal cells with root hairs one-cell thick. Roots absorb and collect nutrients from the surrounding soil over great surface areas. The cortex is directly beneath the epidermis and is composed of root parenchyma cells. The inner layer of the cortex is called the endodermis which contains a waxy layer called the Casparian strip, responsible for controlling ion uptake into trees. The pericycle is below the Casparian strip and is actively creating new endodermal cells. The vascular cylinder is below the endodermis in the middle of the root and is comprised of variations of xylem and phloem. Typically, deposited air pollutants leach into the soil profile and dissolve into soil pore-water interfaces in the rhizosphere. Depending on the pollutant's chemical and physical properties, and existing soil properties, pollutants can enter into roots and diffuse into their cell layers, causing pollutant accumulations in trees. Once pollutants enter the xylem and phloem, they can be transferred to different parts of a tree and impact tree physiology, function, and growth (Rost et al., 2009).

The movement of pollutants into trees depends on the tree species, pollutant physical and chemical properties, and environmental conditions. Differing tree species have unique cell compositions and layers, and varying physiological functions influencing pollutant uptake. Physical and chemical properties such as hydrophobicity, water-solubility, charge, and size of pollutants affect their ability to adsorb and enter tree cells. Environmental conditions, such as

temperature, concentration gradients, humidity, moisture or water content, wind speed and other climatic factors, control the fate of pollutants and their rate of uptake into trees.

2.9 Trembling Aspen and White Spruce

Trembling aspen and white spruce species are assessed in this this study because they are endemic to areas surrounding the AOSR, possess high economic value to Al-Pac, and possess varying anatomical and physiological features, distinguishing potential species-responses to aerial fallout. Trembling aspen and white spruce grow together naturally, in upland regions of the AOSR (Brassard and Chen, 2006; Gosselin et al., 2010). According to the Government of British Columbia's Forest Practices Branch (2008), trembling aspen is a medium-sized (greater than 40 m tall), deciduous, shade-intolerant species with a relatively deep root system. The root system of trembling aspen on well-drained upland areas is typically heart shaped with lateral roots that produce suckers. In contrast, white spruce is a medium-sized (less than 55 m tall) evergreen conifer, shade-tolerant species with a shallow root system (Government of British Columbia, Forest Practices Branch, 2008). Trembling aspen is a hardwood species with a smooth, porous, thin stem bark, whereas white spruce is a softwood species with a rough, thicker, stem bark. Trembling aspen contains branches with broad, thin leaves attached, dominantly located in the upper crown of the tree, whereas white spruce contains branches along the entire trunk of the tree (from the canopy to the forest floor) with small, clustered needles attached. Where they grow together, aspen establishes more quickly than white spruce, providing shade required for white spruce establishment (Cortini et al., 2012). Typically, spruce and aspen mixed-wood stands grow symbiotically due to their varying sunlight requirements and dissimilar roots systems (Government of British Columbia, Forest Practices Branch, 2008). Both trembling aspen and white spruce require similar nutrient regimes and have moderate to high tolerances to most disturbances (frost, pathogens etc.), although trembling aspen is known to be more sensitive to water deficits and low sunlight exposure and white spruce is more sensitive to wind and fires (Government of British Columbia, Forest Practices Branch, 2008). Both of these tree species have high reproductive success and can live up to 100 to 300 years (Government of British Columbia, Forest Practices Branch, 2008).

2.10 Dendrochronology and Dendrochemistry

Dendrochronology is a technique used to determine the annual-radial growth of trees, through inspection of individual tree rings (Speer, 2010). Dendrochemistry is related to dendrochronology and involves tracing chemicals that reside in tree rings, annually, over time (Watmough, 1999). In dendrochronology and dendrochemistry, a series of cores are extracted from individual tree trunks, which are comprised of a suit of tree rings. A single tree ring consists of earlywood and latewood cells, forms of secondary xylem cells, and is representative of one year of growth. Trees produce a new set of earlywood and latewood cells each year from a tree's vascular cambium. The boundary between the light colored earlywood cells and dark coloured latewood cells contrasts and is visually apparent in trees residing in temperate climates, including the AOSR. Earlywood cells accumulate early in the growing season and are responsible for the bulk of new radial-cell growth and bole width. Latewood cells darken and lignify near the end of the growing season, indicating the end of growth for a particular year. Developing earlywood and latewood cells (ring width) partially depend on environmental conditions present each year. Tree rings, in some cases, can act as repositories of aerial fallout, providing temporal and spatial information about atmospheric pollution. Radial growth occurs in trembling aspen and white spruce trees during Alberta's spring and summer months, when climatic conditions are optimal. Radial-growth variation, or ring width, is dominantly controlled by environmental factors that limit tree growth, such as precipitation and temperature (Fritts, 1976). Previous research suggests that atmospheric pollution influences radial growth by reducing ring-width size (Thompson, 1981; Benoit et al., 1982; Juknys et al.; 2003; Wilczynski, 2006; Malik et al., 2012) and increasing the annual variation of ring-width growth (Thompson, 1981; Fox et al., 1986).

The chemistry of elements present in tree rings can be assessed using dendrochemistry, providing information about chemical changes through time. Air pollution rates, emerging from industrial facilities, have been successfully correlated to temporal chemical changes in tree rings, growing near their facilities (Watmough, 1999; Lageard et al., 2008; Zhang et al., 2008). Dendrochemistry techniques have also been unsuccessful in their attempts to relate commercial air-contaminant emittance rates to tree-ring chemistry (Watmough, 1999; Watmough and Hutchinson, 2003; Siwik et al., 2010), indicating that pollutant uptake into tree rings does not occur for all pollutants and is pollutant specific. Pollutants embedded in tree rings are also

subject to translocation between the heartwood and sapwood in certain species, skewing temporal accuracy.

2.11 A Broken-Stick Model

Air pollutant deposition and accumulation on trees, surrounding the AOSR, has been ongoing since commercial production began in 1967. Therefore, a novel analysis technique will be attempted in this study to assess the long-term accumulation of airborne pollution in trees; annual radial-growth signatures will be evaluated using a broken-stick model. A broken-stick model is a form of linear regression that joins two slopes at transition/breakpoints or threshold points (McGee and Carleton, 1970; Toms and Lesperance, 2003). In this study, annual ring-index data, generated from the dendrochronological assessment, will be used to generate change-points of radial growth between sites. The threshold/transition point, which corresponds to a particular year, will reveal the point in time where clusters of radial growth deviate from previous years' radial-growth patterns. The occurrence of a breakpoint has the potential to estimate the point in time when AOSR airborne-contaminant accumulation impacts tree growth. In general, a broken-stick model is designed to account for the onset of changes in biological time-series dependent data (Chiu et al., 2006).

2.12 The Canadian Light Source (XANES and XRF)

The Canadian Light Source (CLS), commonly referred to as the synchrotron, in Saskatoon, Saskatchewan is an emerging and novel chemical-analysis technology that has the ability to assess objects at a molecular scale. The synchrotron inputs, excels, and stores electrons, circulating at light speeds (Lightsource.org, 2016). These accelerated electrons are manipulated by bending magnets, which change the direction of electrons, resulting in the emittance of a specific range of the electromagnetic spectrum, collectively known as 'synchrotron light' (Lightsource.org, 2016). Different beamlines emit and channel varying ranges of the electromagnetic spectrum, through light-manipulating tools such as monochromators and mirrors (Lightsource.org, 2016). Each beamline is unique and their scientific applications are diverse (Lightsource.org, 2016).

The beamline used in this study is known as Industry Development Education Applications Students (IDEAS) beamline. The IDEAS beamline at the CLS is capable of

performing techniques known as X-Ray Fluorescence (XRF) and X-ray Absorbance Near Edge Structure (XANES) spectroscopy. In both techniques, a sample is shot with synchrotron light. On a molecular scale, incoming synchrotron light excites electrons in elements that comprise a sample. Elements electrons absorb this incoming energy, ultimately leading to the ejection of a core electron and release of a photon. In XRF, an electron from a higher energy orbital, or shell, fills the hole produced from an ejected core electron, to keep an element in its lowest energy state. The movement of an electron from a higher energy orbital to a lower energy orbital results in the emission of a photon fluorescent. The release of a characteristic photon/fluorescent correlates to specific elements, allowing for the detection of specific elements in a sample. XRF is a novel technique because it is able to identify a large number of elements, simultaneously, in a relatively short period of time with minimal sample preparation and no sample destruction. The IDEAS beamline can assess 18 elements, inclusive to Argon (Ar), Potassium (K), Calcium (Ca), Titanium (Ti), Scandium (Sc), Vanadium (V), Chromium (Cr), Manganese (Mn), Iron (Fe), Cobalt (Co), Nickel (Ni), Copper (Cu), Zinc (Zn), Gallium (Ga), Germanium (Ge), Arsenic (As), Selenium (Se), and Bromine (Br).

In a XANES analysis, the beam equipment is rearranged and the main synchrotron light is manipulated (narrowed) to expose a sample to electromagnetic waves across a specific energy range, characteristic to a specific elements binding energy. The number of photons emitted from this specific energy range estimates the absorbance of synchrotron light within a sample providing information about the coordination environment and oxidation state of specific compounds (i.e., chemical speciation). In this study, XANES, using the IDEAS beamline, determined the speciation of K-edge Mn in some of my samples. The output of XANES is a graph that provides a fingerprint of specific Mn compounds within a sample. Peaks at specific energies in a XANES graph represent a certain species of Mn, determined by a reference sample, in this case MnO. K-edge Mn was scanned across an energy range of 6480 to 6640 eV. Previous studies have successfully used XRF and XANES to better understand the chemical make-up of various plant and soil media (e.g, Fittschen and Falkenberg, 2011; Lombi et al., 2011; Majumdar et al., 2012; Herndon et al., 2014).

2.13 Building upon Previous Research

This research aims to build upon previous research conducted by an M.Sc. student. Kershaw (2013) identified a decline in radial growth in white spruce trees downwind from Alberta's oil sand facilities. He illustrated this by using a Principle Component Analysis (PCA) on his tree-ring data that correlated closely to AOSR production rates, and simultaneous air pollution, to his observed-ring widths, attributing radial-growth declines to air pollution. Kershaw's PCA analysis provided the evidence of AOSR aerial deposition impacts, and by doing so, a basis for this study.

2.14 References

Aznar, J., M. Richer-Lafleche, C. Begin, and Y. Begin. 2009. Lead exclusion and copper translocation in black spruce needles. Water Air Soil Pollut. 203: 139-145.

Bari, M., W. Kindzierski, and S. Cho. 2014. A wintertime investigation of atmospheric deposition of metals and polycyclic aromatic hydrocarbons in the Athabasca Oils Sands Region, Canada. Sci. Tot. Environ. 485-486: 180-192.

Benoit, L.F., J.M. Skelly, L.D. Moore, and L.S. Dochinger. 1982. Radial growth reductions of Pinus strobus L. correlated with foliar ozone sensitivity as an indicator of ozone-induced loss in eastern forests. Can. J. For. Res. 12: 673-678.

Brassard, B.W., and H. Y. H. Chen. 2006. Stand Structural Dynamics of North American Boreal Forests. Crit. Rev. Plant Sci. 25: 115-137

Canadian Association of Petroleum Producers. 2015a. Canadian Oil and Natural Gas [Online]. Available at http://www.capp.ca/canadian-oil-and-natural-gas/oil (accessed April 2015).

Canadian Association of Petroleum Producers. 2015b. Oil Sands History and Milestones [Online]. Available at http://www.canadasoilsands.ca/en/what-are-the-oil-sands/oil-sands-history-and-milestones (accessed June 2016).

Cheng, Z., B. Buckley, B. Katz, W. Wright, R. Bailey, K. Smith, J. Li, A. Curtis, and A. van Green. 2007. Arsenic in tree rings at a highly contaminated site. Sci. Tot. Environ. 376: 324-334.

Chiu, G. S., R. Lockhart, and R. Routledge. 2006. Bent-cable regression theory and applications. J. Am. Stat. Assoc. 101:542-553.

Cortini, F. P.G. Comeau, and M. Bokalo. 2012. Trembling aspen competition and climate effects on white spruce growth in boreal mixtures of Western Canada. For. Ecol. Manage. 277: 67-73.

Crown, P. and A. Twardy. 1975. Soils of the Fort McMurray Region, Alberta and Their Relation to Agriculture and Urban Development. Alberta Institute of Pedology, University of Alberta.

Fenn, M.E., A. Bytnerowicz, S.L. Schilling, and C.S. Ross. 2015. Atmospheric deposition of nitrogen, sulfur and base cation sin jack pine stands in the Athabasca Oil Sands Region, Alberta, Canada. Environ. Pollut. 196: 497-510.

Fittschen, U., and G. Falkenberg. 2011. Trends in environmental science using microscopic x-ray fluorescence. Spectrochimica Acta Part B 66: 567-580.

Fox, C.A., W.B. Kincaird, T.H. Nash, D.L., and H.C. Fritts. 1986. Tree-ring variation in western larch (*Larix occidentalis*) exposed to sulfur dioxide emissions. Can. J. For. Res. 16: 283-292.

Fritts, H.C. 1976. Tree rings and climate. p. 567. Academic Press, New York.

Gosselin, P., S. Hrudey, A. Naeth, A. Plourde, R. Therrien, G. Van Der Kraak, and Z. Xu. 2010. Environmental and health impacts of Canada's oil industry. The Royal Society of Canada. Ottawa, Ontario.

Government of Alberta. 2015a. Oil sands [Online]. Available at http://www.energy.alberta.ca/OurBusiness/oilsands.asp.asp (accessed April 2016)

Government of Alberta. 2015b. Forest Management [Online]. Available at http://esrd.alberta.ca/lands-forests/forest-management/forest-management-agreements/default.aspx (accessed April 2015).

Government of British Columbia, Forest Practices Branch. 2008. Tree Species Compendium [Online]. Available at https://www.for.gov.bc.ca/hfp/silviculture/compendium/index.htm (accessed June 2016)

Government of Canada. 2010. Canadian Climate Normals 1981 – 2010 Station Data [Online]. Available at http://climate.weather.gc.ca/climate_normals/results_1981_2010_e.html?searchType=stnProv&lstProvince=AB&txtCentralLatMin=0&txtCentralLatSec=0&txtCentralLongMin=0&txtCentralLongSec=0&stnID=2467&dispBack=0 (accessed June 2016).

Government of Canada, Natural Resources Canada. 2016. Overview of Canada's forest industry [Online]. Available at http://www.nrcan.gc.ca/forests/industry/overview/13311 (accessed June 2 016).

Gueguen, C., O. Clarisse, A. Perroud, and A. McDonald. 2011. Chemical speciation and partitionaing of trace metals (Cd, Co, Cu, Ni, Pb) in the lower Athabsaca river and its tributaries (Alberta, Canada). J. of Envrion. Monit. 13: 2865-2872.

Hazewinkel, R., A. Wolfe, S. Pla, C. Curtis, and K. Hadley. 2008. Have atmospheric emissions from the Athabasca oil sands impacted lakes in northestern Alberta*?* Can. J. Fish. Aquat. Sci. 65: 1554-1567.

Helmisaari, H-S., J. Derome, H. Fritze, T. Nieminem, K. Palmgren, M. Salemaa, and I. Vanha-majamaa. 1995. Copper in Scots pine forests around a heavy-metal smelter in south-western Finland. Water Air Soil Pollut. 85: 1727-1732.

Herndon, E.M., C.E., Martınez, and S.L. Brantley. 2014. Spectroscopic (XANES/XRF) characterization of contaminant manganese cycling in a temperate watershed. Biogeochemistry 121: 505-517.

Hojdova, M., T. Navratil, J. Rohovec, K. Zak, A. Vanek, V. Chrastny, R. Bace, and M. Svoboda. 2011. Changes in mercury deposition in mining and smelting region as recorded in tree rings. Water Air Soil Pollut. 216: 73-82.

Hu, Y., K. Jung, D. Zeng, and S. Chang. 2013. Nitrogen-and-sulphur-deposition-altered soil microbial community functions and enzyme activities in a boreal mixedwood forest in western Canada. Can. J. For. Res. 43: 777-784.

Huang, R., K.N. McPhedran, L. Yang, and M.G. El-Din. 2016. Characterization and distribution of metal and nonmetal elements in the Alberta oil sands region of Canada. Chemosphere 147: 218-229.

Juknys, R., J. Vencloviene, V. Stravinskiene, A. Augustaitis, and E. Bartkevicius. 2003. Scots pine (Pinus sylvestris L.) growth and condition in a polluted environment: from decline to recovery. Environ. Pollut. 125: 205-212.

Jung, K., W-J. Choi, S.X. Chang, and M.A. Arshad. 2013a. Soil and tree ring chemistry of *Pinus banksiana* and *Populus tremuloides* stands as indicators of changes in atmospheric environments in the oil sands region of Alberta, Canada. Ecol. Indic. 25: 256-265.

Jung, K., S. Chang, Y. Sik Ok, and M. Arshad. 2013b. Critical loads and H^+ budgets of forest soils affected by air pollution from oil sands mining in Alberta, Canada. Atmos. Environ. 69: 56-64.

Kelly, E., D. Schindler, P. Hodson, J. Short, R. Radmanovich, and C. Nielson. 2010. Oil sands development contributes elements toxic at low concentrations to the Athabasca River and its tributaries. Proc. Natl. Acad. Sci. 107: 16178-16183.

Kershaw, G. 2013. Talking to trees: A dendrochronological assessment of the atmospheric pollution effects of Athabasca bitumen mining downwind from the industry. M.Sc. Thesis. University of Dalhousie. Halifax, Nova Scotia.

Kittredge, J. 1973. *Introduction*. p. 1-6. *In* Forestry Influences: The Effects of Woody Vegetation on Climate, Water, and Soil. Dover Publications Inc., New York, USA.

Kurczynska, E., W. Dmuchowski, W. Wloch, and A. Bytnerowicz. 1997. The influence of air pollutants on needles and stems of scots pine (*Pinus sylvestris L.*) trees. Environ. Pollut. 98: 325-334.

Lombi, E., M. Jonge, E. Donner, C. Ryan, and D. Paterson. 2011. Trends in hard x-ray fluorescence mapping: environmental applications in the age of fast detectors. Anal. Bioanal. Chem. 400: 1637-1634.

Lageard, J., J. Howell, J. Rothwell, and I. Drew. 2008. The utility of *Pinus sylvestris* L. in dendrochemical investigations: pollution impact of lead mining and smelting in Darley Dale, Derbyshire, UK. Environ. Pollut. 153: 284-294.

Laxton, D., S. Watmough, and J. Aherne. 2012. Nitrogen cycling in *Pinus banksiana* and *Populous tremuloides* stands in the Athabasca oil sands region, Alberta, Canada. Water Air Soil Pollut. 223: 1-13.

Lightsource.org. 2016. What is a Light Source? [Online]. Available at http://www.lightsources.org/what-light-source (accessed June 2016).

Liggio, J., S-M. Li, K. Hayden, Y. M. Taha, C. Stroud, A. Darlington, B. D. Drollette, M. Gordon, P. Lee, P. Liu, A. Leithead, S. G. Moussa, D. Wang, J. O'Brien, R. L. Mittermeier, J. R. Brook, G. Lu, R. M. Staebler, Y. Han, T. W. Tokarek, H. D. Osthoff, P. A. Makar, J. Zhang, D. L. Plata, and D. R. Gentner. 2016. Oil sands operations as a large source of secondary organic aerosols. Nature 534: 91 – 94.

Lynam, M.M., J.T. Dvonch, J.A. Barres, M. Morishita, A. Legge, and K. Percy. 2015. Oil sands development and its impact on atmospheric wet deposition of air pollutants to the Athabasca Oil Sands Region, Alberta, Canada. Environ. Pollut. 206: 469-478.

Majumdar, S., J. Peralta-Videa, H. Castillo-Michel, J. Hong, C. Rico, and J. Gardea-Torresdey. 2012. Applications of synchrotron μ-XRF to study the distribution of biologically important elements in different environmental matrices: A review. Analytica Chemica Acta 755: 1-16.

Malik, I., M. Danek, E. Marchwinska- Wyrwal, T. Danek, M. Wistuba, and M. Krapiec. 2012. Scots Pine (*Pinus sylvestris L.*) Growth suppression and adverse effects on human health due to air pollution in the upper silesian industrial district (USID), Southern Poland. Water Air & Soil Pollut. 223: 3345-3364.

McGee., V.E and W.L. Carleton. 1970. Piecewise Regression. J. Am. Stat. Assoc. 65: 1109-1124.

Oleksyn, J., K. Oleksynowa, E. Kozlowska, and L. Rachwal. 1987. Mineral content and sensitivity of black pine (*Pinus nigra*) of various provenances to industrial air pollution. For. Ecol. Manage. 21: 237-247.

Proemse, B., B. Mayer, J. Chow, and J. Watson. 2012a. Isotopic characterization of nitrate, ammonium and sulfate in stack $PM_{2.5}$ emissions in the Athabasca Oil Sands Region, Alberta, Canada. Environ. Pollut. 182: 80-91.

Proemse, B., B. Mayer, and M. Fenn. 2012b. Tracing industrial sulfur contributions to atmospheric sulfate deposition in the Athabasca oil sands region, Alberta, Canada. Appl. Geochem. 27: 2425-2434.

Proemse, B., B. Mayer, M. Fenn, and C. Ross. 2013. A multi-isotope approach for estimating industrial contributions to atmospheric nitrogen deposition in the Athabasca oil sands region in Alberta, Canada. Atmos. Environ. 60: 555-563.

Roberts, T. 1984. Effects of air pollution on agriculture and forestry. Atmos. Environ. 18: 629-652.

Rost, T.L, M.G. Barbour, C.R. Stocking, and T.M. Murphy. 2009. Plant Biology. Second Edition. Nelson Education Limited. Toronto, ON.

Savard, M.M., C. Begin, and J. Marion. 2014. Modelling carbon isotopes in spruce trees reproduces air quality changes due to oil sands operations. Ecol. Indic. 45: 1-8

Schindler, D. 2010. Tar sands needs solid science. Nature 468: 499 – 501.

Schindler, D.W. 2014. Unravelling the complexity of pollution by the oil sands industry. Proc. Natl. Acad. Sci. 111: 3209-3210.

Simpson, I., N. Blake, B. Barletta, D. Diskin, H. Fuelberg, K. Gorham, L. Huey, S. Meinardi, F. Rowland, S. Vay, A. Weinheimer, M. Yang, and D. Blake. 2010. Characterization of trace gases measured over Alberta oil sands mining operations: 76 speciated C2 – C10 volatile organic compounds (VOCs), CO_2, CH_4, CO, NO, NO_2, NO_Y, and SO_2. Atmos. Chem. Phys. 10: 11931-11954.

Shparyk, P., and V. Parpan. 2004. Heavy metal pollution and forest health in the Ukrainian Carpathians. Environ. Pollut. 130: 55-63.

Siwik, E., L. Campbell, and G. Mierle. 2010. Distributions and trends of mercury in deciduous tree cores. Environ. Pollut. 158: 2067-2073.

Smith, W. 1974. Air pollution- effects on the structure and function of the temperate forest ecosystem. Environ. Pollut. 6: 111-129.

Soil Classification Working Group. 1998. The Canadian System of Soil Classification, 3rd (ed.). p. 187. Agriculture and Agri-Food Canada Publication, 1646.

Speer, J. H. 2010. *Fundamentals of tree-ring research*. p. 368. University of Arizona Press, Tucson.

Testa, M. Bridget. 2008. Tar on Tap. Mech. Eng. 12: 30-34.

The Earth Observatory. 2011. World of Change: Athabasca Oil Sands: Featured Articles [Online]. Available at http://earthobservatory.nasa.gov/Features/WorldOfChange/athabasca.php (accessed June 2016)

Thompson, M.A. 1981. Tree rings and air pollution: a case study of Pinus monophylla growing in east-central Nevada. Environ. Pollut. 26: 251-266.

Toms, J. D., and M. L. Lesperance. 2003. Piecewise regression: a tool for identifying ecological thresholds. Ecology 84:2034-2041.

Watmough, S. 1999. Monitoring historical changes in soil and atmospheric trace metal levels by dendrochemcial analysis. Environ. Pollut. 106: 391-403.

Watmough, S., and T. Hutchinson. 2003. A comparison of temporal patterns in trace metal concentration in tree rings of four common European tree species adjacent to a Cu-Cd refinery. Water Air Soil Pollut. 146: 225-241.

Wieder, K., D. Vitt, M. Burke-Scoll, K. Scott, M. House, and M. Vile. 2010. Nitrogen and sulphur deposition and the growth of *sphagnum fuscum* in bogs of the Athabasca oil sands region, Alberta. J. of Limnol. 69: 161-170.

Wilczynski, S. 2006. The variation of tree-ring widths of Scots pine (*Pinus sylvestris L.*) affected by air pollution. Eur. J. For. Res. 125: 213-21

Zhang, C., B. Huang, J.D.A. Piper, and R. Luo. 2008. Biomonitoring of atmospheric particulate matter using magnetic properties of *Salix matsudana* tree ring cores. Sci. Tot. Environ. 393: *177-190.*

3. A DENDROCHRONOLOGICAL ASSESSMENT OF TREMBLING ASPEN (*POPULUS TREMULOIDES*) AND WHITE SPRUCE (*PICEA GLAUCA*) SURROUNDING THE ATHABASCA OIL SANDS REGION IN ALBERTA, CANADA

3.1 Abstract

The Athabasca Oil Sands Region (AOSR), in Alberta, Canada, houses a multitude of large-scale production facilities that are releasing a diverse set of contaminants into the atmosphere. These airborne-contaminants are deposited onto surrounding boreal forest ecosystems by prevailing winds, but their effects on the surrounding environment is largely unknown. The purpose of this study is to determine if AOSR atmospheric pollution is impacting the radial growth of two common tree species, trembling aspen (*Populus tremuloides*) and white spruce (*Picea glauca*). Trembling aspen and white spruce cores, as well as soil samples, were collected from three forest stands surrounding AOSR facilities. Samples were collected from one upwind Control site and two sites located downwind from the AOSR. Master chronologies were constructed for each tree species per site and analyzed using a broken-stick model, which compared Control site growth to each downwind sites' growth. Soil pH, texture, bulk density, and organic carbon content were also assessed, at various depth-increments, per site. Results indicate that trembling aspen's radial growth is responding in a similar manner between the Control site and the two downwind sites, while white spruce is acting differently between the Control and the two downwind sites. The difference in white spruce radial growth occurs specifically over the past decade, even though soil properties are the same at all sites. This timeframe outlines a potential threshold point of airborne-contaminant enrichment in white spruce trees. Radial-growth declines illustrated a more severe departure at sites closer in proximity to AOSR facilities, where airborne pollutant concentrations are at their peak.

3.2 Introduction

Canada produces 2.3 million barrels per day (bpd) of oil which is projected to increase to four million bpd by 2030 (Canadian Association of Petroleum Producers, 2015). Approximately 78% of Canadian oil is extracted and produced from Alberta's oil sand deposits, the third largest oil reserve in the world (Canadian Association of Petroleum Producers, 2015; Government of

Alberta, 2015). Alberta's oil sand deposits are located within Canada's boreal forest, and are split into three zones: Athabasca, Cold River, and Peace Lake, collectively covering an area of 142,000 km^2. The Athabasca Oil Sands Region (AOSR) is the largest and most commercially developed zone in Canada (Gosselin et al., 2010) and its rampant expansion is of utmost concern, due to its extensive and controversial pollution output. AOSR atmospheric emissions are particularly worrying because of their potential to alter circumambient ecosystems, great distances away from AOSR boundaries. Kelly et al. (2010) and Bari et al. (2014) determined that airborne pollutants emitted from the AOSR are carried by prevailing winds and deposited onto boreal forest ecosystems through wet (fog, rain, or snowfall) and dry (gravitational settling) deposition events. Airborne deposition into river systems allows these pollutants to flow and travel even further distances from their original source. Collectively, the movement of atmospheric pollutants, released from oil sand facilities, and subsequent deposition onto boreal forest ecosystems is referred to as atmospheric or aerial fallout (Bari et al., 2014). The extent and ramification of AOSR aerial fallout on surrounding boreal forest ecosystems remains controversial and misunderstood, and as a result, research contributing to this topic is urgently needed and is indispensable to local community members, scientists, government, and local stakeholders (Schindler, 2010).

Bitumen extraction and production, in the AOSR, is a large-scale, complex operation involving many stages of processing. Originally, a single company controlled commercial oil production and extraction, beginning in 1967 (Gosselin et al., 2010). Over the past 50 years, oil facilities have evolved and expanded to include multiple large-scale companies. The recovery of oil through open pit mining and *in situ* methods, such as Cyclic Steam Stimulation and Steam Assisted Gravity Drainage, as well as, upgrading procedures, inclusive to distillation, coking, hydro-conversion, solvent de-asphalting, and hydrotreating, are landscape destructive and energy- and water-intensive processes that emit vast and diverse quantities of contaminants into the atmosphere, changing ambient air quality and landscape composition (Government of Alberta, 2015; Testa, 2008; Wang and Naterer, 2010). Pollutants emitted from the AOSR include multiple chemical-speciation's of polycyclic aromatic hydrocarbons (PAH)'s, volatile organic compounds (VOC)'s, particulate matter, sulphur, nitrogen, carbon, metals, and ozone (Kelly et al., 2010; Gosselin et al., 2010; Simpson et al., 2010, Schindler, 2010; Bari et al., 2014; Lynam et al., 2015; Huang et al., 2016; Liggio et al., 2016).

The impact of AOSR emissions on circumambient boreal forest ecosystem components is largely unknown. Biotic elements, studied thus far, include: isotope analyses of cores from several endemic tree species (*Pinus banksiana, Populus tremuloides, Picea mariana,* and *Picea glauca*) (Jung et al., 2013a; Savard et al., 2014), *Pinus banksiana,* and *Populus tremuloides* leaves and branches (Laxton et al., 2012), soil microbe communities (Hu et al., 2013), *sphagnum fucsum* moss (Weider et al., 2010), diatom assemblages (Hazewinkel et al., 2008), and several endemic fish species (Schindler, 2014). Abiotic elements studied in this region include soil chemical parameters (Jung et al., 2013a; Jung et al., 2013b), the Athabasca river (Kelly et al., 2010; Gueguen et al., 2011; Schindler, 2014), snowpack (Kelly et al., 2010; Bari et al., 2014), land changes (Rooney et al., 2011), and measurements of airborne-contaminant deposition through direct and passive catchment and isotopic tracer methods (Kelly et al., 2010; Simpson et al., 2010; Proemse et al., 2012a; Proemse et al., 2012b; Jung et al., 2013a; Proemse et al., 2013; Bari et al., 2014; Fenn et al., 2015; Lynam et al., 2015; Liggio et al., 2016). Previous literature has revealed insights into the spatial variation of atmospheric emissions on circumambient boreal forest ecosystem components, indicating that aerial fallout decreases with distance from the AOSR, and is dramatically reduced for certain pollutants, approximately 50 km's away (Kelly et al., 2010; Simpson et al., 2010; Proemse et al., 2012b; Proemse et al., 2013; Hodson, 2013; Bari et al., 2014; Schindler, 2014; Fenn et al., 2015; Lynam et al., 2015; Huang et al., 2016). Conversely, evidence has revealed no significant enrichment accruing in circumambient boreal forest ecosystem components (Wieder et al., 2010; Laxton et al., 2012; Jung et al., 2013b). It is important to understand that several key biotic and abiotic components and parameters have yet to be studied, contributing to the misunderstanding of the implications and dynamics of AOSR emissions on boreal ecosystems as a whole.

The focus of this study is to perform a dendrochronological assessment on two of the region's tree species, trembling aspen (*Populus tremuloides*) and white spruce (*Picea glauca*), to investigate the implications of AOSR emissions on circumambient tree growth. Dendrochronology is a technique used to determine the annual-radial growth of trees, through inspection of individual tree rings (Speer, 2010). Radial-growth variation, or ring width, is dominantly controlled by environmental factors that limit tree growth, such as precipitation and temperature (Fritts, 1976); although previous research has demonstrated that atmospheric pollution can become a limiting factor and reduce ring-width size (Thompson, 1981; Benoit et

al., 1982; Juknys et al., 2003; Wilczynski, 2006; Malik et al., 2012) and increase the annual variation of ring-width growth (Thompson, 1981; Fox et al., 1986).

Globally, commercial aerial fallout is known to significantly hinder tree physiological processes and growth (Thompson, 1981; Smith, 1974; Roberts, 1984; Oleksyn et al., 1987; Helmisaari et al., 1995; Kurczynska at al., 1997; Juknys et al., 2003; Watmough and Hutchinson, 2003; Shparyk and Parpan, 2004; Wilczynski, 2006; Cheng et al., 2007; Lageard et al., 2008; Aznar et al., 2009; Siwik et al., 2010; Hojdova et al., 2011; Malik et al., 2012). Airborne contaminants can diffuse into plant cells and enter tree metabolisms through its tree parts such as leaves, branches, stem barks, and roots. Contaminants can also deposit onto forest floors, leach into the soil profile by precipitation events, and become absorbed by tree roots.

Dendrochronology is a well-established science but has yet to be utilized in the AOSR. I will therefore use dendrochronology to try to provide a signature of annual-radial growth for trembling aspen and white spruce at sites located at varying distances around AOSR facilities. Airborne contamination has been ongoing since production began in 1967, allowing for approximately 50 years of fluctuating pollutant exposure and accumulation to occur on nearby trembling aspen and white spruce trees. I hypothesize that white spruce and trembling aspen stands downwind from the AOSR will exhibit a reduction in annual-radial growth after 1967, the time period when Alberta's oil sands began commercial production. Specific objectives of this study are: 1) to use dendrochronology to determine if AOSR atmospheric pollution is adversely impacting the radial-growth of trembling aspen and white spruce downwind from the AOSR; 2) determine if soil properties differ per site, and 2) determine if radial-growth responses differ between tree species.

3.3 Materials and Methods

3.3.1 Site descriptions

Figure 3.1 illustrates the Control site which was selected approximately 190 km's (56º73'31.7" N, 114º59'27.3" W) upwind from the AOSR. Two other sites were selected downwind at 50 km (Site 50 km - 56º64'35.3" N, 111º06'56.4" W) and near the edge of the AOSR (Site 0 km – 56º88'42.5" N, 111º45'21.0" W). The Control site was selected so that it could represent an unspoiled and baseline radial-growth record within the region. The other two sites were located within the proposed 50 km zone of enrichment (Kelly et al., 2010; Simpson et

al., 2010; Hu et al., 2013; Proemse et al., 2012b; Proemse et al., 2013; Hodson, 2013; Bari et al., 2014; Schindler, 2014; Fenn et al., 2015; Lynam et al., 2015; Huang et al., 2016), and represented areas suspected to receive atmospheric fallout following prevailing wind patterns within the region. It was assumed that radial-growth patterns that deviate from the Control site will indicate the timeframe and magnitude of a disturbance event that has occurred at the site.

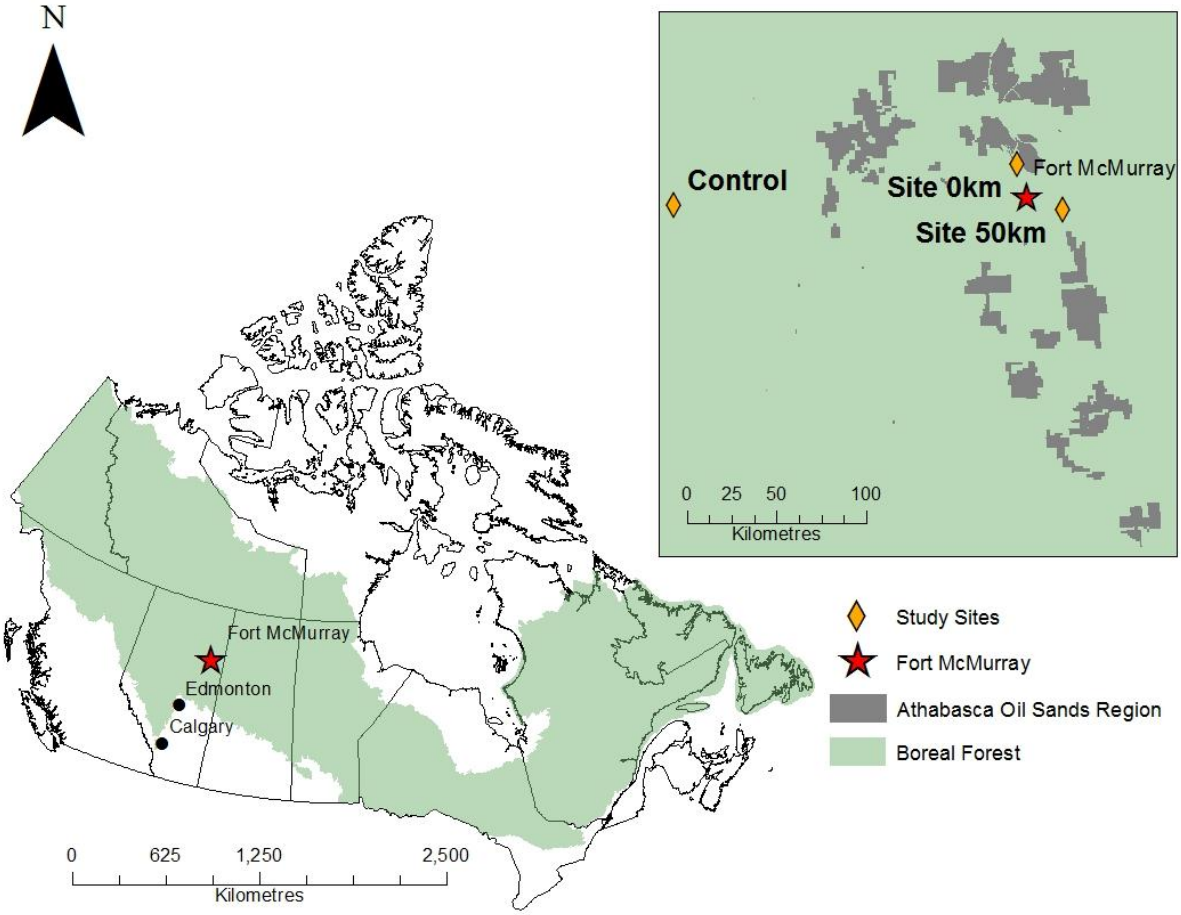

Figure 3.1 Location of the study sites in Alberta's AOSR (operating and approved projects). (EsriCanadaEd, 2001; Government of Alberta, Alberta Environment and Parks, 2015; MapCruzin, 2016; Government of Canada, Agriculture and Agri-Food Canada, 2016).

Three mixed-wood stands of trembling aspen and white spruce were chosen for the study sites and were comprised of similar site characteristics, ideal for radial-growth comparison. Sites were selected within a 200 km radius of one another to ensure climate conditions were similar per site. Climate conditions, within the region, are characterized by short warm summers (four month growing season), and long cold winters, with average temperatures ranging from +14.3ºC to -12.1 ºC (Government of Canada, 2010). Average-annual

precipitation is relatively low, most prevalent in the summer months, at 418.6 mm (Government of Canada, 2010). All sites occurred on well-drained upland regions, without the occurrence of standing water, to prevent the uptake from potentially contaminated underground aquifers. Sites were selected at a minimum of 10 meters away from the nearest forest cut line, road, and/or highway, to avoid forest-edge effects. All tree and soil samples were collected on land with little to no slope. A qualitative assessment of soils, through soil pit descriptions, revealed that all soils, for each site, were Luvisols containing similar horizons; a thick LFH, above an eluviated Ae horizon, overlying a thick Bt horizon (Soil Classification Working Group, 1998; Appendix A). No effervescence was found in any of the pits, at any of the sites, meaning inorganic soil carbonates were not present (Appendix A). Coarse fragments were comparable and minimal at all study locations, and loam was identified as the dominant texture class for each depth increment at each site (Appendix A). Soil samples were collected in detail to ensure that any radial-growth differences were not attributed to changes in soil characteristics.

Increment cores were extracted from two tree species, trembling aspen and white spruce, from three study sites, located around the AOSR on June of 2015. They were selected to represent both the most common deciduous and coniferous tree species in the region and this also allowed for an inter-species comparison to be made at each site.

3.3.2 Field sampling: cores and soils

Twenty white spruce and 20 trembling aspen trees were cored at each site using a 5.15 mm increment borer. Only mature trees were selected for coring. Two cores were extracted for each tree at breast height and at perpendicular angles to one another, to account for potential compression growth effects on the sample (Speer, 2010). A total of 40 trembling aspen and 40 white spruce cores were extracted at each site, for a total of 240 cores from the three locations. Once extracted, tree cores were transported to the University of Saskatchewan's Mistik Askiwin Dendrochronology Lab for processing.

Four soil pits were dug at representative locations at each site. Representative locations were areas where level topography and native vegetation occurred. Pits varied in size from 55 - 60 cm deep. Each pit was dug within a 20 m radius of selected sites near cored trees. Five ≈ 60 g samples were obtained from each pit at various depth increments. One sample per depth increment was extracted with a soil knife. Depth increments were identified as: 1) Leaf Litter, 2) 0 to 5 cm, 3) 5 to 20 cm 4) 20 to 45 cm, and 5) 45 to 60 cm. Twenty samples were collected per

site, for a total of 60 soil samples. Two bulk density samples were also extracted per pit between the 5 to 20 cm depth increment before individual depth increment samples were obtained. Bulk density samples were collected using a metal cylinder, 5 cm in depth by 6 cm diameter. All soil samples were then deposited into plastic zip-lock bags and stored in coolers for transport back to the University of Saskatchewan. Bulk density samples were immediately stored in freezers at the University of Saskatchewan to retain field-moist conditions. Horizon depth, designation, texture, color, mottles, coarse fragments, and effervescence were recorded for each pit before the extraction of soil samples (Appendix A).

3.3.3 Dendrochronological processing and analytical techniques

Each core was processed to reveal individual tree rings by first gluing each core onto a slotted mounting board, then sanding each core with progressively finer sandpaper (60-800 grit) until cellular structures were revealed and individual tree rings were clearly visible. The radial growth of each tree ring was manually measured under a 62X microscope and a Velmex stage system. The Velmex stage system was linked to a software program called J2X (VoorTech Consulting, 2004), which digitally recorded each measured tree-ring width. Measurements were recorded to a precision of 0.001mm (Appendix B).

Each chronology was cross-dated and standardized to provide an average radial-growth pattern at each site. Cores were crossdated using the program COFECHA (Holmes, 1983; Grissino-Mayer, 2001), which compares each core in a chronology to a master chronology made up of all the cores. A master chronology is the average radial-growth per year of all cores in a series. A series is defined as all cores per tree species per site. Cores were compared to the master chronology over 30-year time segments. COFECHA provided a sequence of statistics to help identify important average chronology characteristics at each site. The statistical outputs used in this study that were derived from the COFECHA output are mean series intercorrelation (MSI), mean sensitivity (MS), autocorrelation, time-span of the series, and mean tree age (MTA).

MSI is the correlation coefficient (R-value) of all trees in a master chronology, generated from the average correlation coefficients of cores compared to the master chronology. High MSI values signify mutually-related radial growth whereas low MSI values signify poorly-related radial growth. MS measures annual variations (relative percent changes) of radial growth to determine the responsiveness of trees to their environment (Fritts, 1979). High MS values

(values above 0.300) indicate a high degree of annual variation over time and a mix of wide and narrow tree-rings within a chronology. A low MS value (values below 0.100) indicates a low degree of annual variation over time and relatively similar ring widths. Autocorrelation measures any lag in growth within a series and expressed the degree to which previous growing conditions affect future growth (Grissino-Mayer, 2001). The time-span of the series described the total length of years each series spanned using all possible chronologies. Finally, MTA refers to the average age of trees used in the master chronology.

Ring-widths generally decrease from pith to bark because trees accumulate a disproportionately large amount of radial cells during their initial stage of growth. Radial-growth rates decline as trees mature, following a negative exponential growth pattern. Each chronology was detrended to remove this biological growth. Chronologies were standardized using program ARSTAN (Cook, 1985), which fits a negative exponential growth curve to each chronology to remove this innate radial-growth trend. In cases where a negative exponential curve did not fit individual chronologies, radial-growth was detrended with a horizontal line though the mean. The final result produced from ARSTAN was a unitless tree-ring index of growth over an annual-time series (Appendix B). A ring-index value of one indicated average radial growth. A ring index value greater than one indicated above-average radial growth and a ring index value less than one indicated below-average radial growth.

3.3.4 Broken-stick model

Each downwind site's radial-growth was compared to the Control site's radial-growth, per tree species, using a broken-stick model (McGee and Carelton, 1970; Toms and Lesperance, 2003; Chiu et al., 2006). A broken-stick model is a form of non-parametric linear regression which fits two linear slopes, to similar clusters of data, which diverge at a calculated transition/break/threshold point. Slopes were calculated and fit to individual change points using R Version 3.1.2's "piecewise.linear" function (Sonderegger, 2015). An individual (annual) change point was determined by the log(*ratio*) of a downwind site's ring index divided by the Control site's ring index for each tree species. Ring index values represent standardized average radial growth per year, per tree species, per site.

i.e., Annual change point = $\log\left(\frac{Site\ 50\,km\ or\ Site\ 0\,km\ ring\ \ index}{Control\ \ ring\ \ index}\right)$

for white spruce or trembling aspen.

A log(*ratio*) that equals zero implies that the compared ring indices were the same, and change does not exist. A log(*ratio*) greater than or less than zero indicates that the compared ring indices were different, and a change point does exist. A greater log(*ratio*) value signifies a larger degree of change and are illustrated as further distances from zero. The second slope begins at a calculated transition point, which is the point where clusters of data deviate from previous year's clusters of data (the point with the largest residual sum of squares). The ability of the broken-stick model to detect a threshold/breakpoint, allows one to associate a year to dominant radial-growth changes (if any occur). A major assumption of this model is that calculated transition points manifest themselves in a sharp/abrupt manner, which in reality, may be more representative of a smooth or polymeric transition (McGee and Carleton, 1970; Toms and Lesperance, 2003; Chiu et al., 2006).

3.3.5 Soil processing and analytical techniques

Four soil parameters were analyzed; acidity, bulk density, organic carbon content, and texture. These parameters were chosen to identify if varying soil characteristics occurred at each site. Prior to analysis, all soils were sieved with a 2 mm mesh sieve and air dried for one week. Mean pH values were calculated from four replicates per depth increment per site. The pH ($CaCl_2$) was assessed with a Fisher Science Education ® 510 bench pH meter following the method of Hendershot et al. (2008). The pH meter was calibrated with three Fisher Scientific ® solutions at 4.0, 7.0 and 10.0. Mean bulk density values were calculated from four replicates per site, for the 5 to 20 cm depth increment. Bulk density was determined following Sheppard and Addison (2008) sample and handling methods and modified calculations established by Ellert et al. (2008). Mean (%) organic carbon was calculated from four replicates per depth increment per site. Organic carbon was determined using the dry carbon combustion method outlined by Baldock and Skjemstad (1999) using a LECO C-632 Carbon Analyzer®. Two blanks and three Standard Reference Materials were run prior to analysis, and every 20 samples, to ensure adequate machine performance. Finally, particle-size analysis determined mean (%) silt, (%) clay and (%) sand fractions calculated from four replicates per depth increment per site using the method of Indorante (1990) with settling times of 3 hours and 57 minutes, and 3 hours and 51 minutes per batch (24 samples).

Soil parameters (pH, bulk density, organic carbon (%), and sand, silt and clay fractions (%)) were compared to one another per site using the Kruskal-Wallis rank sum test (Kruskal and

Wallis, 1952; Hollander and Wolfe, 1973), otherwise known as the one-way ANOVA on ranks, using code in R Version 3.1.2 (R Core Team and contributors worldwide, 2016). The Kruskal-Wallis rank sum test was used because of the soil data's small sample size and absence of normal distributions. Data did not follow normal distributions even after transformations were performed. The Kruskal-Wallis rank sum test assigns a rank to each data point and compares average ranks per grouping. A ranking of 1 was assigned to the lowest observable value. Higher rankings were denoted to higher values and similar ranks were given to similar values. P-values greater than 0.05 indicate to accept the null hypothesis which states that mean ranks are the same per group, meaning soil parameters are similar per site. P –values less than 0.05 indicate to accept the alternative hypothesis which states at least one mean rank is different per grouping, meaning soil parameters differ per site. A post-hoc test, Dunn's test (Dunn, 1961), was performed if the Kruskal-Wallis test showed statistically significant results, using code in R Version 3.1.2 (Dinno, 2016). The post-hoc test was used to determine which sites were statistically different from one another for each soil parameter.

3.4 Results

The MS values from the COFECHA analysis did not differ per site for the same species but showed significant changes between tree species (Table 3.1). Values of MS are consistently lower for white spruce compared to trembling aspen, inferring that white spruce rings are less sensitive and exhibit less year-to-year variation, whereas trembling aspen are more sensitive

Table 3.1 COFECHA results generated for each series. MSI = mean series intercorrelation; MS = mean sensitivity; MTA = mean tree age

Site	Tree Species	No. of Cores	Time-span	MTA	Auto-correlation (unfiltered)	MSI	MS
Control	White Spruce	39	1925-2014	66	0.660	0.668	0.205
Site 50 km	White Spruce	39	1918-2014	80	0.787	0.663	0.206
Site 0 km	White Spruce	35	1953-2014	57	0.881	0.629	0.199
Control	Trembling Aspen	35	1910-2014	94	0.750	0.741	0.339
Site 50 km	Trembling Aspen	38	1904-2014	99	0.700	0.701	0.330
Site 0 km	Trembling Aspen	37	1927-2014	65	0.749	0.725	0.339

and exhibit more year-to-year variation in their rings. Intra-species MSI did not change per site but inter-species changes did occur. Trembling aspen's radial growth appears to be more mutually-related than white spruce, although intra-species growth is highly mutually-related per site. Additionally, all sites MSI's fell far above the 0.4226 threshold value, indicating a positive significant radial growth correlation at a 99% confidence interval for all species at all sites. Autocorrelation values did not significantly change per species and site, although, white spruce portrayed more variation than trembling aspen. Finally, MTA and time-spans revealed that trembling aspen is older than white spruce at all sites. Site 50 km has the oldest trees, whereas Site 0 km had the youngest trees, for both tree species.

Trembling aspen's downwind sites follow the Control site's radial-growth pattern (Figure 3.2). Radial-growth trends for white spruce's downwind sites deviated from the Control site's radial growth from 2004 onward, illustrating gradually reduced or below-average ring-width growth at the two downwind sites (Figure 3.3; Figure 3.4; Figure 3.5). Trembling aspen and white spruce stand's followed similar variations in annual-radial growth, with the exception of white spruce's downwind sites from 2004 onward (Figure 3.6). Trembling aspen's growth appeared to be more responsive to climate changes at all three sites, illustrated by their more elongated ring index peaks (Figure 3.6).

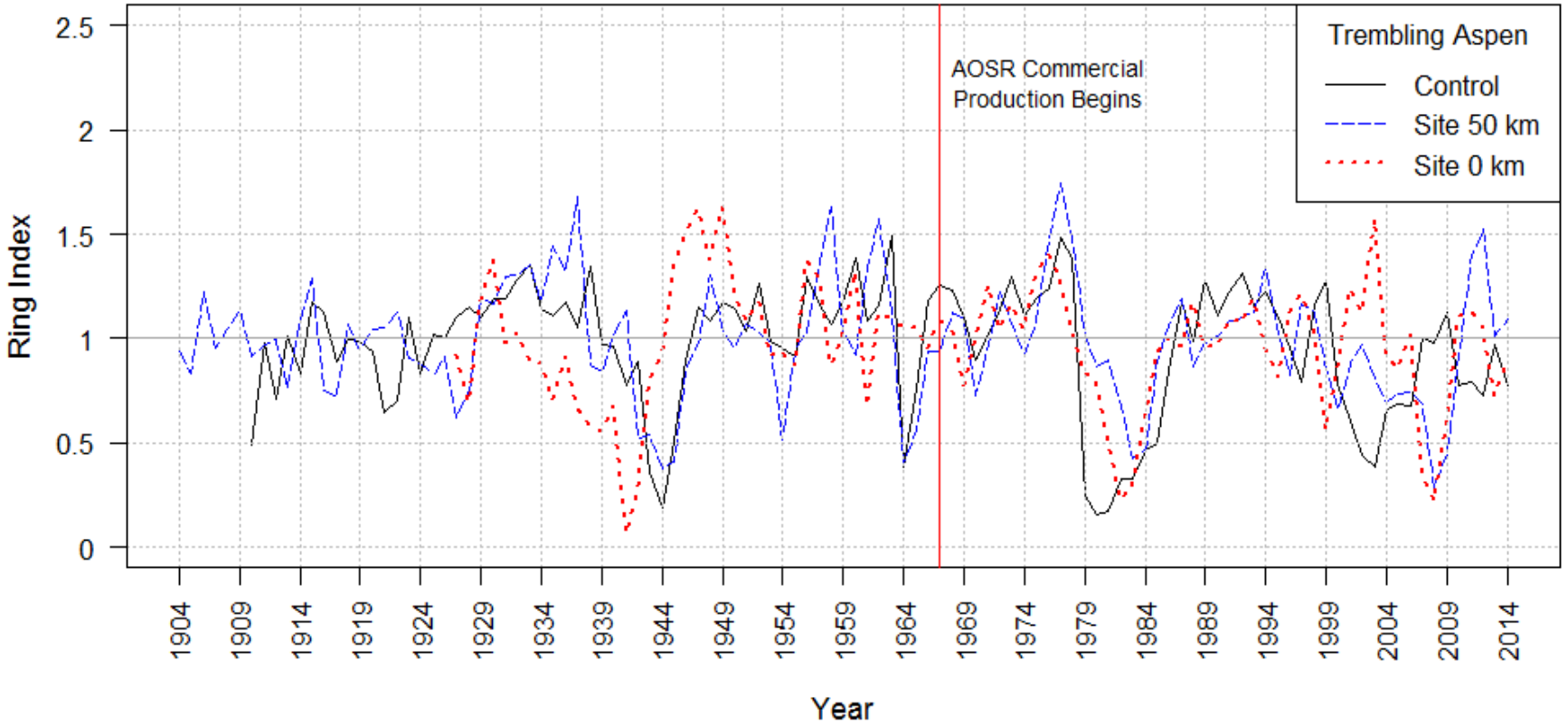

Figure 3.2 Standardized radial-growths of trembling aspen downwind sites (blue slashed or red dotted line) compared to the Control site (black solid line). Ring index values below one represent below-average growth, ring index values above one represent above-average growth, and ring index values at one represent average growth.

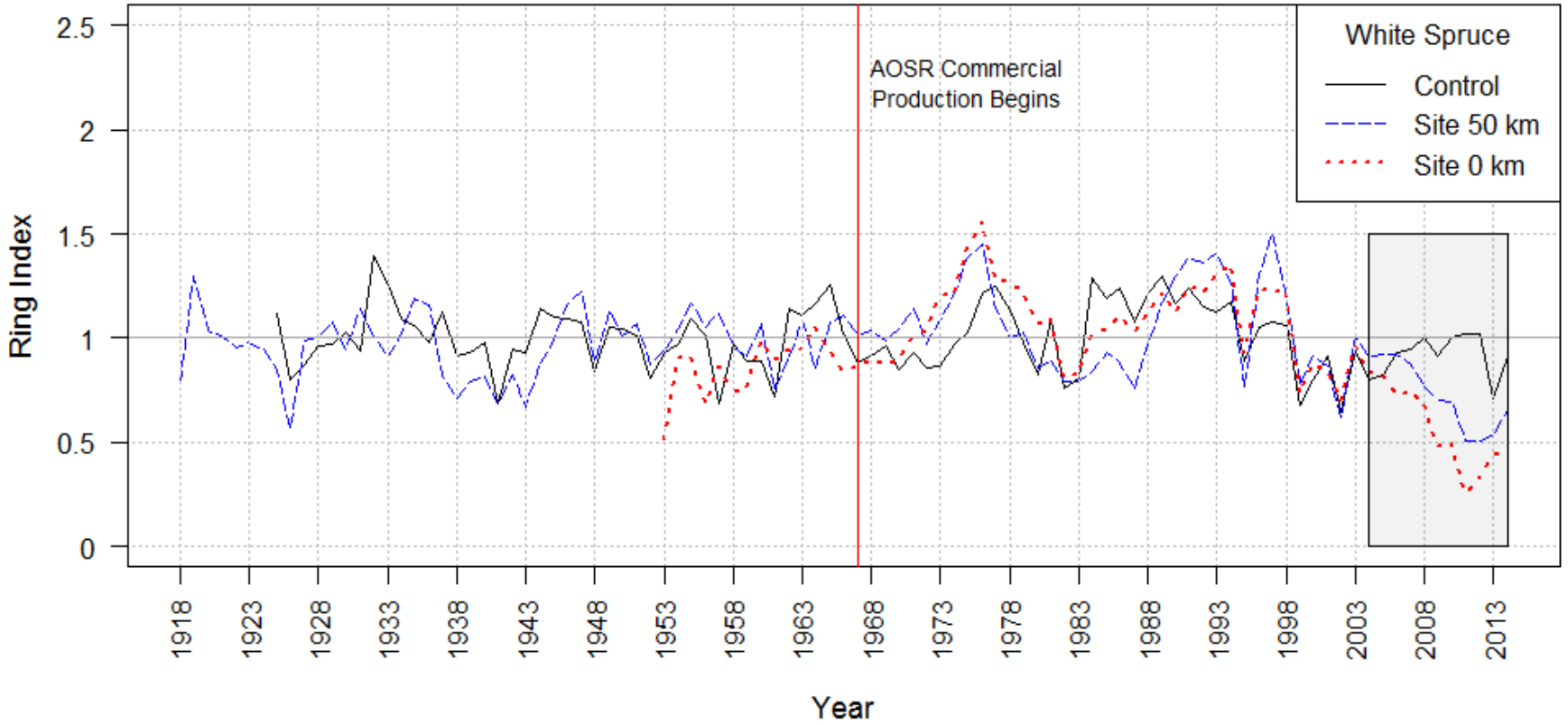

Figure 3.3 Standardized radial-growth of white spruce downwind sites (blue slashed or red dotted line) compared to the Control site (black solid line). Ring index values below one represent below-average growth, ring index values above one represent above-average growth, and ring index values at one represent average growth.

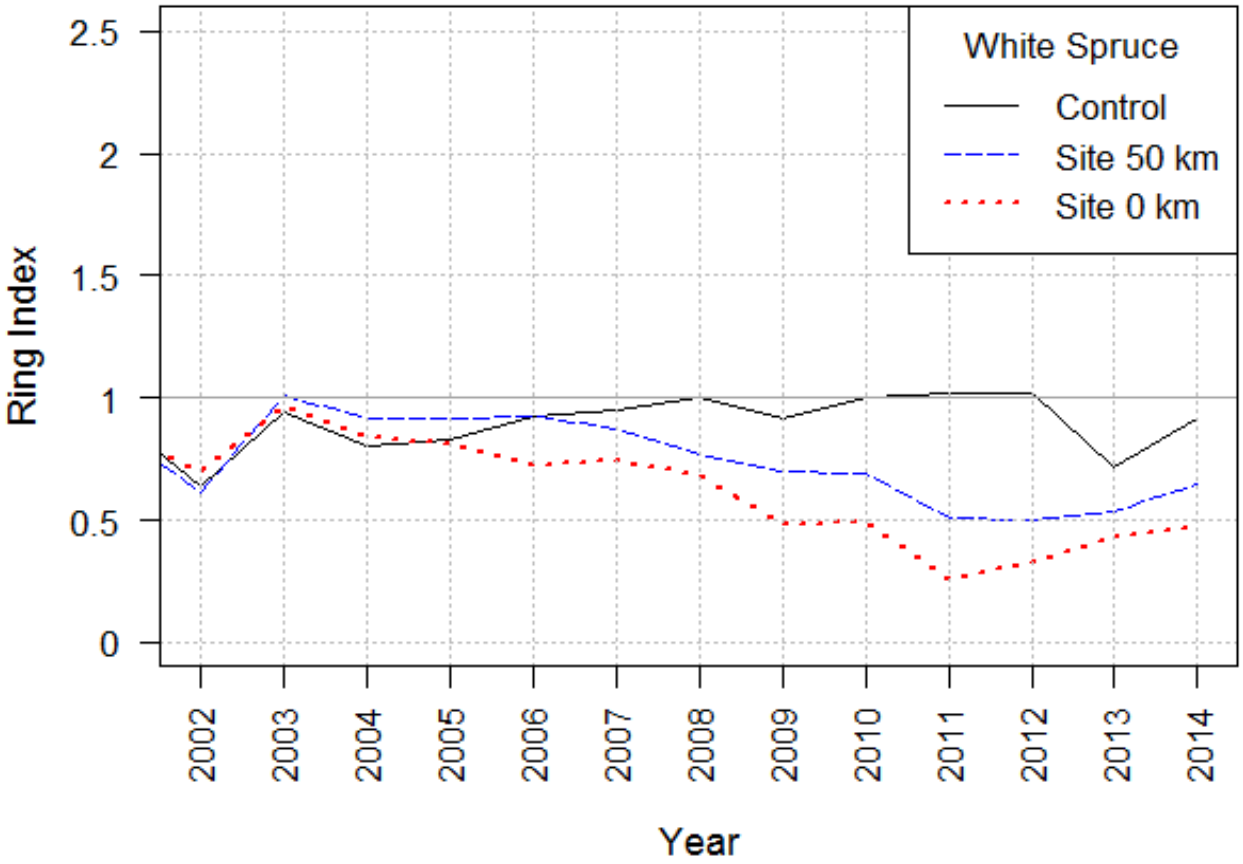

Figure 3.4 Close-up of standardized radial-growth of white spruce downwind sites (blue slashed and red dotted lines) compared to the control site (black solid line) at the last decade of growth. Ring index values below one represent below-average growth, ring index values above one represent above-average growth, and ring index values at one represent average growth.

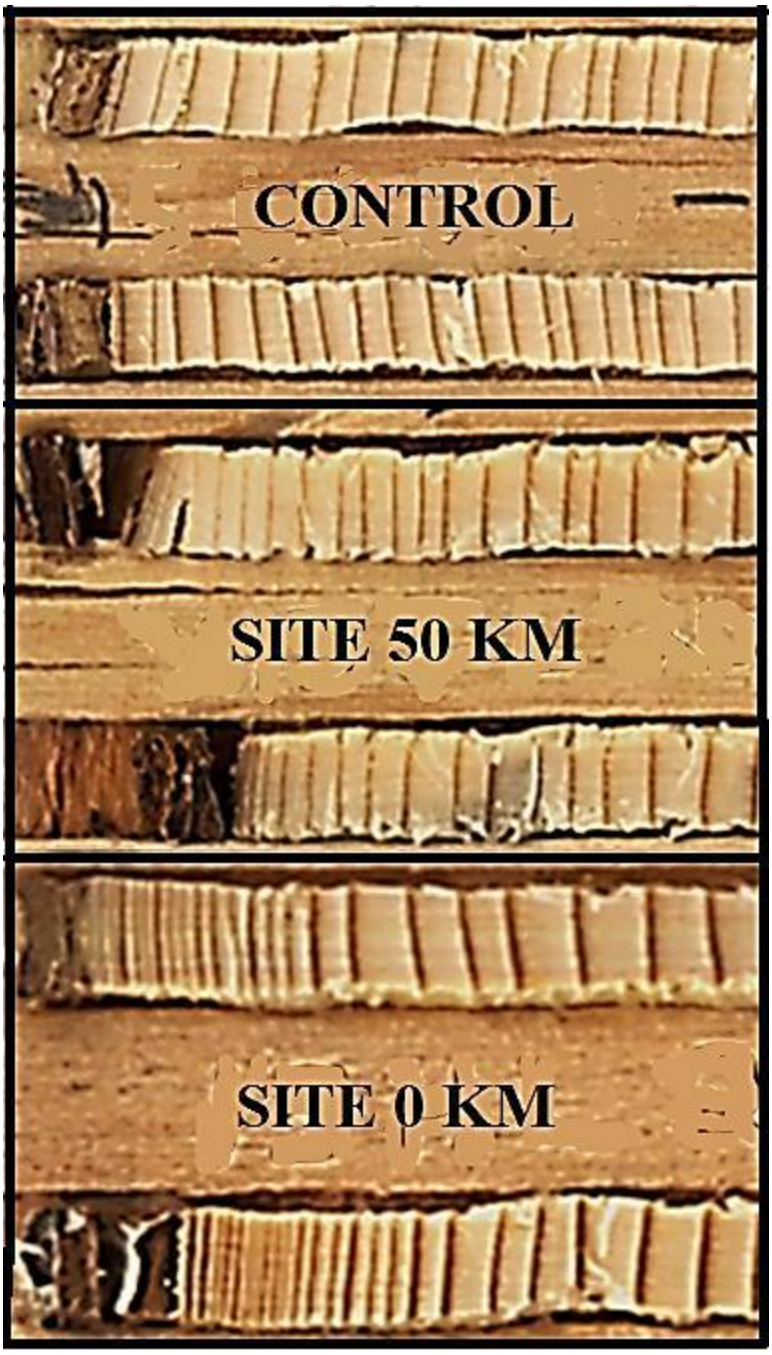

Figure 3.5 Image of three pairs of cores, of similar age, taken from each site. The top pair of cores was taken from the Control site. The middle pair of cores was taken from Site 50 km. The bottom pair of cores was taken from Site 0 km. Notice the change in ring pattern for each pair of cores near the bark (last decade of tree growth). The Site 50 km and Site 0 km ring widths are reduced compared to the Control site.

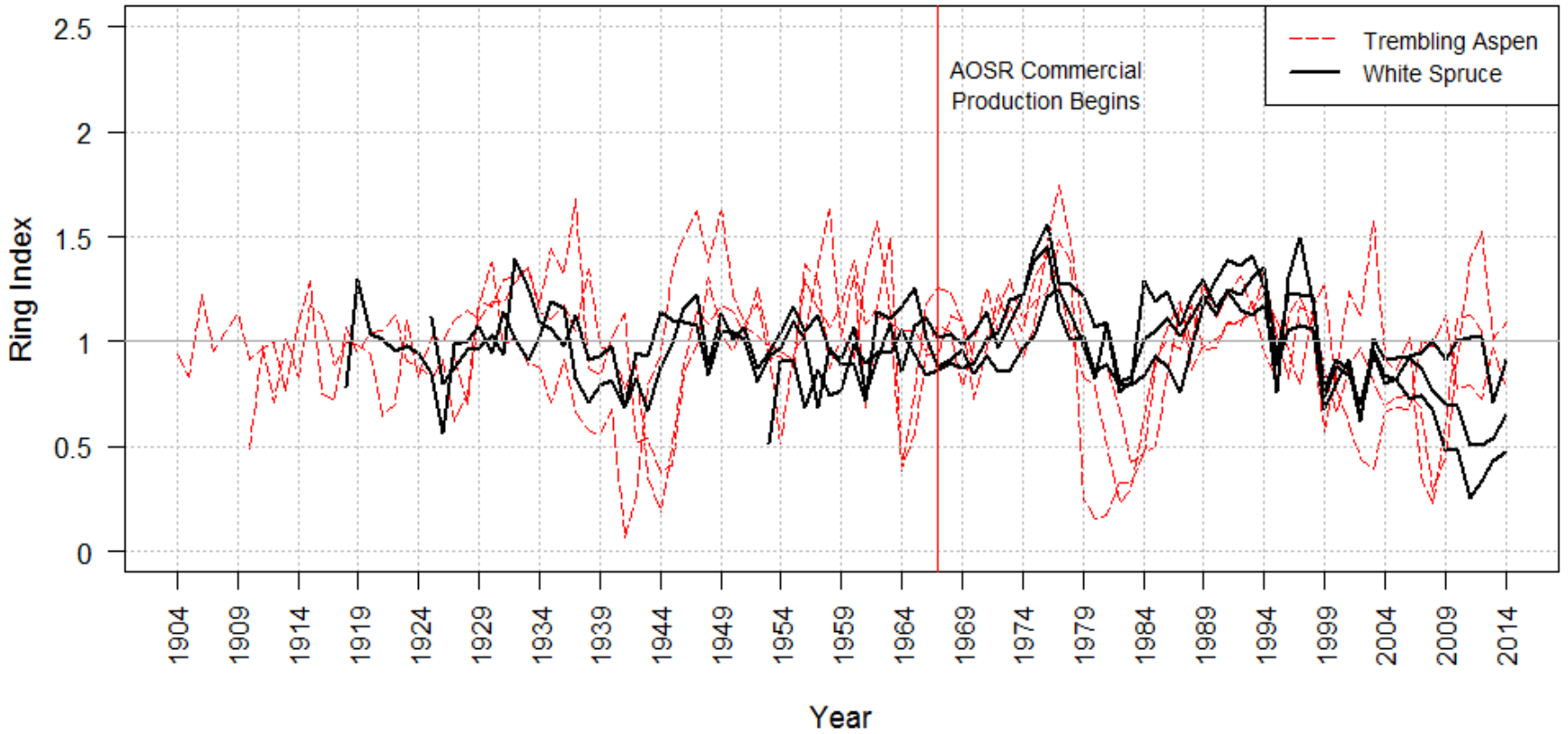

Figure 3.6 Standardized radial growth of white spruce (bolded-black solid lines) compared to trembling aspen (red slashed lines). Three trembling aspen lines and three white spruce lines represent standardized radial growths per site (Control, Site 50 km, Site 0 km). Ring index values below one represent below-average growth, ring index values above one represent above-average growth, and ring index values at one represent average growth.

The broken-stick model did not fit trembling aspen's data and was unable to detect a sensible transition point (Appendix C). Transition points were detected for Site 50 km and Site 0 km white spruce stands (Figure 3.7). A transition point was calculated to occur in 2004 for Site 50 km, and two years sooner (at year 2002) for Site 0 km. Slopes illustrated similar trends for both downwind white spruce sites. A dramatic decline occurred for the second slope, indicating a decline in radial growth between the Control and downwind site's, after a transition point. Both sites' second slope's varied in magnitude and in their endpoints. Site 0 km's second slope was steeper and ended at -1.0, whereas Site 50 km's second slope was less steep and ended at -0.6.

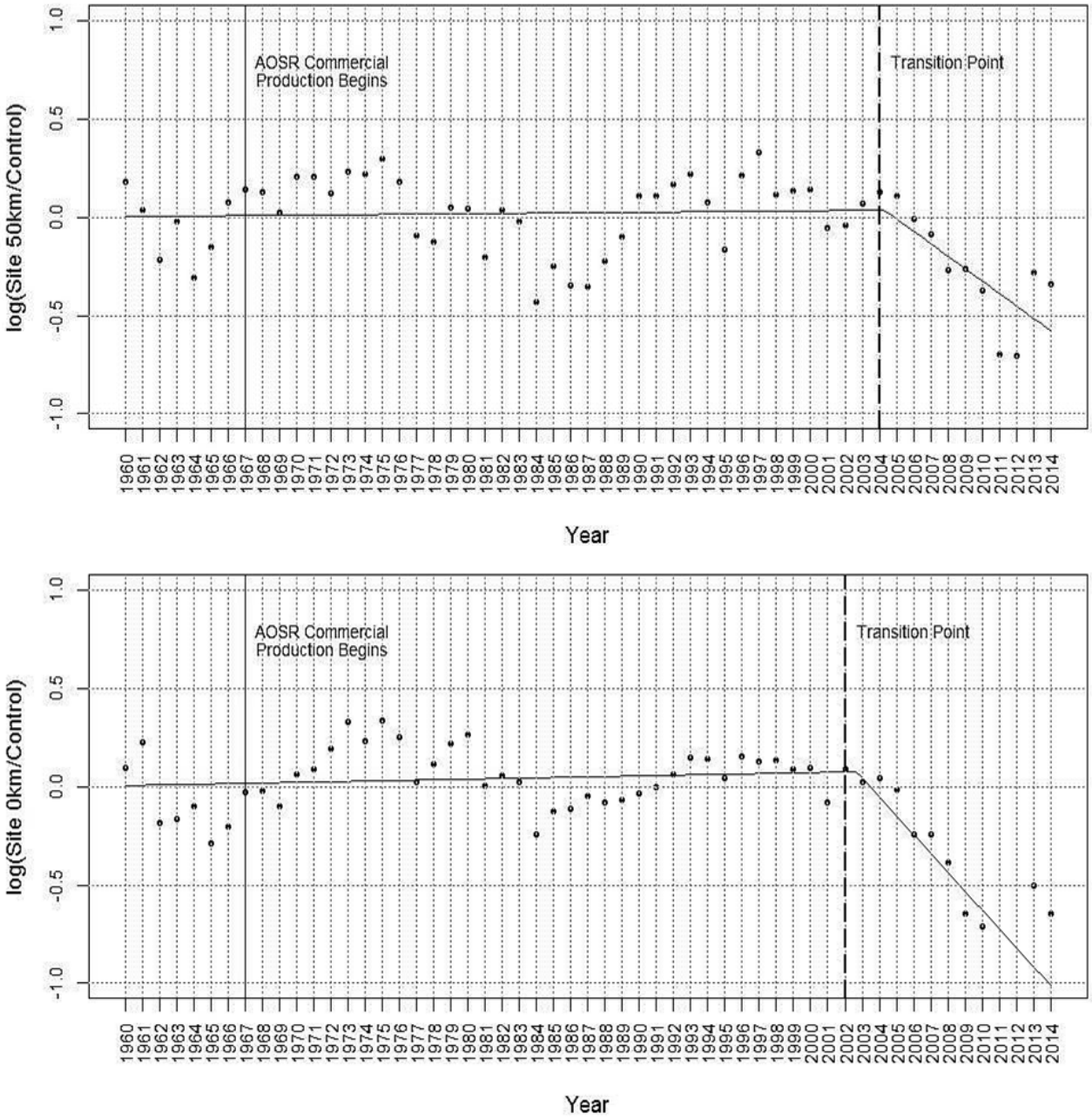

Figure 3.7 Broken-stick model results for white spruce Site 50 km and Site 0 km. The black dots represent individual change points per year. The top graph illustrates change points for white spruce at Site 50 km. The bottom graph illustrates change points for white spruce at Site 0 km. The slashed-black vertical line indicates the transition or threshold point and the beginning of the second slope.

Seventeen out of the 22 soil parameters tested portrayed p-values above 0.05 and to accept the null hypothesis (Appendix D), meaning the majority of soil parameters are similar per site and per depth increment. All bulk density values did not statistically vary per site in the 5 to 20 cm depth increment, ranging from 0.99 to 1.09 g/cm^3 (Table 3.2; Appendix D). All pH values did not statistically vary per site for each depth increment, ranging from 4 to 6 for all depth increments (Table 3.3; Appendix D). Acidity decreased with depth, for all sites. Percent organic carbon in the leaf litter, 5 to 20 cm, 20 to 45 cm, and 45 to 60 cm depth increments did not statistically vary per site (Appendix D). Carbon was statistically different in the 0 to 5 cm depth increment between Site 0 km and the Control site by approximately 6% (Table 3.4). The majority of organic carbon occurred in the leaf litter (LFH horizon), ranging from 35% to 41% mean organic carbon for all sites. The majority of sand (%), silt (%) and clay (%) fractions were similar per site and per depth increment (Table 3.5; Appendix D). Silt and sand percentages were statistically different for the 0 to 5 cm depth increment between the Control site vs. Site 0 km and Site 0 km vs. Site 50 km (Appendix D). Clay percentages were statistically different for the 0 to 5 cm depth increment and the 5 to 20 cm depth increment (Appendix D). Clay in the 0 to 5 cm depth increment, varied between the Control site and Site 0 km. Clay in the 5 to 20 cm depth increment, appeared statistically different for the Control site vs Site 0 km and the Control site vs. Site 50 km.

Table 3.2 Mean bulk density (g/cm^3) in the 5 to 20 cm depth increment per site.

Site	Average Bulk Density
	g/cm^3
Control	1.1 ± 0.2
Site 50 km	1.0 ± 0.1
Site 0 km	1.1 ± 0.03

Table 3.3 Mean pH ($CaCl_2$) per depth increment per site.

Site	Depth Increment	Mean pH
	cm	
Control	0 to 5	5.1 ± 0.7
Control	5 to 20	5.5 ± 0.9
Control	20 to 45	5.5 ± 1.1
Control	45 to 60	5.9 ± 1.1
Site 50 km	0 to 5	4.5 ± 0.4
Site 50 km	5 to 20	4.9 ± 0.1
Site 50 km	20 to 45	5.9 ± 0.9
Site 50 km	45 to 60	6.9 ± 0.6
Site 0 km	0 to 5	4.9 ± 1.0
Site 0 km	5 to 20	5.0 ± 1.0
Site 0 km	20 to 45	5.2 ± 0.5
Site 0 km	45 to 60	5.7 ± 1.0

Table 3.4 Mean (%) organic carbon per depth increment per site.

Site	Depth Increment	Average Organic Carbon
	cm	%
Control	Leaf Litter	35.4 ± 12.7
Control	0 to 5	4.3 ± 2.8
Control	5 to 20	1.2 ± 0.3
Control	20 to 45	0.9 ± 0.1
Control	45 to 60	0.8 ± 0.09
Site 50 km	Leaf Litter	41.6 ± 7.8
Site 50 km	0 to 5	1.0 ± 0.1
Site 50 km	5 to 20	0.8 ± 0.1
Site 50 km	20 to 45	0.8 ± 0.2
Site 50 km	45 to 60	0.9 ± 0.2
Site 0 km	Leaf Litter	41.7 ± 11.4
Site 0 km	0 to 5	0.9 ± 0.2
Site 0 km	5 to 20	0.7 ± 0.2
Site 0 km	20 to 45	0.6 ± 0.2
Site 0 km	45 to 60	0.8 ± 0.2

Table 3.5 Mean (%) Sand, (%) Silt, and (%) Clay per depth increment per site.

Site	Depth Increment	Mean Clay	Mean Sand	Mean Silt	Texture Class
	cm	%	%	%	
Control	0 to 5	19.0 ± 4.5	34.5 ± 12.2	46.5 ± 10.2	Loam
Control	5 to 20	25.0 ± 1.3	37.5 ± 14.4	37.5 ± 13.2	Loam
Control	20 to 45	27.6 ± 2.3	45.5 ± 3.2	26.8 ± 2.6	Sandy Clay Loam
Control	45 to 60	27.2 ± 4.0	45.7 ± 3.9	27.2 ± 0.7	Sandy Clay Loam
Site 50 km	0 to 5	9.7 ± 0.8	48.8 ± 4.9	41.5 ± 5.5	Loam
Site 50 km	5 to 20	17.3 ± 2.7	45.6 ± 8.4	37.1 ± 6.1	Loam
Site 50 km	20 to 45	26.1 ± 3.1	47.9 ± 4.3	26.1 ± 2.2	Sandy Clay Loam
Site 50 km	45 to 60	24.6 ± 0.5	47.1 ± 0.6	28.3 ± 0.6	Loam
Site 0 km	0 to 5	3.6 ± 2.0	61.7 ± 3.2	34.7 ± 1.8	Sandy Loam
Site 0 km	5 to 20	12.5 ± 7.8	51.7 ± 9.9	35.8 ± 3.8	Loam
Site 0 km	20 to 45	23.2 ± 13.0	52.8 ± 15.9	24.0 ± 3.4	Sandy Clay Loam
Site 0 km	45 to 60	27.3 ± 5.0	44.5 ± 8.8	28.2 ± 4.3	Clay Loam

3.5 Discussion

3.5.1 Radial growth of trembling aspen and white spruce surrounding the AOSR

White spruce illustrated radial-growth declines at the downwind sites (Site 50 km and Site 0 km) but not at the Control site. In white spruce, the Control site's growth matched the downwind sites' growth up until the last decade, when signatures started to show a gradual and persistent radial-growth decline in the two downwind sites. The broken-stick model detected a second slope that ended at a greater endpoint, that was more steep, and transitioned earlier at Site 0 km compared to Site 50 km, suggesting that radial-growth declines are more severe and occur earlier in sites closer in proximity to the AOSR, compared to farther away.

Radial-growth declines occur in white spruce within the proposed 50 km zone of airborne pollutant enrichment and match previously determined aerial fallout patterns (Kelly et al., 2010; Simpson et al., 2010; Proemse et al., 2012b; Proemse et al., 2013; Hodson, 2013; Bari et al., 2014; Schindler, 2014; Fenn et al., 2015; Lynam et al., 2015; Huang et al., 2016). More severe radial-growth declines occur at sites in closer proximity to AOSR facilities, which are known to exhibit greater concentrations of airborne pollutants, and less severe radial-growth declines occurred further away from AOSR facilities, where air contaminant concentrations are known to decline. Globally, radial-growth declines have occurred in other tree species surrounding industrial facilities that emit atmospheric pollution: Scots pine (*Pinus sylvestris*) illustrated

reduced ring-widths 5 to 20 km away from coal-powered electrical and steel commercial hubs attributed to nitrogen, sulfur, and dust emissions in Southern Poland (Wilczynski, 2006; Malik et al., 2012). Radial-growth declines occurred in scots pine near a mineral fertilizer plant known to emit nitrogen, sulfur, and carbon oxides, as well as fertilizer dusts in Lithuania, Europe (Juknys et al., 2003). Average radial-growth increments decreased in white pine (*Pinus strobus*) at Blue Ridge Mountains in Virginia, USA due to human-induced increases in ambient ozone (Benoit et al., 1982). Finally, pinyon pine (*Pinus monophylla)* near a copper smelter in McGill, Nevada, USA illustrated reduced tree-rings widths attributed to smelter emissions (Thompson et al., 1981).

Contrary to white spruce, trembling aspen did not illustrate radial-growth declines at any site. Trembling aspen's downwind sites' growth matched the Control site's growth, suggesting that species-different radial-growth responses exist at the downwind sites.

COFECHA statistics (MSI, MS, MTA, etc.) revealed intra-species similarities per site, implying that stand growth is similar and comparable per species. Only inter-species differences exist. White spruce portrayed greater autocorrelation variability than trembling aspen, implying that white spruce's radial growth is more dependent on its previous year's growth than trembling aspen.

3.5.2 What are the potential factors causing a decline in radial growth in white spruce?

Declines in radial growth manifest in trees due to a variety of natural causes, other than atmospheric pollution. Climate changes (droughts and floods), topographical differences, varying soil properties, insect infestations, fires, pathogens, age differences, competition between tree species, and nutrient depletion or toxicities have potential to cause radial-growth declines in white spruce.

Climate, topography, and soil were held constant per site and are unlikely factors causing a decline in radial-growth in white spruce at the downwind sites. Climate is considered the most important factor controlling forest growth, greater than soil and other disturbances (Toledo et al., 2011) and is responsible for the majority of ring-width variation illustrated at each site over time (Fritts, 1976). Each site was located within a 200 km radius of one another, meaning climate conditions remained constant. Kershaw (2013) found that precipitation over the summer months (June – August) controlled some ring-width variation in white spruce trees situated in similar locations as this study's sites. Precipitation has decreased since approximately year 2000

potentially explaining part of the decline in ring-width in white spruce over the past decade (Appendix E). White spruce tree rings may be impacted by precipitation decreases more than trembling aspen due to their more shallow root systems (Government of British Columbia, Forest Practices Branch, 2008). All sites were chosen on well-drained upland areas, without inclines, and without standing water, suggesting that topography and resulting water movement/percolation to tree roots is similar per site. Soil pit descriptions and tests revealed some texture and organic carbon differences in some topsoil layers (0 to 5 cm and 5 to 20 cm depth increments) between sites, potentially altering water/pollutant uptake into white spruce roots located at the top of the soil column, subsequently reducing ring-width to an extent. More importantly, the vast majority of white spruce and trembling aspen roots occur below the topsoil, in the rooting zone, where soil properties illustrate no statistical differences between sites. In summary, there were indistinguishable differences in the majority of depth increments for texture, pH, bulk density, and organic carbon per depth increment for all sites exist, suggesting that for the most part, soil properties were also held constant.

Insect infestations, fires, and pathogens are natural occurrences that can lead to radial-growth declines, but in this case there is no evidence to suggest that any of these factors played a part in this study. Insect infestations, such as spruce budworm, and fire outbreaks produce radial-growth decline patterns that manifest as sharp a drop-off in radial growth after a lag period of one to five years, with rebounding growth shortly after (Krause and Morin, 1999; Lageard et al., 2000; Parish and Antos, 2002; Drobyshev and Niklassen, 2004; Gori et al., 2014). Dissimilar to radial-growth decline patterns caused by insect infestations and fire outbreaks, white spruce trees from the downwind sites, decline gradually not sharply. Thirdly, pathogens, such as armillaria root rot, reduce the rate of radial growth leading to overall radial-growth declines, but ring-width patterns still appear to respond to climate variations (Mallett and Volney, 1999). Unlike radial-growth decline patterns caused by pathogens, white spruce stands at the downwind sites, appear to be unresponsive to variations in climate, during last decade of its life.

Age and species competition also have the ability to cause radial-growth declines in white spruce trees. Average white spruce ages were 80 and 57 years old, at Site 50 km and Site 0 km, respectively, meaning senescence is a highly unlikely factor contributing to the decline in radial growth seen in white spruce at the downwind sites, especially at Site 0 km where trees were the youngest overall. Competition between tree species, especially in dense forest stands,

reduces the availability of nutrients and water to competitors, ultimately impacting radial growth. Trembling aspen is the only competitor to white spruce at these study sites. All stands were well-established and evenly-aged per species, with trembling aspen remaining consistently older than white spruce, suggesting that competition factors did not change at the downwind sites, within the past decade.

Nutrient alterations may be a potential factor causing a decline in radial growth in white spruce at the downwind sites. Nutrient acquirement is essential for proper radial growth. Radial growth is hindered if nutrient deficiencies (too little) and toxicities (too much) occur (Landsberg and Gower, 1997). Nutrient contents were not assessed in this part of the study, but radial-growth declines could likely be caused by nutrient toxicities or deficiencies. Aerial fallout can alter ambient nutrient cycles by inputting pollutants into surrounding tree environments. Aerially deposited contaminants can directly enter atmospherically-exposed tree tissues, altering tissue/cellular nutrient concentrations, impacting a trees metabolic functioning and subsequent radial growth. Soil-nutrient dynamics may become compromised or imbalanced, due to aerial-pollution input beyond a soil's buffering capacity, altering nutrient-pollutant uptake through root systems (Smith, 1974). Trembling aspen roots may be less impacted by topsoil-nutrient changes because their roots are located at greater depths within the soil profile (Government of British Columbia, Forest Practices Branch, 2008). Different species of trees require unique nutrient inputs, meaning white spruce nutrient requirements may differ from trembling aspen nutrient requirements, and therefore, white spruce may be more prone to nutrient toxicities and deficiencies caused by aerial fallout than trembling aspen. Trembling aspen is known to be less sensitive to enrichment of nitrogen in soil (Hu et al., 2015).

3.5.3 Implications of research: Al-Pac and Alberta's oil sand reclamation

This study suggests that trembling aspen does not alter its radial growth downwind from AOSR facilities when compared to the Control site upwind, but white spruce does. Alberta's oil industry is required to reclaim land impacted by oil sands activities (Audet et al., 2015). White spruce is an essential resource and is commonly utilized by Al-Pac, so any decline in radial growth in white spruce would reduce Al-Pac's available selection of merchantable timber (Alberta-Pacific Forest Industries Inc., 2016). The projected expansion of Alberta's oil sand industry may adversely impact the growth of a greater portion of white spruce located downwind from Alberta's oil sand facilities, which could mean a substantial loss of resources for this

company. Long-term, oil sand operations could even potentially reduce the value of downwind FMA areas, due to the potential to deliver vast amounts of bio-available nutrients into downwind forests.

3.6 Conclusions

Results illustrated a decline in radial growth occurring in white spruce stands downwind from AOSR facilities. The broken-stick model determined that radial-growth declines in white spruce at Site 0 km are more severe and are occurring earlier than Site 50 km. Radial-growth declines occur within the proposed 50 km zone of air pollution enrichment and match previously determined aerial deposition patterns within the region. Contrary to white spruce, the radial growth of trembling aspen did not differ per site. Trembling aspen appears to be responding to its environment differently than white spruce. The soil assessment determined that soil properties (pH, bulk density, texture, and organic carbon content) were relatively similar per depth increment per site. COFECHA statistics determined that tree growth is similar and comparable amongst species per site but differ between the two species.

Other factors that could potentially cause declines in radial growth, other than air pollution, were discussed in this paper and include climate differences, topographical differences, varying soil properties, insect infestations, fire outbreaks, pathogens, age, competition between tree species, and nutrient depletion or toxicities. Of those factors, nutrient depletion or toxicity was the most probable factor potentially causing a decline in radial growth in white spruce at the two downwind sites. Recent precipitation declines may have also attributed to the observed ring-width declines over the past decade, or perhaps may have stressed the tree so that any toxicity issues were amplified. Future studies should perform a chemical or nutrient analysis of surrounding trembling aspen and white spruce stands to better understand the radial-growth declines occurring in white spruce downwind of the AOSR.

3. 7 References

Alberta-Pacific Forest Industries Inc. 2016. Corporate Social Responsibility Report 2007-2009 [Online]. Available at https://alpac.ca/application/files/8914/1876/0229/CSR_Report_2007-2009.pdf (accessed June 2016).

Audet, P., B.D. Pinno, and E. Thiffault. 2015. Reclamation of boreal forest after oil sands mining: anticipating novel challenges in novel environments. Can. J. For. Res. 45: 364-371.

Aznar, J., M. Richer-Lafleche, C. Begin, and Y. Begin. 2009. Lead exclusion and copper translocation in black spruce needles. Water Air Soil Pollt. 203: 139-145.

Baldock, J. A. and J.O. Skjemstad. 1999. *Soil organic carbon/soil organic matter.* p. 159-170. *In* K. I. Peverill, L. A. Sparrow, and D. J. Reuter (eds.) Soil Analysis: an Interpretation Manual. CSIRO Publishing, Collingwood, ON.

Bari, M., W. Kindzierski, and S. Cho. 2014. A wintertime investigation of atmospheric deposition of metals and polycyclic aromatic hydrocarbons in the Athabasca Oils Sands Region, Canada. Sci. Tot. Environ. 485-486: 180-192.

Benoit, L.F., J.M. Skelly, L.D. Moore, and L.S. Dochinger. 1982. Radial growth reductions of *Pinus strobus* L. correlated with foliar ozone sensitivity as an indicator of ozone-induced loss in eastern forests. Can. J. For. Res. 12: 673-678.

Canadian Association of Petroleum Producers. 2015. *Canadian Oil and Natural Gas* [Online]. Available at http://www.capp.ca/canadian-oil-and-natural-gas/oil (accessed April 2015).

Cheng, Z., B. Buckley, B. Katz, W. Wright, R. Bailey, K. Smith, J. Li, A. Curtis, and A. van Green. 2007. Arsenic in tree rings at a highly contaminated site. Sci. Tot Environ. 376: 324-334.

Chiu, G. S., R. Lockhart, and R. Routledge. 2006. Bent-cable regression theory and applications. J. Am. Stat. Assoc. 101:542-553.

Cook, E.R. 1985. A time series analysis approach to tree ring standardization. Ph.D. Dissertation, University of Arizona, Tucson.

Dinno, A. 2016. Dunn's Test of Multiple Comparisons Using Rank Sums. [Online].Available at https://cran.r-project.org/web/packages/dunn.test/dunn.test.pdf (accessed September 2016).

Dunn, O. J. 1961. Multiple comparisons among means. J. Am. Stat. Assoc. 56: 52–64.

Drobyshev, I., and M. Niklasson. 2004. Linking tree rings, summer aridity, and regional fire data: an example from the boreal forest of Komi Republic, East European Russia. Can. J. For. Res. 34: 2327-2339.

Ellert, B.H., H. Janzen, A.J. VanderBygaart, and E. Bremmer. 2008. *Chapter 3. Measuring Change in Soil Organic Carbon Storage*. p. 25-38. *In* M.R. Carter and E.G. Gregorich (eds.) Soil Sampling and Methods of Analysis. Second Edition. Tayler and Francis Group, Boca Raton, FL.

EsriCanadaEd. 2001. Provinces and Territories of Canada. Available at ArcGIS.

Fenn, M.E., A. Bytnerowicz, S.L. Schilling, and C.S. Ross. 2015. Atmospheric deposition of nitrogen, sulfur and base cation sin jack pine stands in the Athabasca Oil Sands Region, Alberta, Canada. Environ. Pollut. 196: 497-510.

Fox, C.A., W.B. Kincaird, T.H. Nash, D.L., and H.C. Fritts. 1986. Tree-ring variation in western larch (*Larix occidentalis)* exposed to sulfur dioxide emissions. Can. J. For. Res. 16: 283-292.

Fritts, H.C. 1976. Tree rings and climate. 567 pp. Academic Press, New York.

Gori, Y., F. Camin, N.L. Porta, M. Carrer, and A. Battisti. 2014. Tree rings and stable isotopes reveal the tree-history prior to insect defoliation on Norway spruce (*Picea abies* (L.) Karst.). For. Ecol. Manage. 319: 99-106.

Gosselin, P., S. Hrudey, A. Naeth, A. Plourde, R. Therrien, G. Van Der Kraak, and Z. Xu. 2010. *Environmental and health impacts of Canada's oil industry*. The Royal Society of Canada. Ottawa, Ontario.

Government of Alberta. 2015. Oil sands [Online]. Available at http://www.energy.alberta.ca/OurBusiness/oilsands.asp.asp (accessed April 2016)

Government of Alberta, Alberta Environment and Parks. 2015. Shapefiles for Oil Sands Project Boundaries and Points: 1985 to 2013 [Online]. Available at http://osip.alberta.ca/library/Browser#SearchByKeyword=shapefile&Location=ATHAB&Location=AB&Page=3&Sort=Title (accessed June 2016).

Government of British Columbia, Forest Practices Branch. 2008. Tree Species Compendium [Online]. Available at https://www.for.gov.bc.ca/hfp/silviculture/compendium/index.htm (accessed June 2016)

Government of Canada, Agriculture and Agri-Food Canada. 2016. Ecozones of Canada. Available at ArcGIS.

Grissino-Mayer, H.D. 2001. Evaluating crossdating accuracy: A manual and tutorial for the computer program COFECHA. Tree-ring Res. 57: 205-221.

Gueguen, C., O. Clarisse, A. Perroud, and A. McDonald. 2011. Chemical speciation and partitionaing of trace metals (Cd, Co, Cu, Ni, Pb) in the lower Athabsaca river and its tributaries (Alberta, Canada). J. Envrion. Monitor. 13: 2865-2872.

Hazewinkel, R., A. Wolfe, S. Pla, C. Curtis, and K. Hadley. 2008. Have atmospheric emissions from the Athabasca oil sands impacted lakes in northestern Alberta*?* Can. J. Fish. Aquat. Sci. 65: 1554-1567.

Helmisaari, H-S., J. Derome, H. Fritze, T. Nieminem, K. Palmgren, M. Salemaa, and I. Vanha-majamaa. 1995. Copper in Scots pine forests around a heavy-metal smelter in south-western Finland. Water Air Soil Pollut. 85: 1727-1732.

Hendershot, W. H., H. Lalande, and M. Duquette. 2008. *Chapter 16. Soil Reaction and Exchangeable Acidity*. p. 173-178. *In* M. R. Carter and E. G. Gregorich (ed.) Soil Sampling and Methods of Analysis. Second Edition. CRC Press, Boca Raton FL.

Hodson, P.V. 2013. History of environmental contamination by oil sands extraction. Proc. Natl. Acad. Sci. 110: 1569-1570.

Hojdova, M., T. Navratil, J. Rohovec, K. Zak, A. Vanek, V. Chrastny, R. Bace, and M. Svoboda. 2011. Changes in mercury deposition in mining and smelting region as recorded in tree rings. Water Air Soil Pollut. 216: 73-82.

Hollander, M. and D. A. Wolfe. 1973.Nonparametric Statistical Methods. p. 115–120. John Wiley & Sons, New York.

Holms, R.L. 1983. Computer-assisted quality control in tree-ring dating and measurement. Tree-ring Bull. 43: 69-78.

Hsu, Y., T. Harner, H. Li, and P. Fellin. 2015. PAH measurements in air in the Athabasca oil sand region. Environ. Sci. Tech: A-I.

Hu, Y., K. Jung, D. Zeng, and S. Chang. 2013. Nitrogen-and-sulphur-deposition-altered soil microbial community functions and enzyme activities in a boreal mixedwood forest in western Canada. Can. J. For. Res. 43: 777-784.

Hu, Y-L. Y. Hu, D-H. Zeng, X. Tan, and S.X. Chang. 2015. Exponential fertilization and plant competition effects on the growth and N nutrition of trembling aspen and white spruce seedlings. Can. J. For. Res. 45: 78-86.

Huang, R., K.N. McPhedran, L. Yang, and M.G. El-Din. 2016. Characterization and distribution of metal and nonmetal elements in the Alberta oil sands region of Canada. Chemosphere 147: 218-229.

Indorante, S.J., L.R. Follmer, R,.D Hammer, and P.G. Koeing. 1990. Particle-size analysis by a modified pipette procedure. Soil Sci. Soc. Am. J. 54: 560-563.

Juknys, R., J. Vencloviene, V. Stravinskiene, A. Augustaitis, and E. Bartkevicius. 2003. Scots pine (Pinus sylvestris L.) growth and condition in a polluted environment: from decline to recovery. Environ. Pollut. 125: 205-212.

Jung, K., W-J. Choi, S.X. Chang, and M.A. Arshad. 2013a. Soil and tree ring chemistry of *Pinus banksiana* and *Populus tremuloides* stands as indicators of changes in atmospheric environments in the oil sands region of Alberta, Canada. Ecol. Indic. 25: 256-265.

Jung, K., S. Chang, Y. Sik Ok, and M. Arshad. 2013b. Critical loads and H^+ budgets of forest soils affected by air pollution from oil sands mining in Alberta, Canada. Atmos. Environ. 69: 56-64.

Kelly, E., D. Schindler, P. Hodson, J. Short, R. Radmanovich, and C. Nielson. 2010. Oil sands development contributes elements toxic at low concentrations to the Athabasca River and its tributaries. Proc. Natl. Acad. Sci. 107: 16178-16183.

Krause, C. and H. Morin. 1999. Tree-ring patterns in stems and root systems of black spruce (*Picea mariana*) caused by spruce budworms. Can. J. For. Res. 29: 1583-1591.

Kruskal, W. H. and A.Wallis. 1952. Use of ranks in one-criterion variance analysis. J. Am. Stat. Assoc. 47: 583–621.

Kurczynska, E., W. Dmuchowski, W. Wloch, and A. Bytnerowicz. 1997. The influence of air pollutants on needles and stems of scots pine (*Pinus sylvestris L.*) trees. Environ. Pollut. 98: 325-334.

Lageard, J.G.A., P.A Thomas, and F.M. Chambers. 2000. Using fire scars and growth release in subfossil Scots pine to reconstruct prehistoric fires. Palaeogeogr. Palaeoclimatol. Palaeoecol. 164: 87-99.

Lageard, J., J. Howell, J. Rothwell, and I. Drew. 2008. The utility of *Pinus sylvestris* L. in dendrochemical investigations: pollution impact of lead mining and smelting in Darley Dale, Derbyshire, UK. Environ. Pollut. 153: 284-294.

Landsberg, J.J., and S.T. Gower. 1997. *Chapter 7. Nutrient Cycling and Distribution*. p. 187-188. *In* Applications of Physiological Ecology to Forest Management.Academic Press, Inc. San Diego, California.

Laxton, D., S. Watmough, and J. Aherne. 2012. Nitrogen cycling in *Pinus banksiana* and *Populous tremuloides* stands in the Athabasca oil sands region, Alberta, Canada. Water Air Soil Pollut. 223: 1-13.

Liggio, J., S-M. Li, K. Hayden, Y. M. Taha, C. Stroud, A. Darlington, B.D. Drollette, M. Gordon, P. Lee, P. Liu, A. Leithead, S.G. Moussa, D. Wang, J. O'Brien, R.L. Mittermeier, J. R. Brook, G. Lu, R. M. Staebler, Y. Han, T. W. Tokarek, H. D. Osthoff, P. A. Makar, J. Zhang, D. L. Plata, and D. R. Gentner. 2016. Oil sands operations as a large source of secondary organic aerosols. Nature 534: 9-94.

Lynam, M.M., J.T. Dvonch, J.A. Barres, M. Morishita, A. Legge, and K. Percy. 2015. Oil sands development and its impact on atmospheric wet deposition of air pollutants to the Athabasca Oil Sands Region, Alberta, Canada. Environ. Pollut. 206: 469-478.

Malik, I., M. Danek, E. Marchwinska- Wyrwal, T. Danek, M. Wistuba, and M. Krapiec. 2012. Scots Pine (*Pinus sylvestris L*.) Growth suppression and adverse effects on human health due to air pollution in the upper silesian industrial district (USID), Southern Poland. Water Air & Soil Pollut. 223: 3345-3364.

Mallett, K.I., and W.J.A. Volney. 1999. The effect of Armillaria root disease on lodgepole pine tree growth. Can. J. For. Res. 29: 252-259.

MapCruzin. 2016. Download Free Canada Alberta ArcGIS GIS Shapefile Map Layers: Location GIS Shapefile [Online]. Available at http://www.mapcruzin.com/free-canada-alberta-arcgis-maps-shapefiles.htm (accessed June 2016).

McGee., V.E and W.L. Carleton. 1970. Piecewise Regression. J. Am. Statist. Assoc. 65: 1109-1124.

Oleksyn, J., K. Oleksynowa, E. Kozlowska, and L. Rachwal. 1987. Mineral content and sensitivity of black pine (*Pinus nigra*) of various provenances to industrial air pollution. For. Ecol. Manage. 21: 237-247.

Parish, R. and J.A. Antos. 2002. Dynamics of an old-growth, fire-initiated, subalpine forest in southern interior British Columbia: tree-ring reconstruction of 2 year cycle spruce budworm outbreaks. Can. J. For. Res. 32: 1947-1960.

Proemse, B., B. Mayer, J. Chow, and J. Watson. 2012a. Isotopic characterization of nitrate, ammonium and sulfate in stack $PM_{2.5}$ emissions in the Athabasca Oil Sands Region, Alberta, Canada. Environ. Pollut. 182: 80-91.

Proemse, B., B. Mayer, and M. Fenn. 2012b. Tracing industrial sulfur contributions to atmospheric sulfate deposition in the Athabasca oil sands region, Alberta, Canada. Appl. Geochem. 27: 2425-2434.

Proemse, B., B. Mayer, M. Fenn, and C. Ross. 2013. A multi-isotope approach for estimating industrial contributions to atmospheric nitrogen deposition in the Athabasca oil sands region in Alberta, Canada. Atmos. Environ. 60: 555-563.

R Core Team and contributors worldwide. 2016. *The R Stats Package*. kruskal.test. [Online]. Available at https://stat.ethz.ch/R-manual/R-devel/library/stats/html/00Index.html (accessed September 2016).

Roberts, T. 1984. Effects of air pollution on agriculture and forestry. Atmos. Environ. 18: 629-652.

Rooney, R., S. Bayley, and D. Schindler. 2011. Oil sands mining and reclamation cause massive loss of peatland and stored carbon. Proc. Natl. Acad. Sci. 109: 4933-4937.

Schindler, D. 2010. Tar sands needs solid science. Nature 468: 499-501.

Schindler, D.W. 2014. Unravelling the complexity of pollution by the oil sands industry. Proc. Natl. Acad. Sci. 111: 3209-3210.

Simpson, I., N. Blake, B. Barletta, D. Diskin, H. Fuelberg, K. Gorham, L. Huey, S. Meinardi, F. Rowland, S. Vay, A. Weinheimer, M. Yang, and D. Blake. 2010. Characterization of trace gases measured over Alberta oil sands mining operations: 76 speciated $C_2 – C_{10}$ volatile organic compounds (VOCs), CO_2, CH_4, CO, NO, NO_2, NO_Y, and SO_2. Atmos. Chem. Phys. 10: 11931-11954.

Sheppard, S.C. and J.A. Addison. 2008. Chapter 4. Soil Sample Handling and Storage. p. 39-50. *In* M.R. Carter and E.G. Gregorich (eds.) Soil Sampling and Methods of Analysis. Second Edition. Tayler and Francis Group, Boca Raton, Florida.

Shparyk, P., and V. Parpan. 2004. Heavy metal pollution and forest health in the Ukrainian Carpathians. Environ. Pollut. 130: 55-63.

Siwik, E., L. Campbell, and G. Mierle. 2010. Distributions and trends of mercury in deciduous tree cores. Environ. Pollut. 158: 2067-2073.

Smith, W. 1974. Air pollution- effects on the structure and function of the temperate forest ecosystem. Environ. Pollut. 6: 111-129.

Soil Classification Working Group. 1998. The Canadian System of Soil Classification, p. 187. Third Edition. Agriculture and Agri-Food Canada Publication.

Sonderegger, D. 2015. SiZer: Significant Zero Crossings [Online]. Available at http://www.r-project.org (accessed April 2016).

Speer, J. H. 2010. *Fundamentals of tree-ring research*. 368 pp. University of Arizona Press, Tucson.

Testa, M. Bridget. 2008. Tar on Tap. Mech. Eng. 12: 30-34.

Thompson, M.A. 1981. Tree rings and air pollution: a case study of Pinus monophylla growing in east-central Nevada. Environ. Pollut. 26: 251-266.

Toledo, M., L. Poorter, M. Pena-Claros, A. Alarcon, J. Balcazar, C. Leano, J. C. Licona, O. Llanque, P. Zuidema, and F. Bongers. 2011.Climate is a stronger driver of tree and forest growth rates than soil and disturbance. J. Ecol. 99: 254-264.

Toms, J. D., and M. L. Lesperance. 2003. Piecewise regression: a tool for identifying ecological thresholds. Ecology 84:2034-2041.

VoorTech Consulting. 2004. MeasureJ2X. VoorTech Consulting, Holderness, N.H.

Wang, Z.L., and G.F. Naterer. 2010. Greenhouse gas reduction in oil sands upgrading and extraction operations with thermochemical hydrogen production. Int. J. Hydrogen Energy 35: 11816-11828.

Watmough, S., and T. Hutchinson. 2003. A comparison of temporal patterns in trace metal concentration in tree rings of four common European tree species adjacent to a Cu-Cd refinery. Water Air Soil Pollut. 146: 225-241.

Wieder, K., D. Vitt, M. Burke-Scoll, K. Scott, M. House, and M. Vile. 2010. Nitrogen and sulphur deposition and the growth of *sphagnum fuscum* in bogs of the Athabasca oil sands region, Alberta. J. Limnol. 69: 161-170.

Wilczynski, S. 2006. The variation of tree-ring widths of Scots pine (*Pinus sylvestris L.*) affected by air pollution. Eur. J. For. Res. 125: 213-21

4. AN ELEMENTAL ASSESSMENT OF TREMBLING ASPEN (*POPULUS TREMULOIDES*) AND WHITE SPRUCE (*PICEA GLAUCA*) SURROUNDING THE ATHABASCA OIL SANDS REGION IN ALBERTA, CANADA

4.1 Abstract

The Athabasca Oil Sands Region (AOSR) in Alberta, Canada, is a renowned source of air pollution. Air pollutants are emitted into the atmosphere through various oil sands upgrading operations and mining activities. These pollutants get transported distances beyond AOSR production boundaries through prevailing winds within the region and are deposited onto the surrounding ecosystem components, a phenomenon identified as aerial fallout. In this study, the elemental composition of trembling aspen (*Populus tremuloides*) and white spruce (*Picea glauca*) tree components, inclusive to branches, leaves, stem wood, stem bark, and three layers of mature root, were assessed through X-Ray Fluorescence (XRF) using a synchrotron beamline at the Canadian Light Source. Three study sites were selected at varying distances away from AOSR facilities; an upwind Control site and two downwind sites. All tree and soil media at the downwind sites were compared to tree and soil media at the upwind Control site to determine if aerial fallout was causing elemental enrichment or alteration. Eight elements: Potassium (K), Calcium (Ca), Titanium (Ti), Zinc (Zn), Nickel (Ni), Manganese (Mn), Chromium (Cr), and Iron (Fe) were identified in all tree and soil media. Of these elements, Mn was consistently elevated in the majority of trembling aspen and white spruce tree media and topsoil at the downwind sites compared to the Control site. Other elements were sometimes elevated at the downwind sites compared to the Control site, but they did not illustrate any distinct trend, as seen for Mn. X-ray Absorption Near Edge Structure (XANES) spectroscopy of K-edge Mn was performed on white spruce tree media at one downwind site which revealed the speciation of Mn. Aqueous and organic Mn (II) was identified within all white spruce tree media (roots, stem wood, stem bark, leaves), whereas Mn (III/IV)-oxide was identified in the leaf litter. Manganese is toxic to trees and plants in excess and may be causing a decline in radial growth in white spruce trees downwind from the AOSR. Trembling aspen appears to be more tolerant Mn input by aerial deposition.

4.2 Introduction

The Athabasca oil sands region (AOSR) in Alberta, Canada is a globally renowned source of air pollution. Airborne pollutant release from the AOSR has been grossly underestimated in the past (Liggio et al., 2016). The impact and extent of air pollution released from the AOSR on circumambient ecosystems is in the midst of being uncovered, and is a meaningful and relevant issue to citizens and scientists alike (Schindler, 2010). Assessing airborne pollutant releases from Alberta's oil sand facilities is complex, since a diverse suite of contaminants are emitted annually from oil sands operating and processing events, including volatile organic compounds (VOC)'s, polycyclic aromatic hydrocarbons (PAH)'s, metals, ozone, and carbon, nitrogen, and sulfur compounds (Gosselin et al., 2010; Simpson et al., 2010, Schindler, 2010; Kelly et al., 2010; Bari et al., 2014; Lynam et al., 2015; Huang et al., 2016). Current AOSR emissions are being carried away from their source by prevailing winds within the region, and are deposited onto the surrounding ecosystems, a process termed aerial fallout (Kelly et al., 2010; Bari et al., 2014). Peak concentrations of airborne contaminants occur within a 50 km radius of Alberta's oil sand facilities (Kelly et al., 2009; Simpson et al., 2010; Proemse et al., 2012; Hodson, 2013; Proemse et al., 2013; Bari et al., 2014; Schindler, 2014; Fenn et al., 2015; Lynam et al., 2016; Huang et al., 2016). Boreal forest surrounds AOSR facilities, within the proposed 50 km radius of enrichment, making these ecosystem components potentially susceptible to airborne contamination and alteration.

Trees are essential ecosystem components that comprise the bulk of the boreal forest ecosystem. Aerial fallout, from commercial facilities, onto surrounding forests has been known to alter tree growth and their physiological processes, across the globe. Increased concentrations of heavy metals (Cu, Pb, As, Cr, Cd, Zn, Fe) and sulfur were found in the needles and/or stem wood of scots pine (*Pinus sylvestris*) nearby smelter plants in Poland, England, and Finland, resulting in decreased numbers of cambial and phloem cells in the stem wood and nutrient alterations (Helmisaari et al., 1995; Kurczynska et al., 1997; Lageard et al., 2008). Concentrations of heavy metals and sulfur in these studies decreased in scots pine farther away from the smelters. This spatial trend, of elevated aerially-deposited pollutant concentrations (heavy metals, nitrous and sulfuric gases, and ozone) in tree components in closer proximity to smelters and industrial regions, was found in other tree species including spruce (*Picea mariana*; *Picea alba*; *Picea abies*), beech (*Fagus sylvatica*), oak (*Quercus robar*; *Quercus stellata*),

sycamore (*Acer pseudoplatonus*), lime (*Tilia europaea*), poplar (*Populus deltoids*) and willow (*Salix spp.*) in central Czech Republic, Ukraine, Canada, New England, and the United States of America (Watmough and Hutchinson, 2003; Shparyk and Parpan, 2004; Cheng et al., 2007; Aznar et al., 2009; Siwik et al., 2010; Hojdova et al., 2011). Fluxes of Pb and Cd concentrations in tree rings of beech and oak temporally matched emission rates from nearby industrial facilities in the Czech Republic, England, and United States of America (Watmough and Hutchinson, 2003; Cheng et al., 2007; Hojdova et al., 2011). The impacts of aerial deposition on forests vary but can range from no apparent impacts to suppressed growth and physiological functioning (photosynthesis and respiration), reduced reproduction (seeds, flowers, etc.), increased morbidity, acute morbidity, and acute mortality (Smith, 1974; Roberts, 1984; Oleksyn et al., 1987). In the AOSR, endemic tree species have been used as mediums to describe air-pollutant depositional patterns (Laxton et al., 2012; Jung et al., 2013; Savard et al., 2014), but the actual impact of Alberta's air pollution on surrounding forest growth has only been assessed by Kershaw (2013) and in Chapter three. Both studies conducted dendrochronological assessments and discovered a decline in radial growth occurring in white spruce trees, surrounding the AOSR, with both attributing the decline to likely air pollution. Chapter three determined that this decline in radial growth did not occur in trembling aspen trees located at similar locations. To better understand white spruce radial-growth declines, trembling aspen and white spruce trees surrounding the AOSR were assessed from a chemical perspective in this study.

Very few compounds have been assessed in tree components surrounding the AOSR, except nitrogen, sulfur, and carbon (Laxton et al., 2012; Jung et al., 2013; Savard et al., 2014). The proper growth and function of a tree is complex and is partly controlled by a combination of macro- and micronutrients. The focus of this paper is to assess white spruce and trembling aspen by observing the elemental chemistry present in their tree components. Synchrotron technology, specifically, a technique known as X-Ray Fluorescence (XRF), will be used to assess the chemical composition of various tree components; leaves, branches, roots, stem woods, stem barks, and soil, in trembling aspen and white spruce stands. XRF is a novel technique because it is able to assess a large number of elements simultaneously, in a relatively short period of time with minimal sample preparation. Previous studies have successfully used XRF on various plant and soil media (Fittschen and Falkenberg, 2011; Lombi et al., 2011; Majumdar et al., 2012), boasting its highly accurate detection capabilities and widespread use. I hypothesize that tree

chemistry will differ in trembling aspen and white spruce stands, and soils, at the downwind sites due to aerial fallout from AOSR emissions. Specific objectives of this paper are: 1) to use XRF and XANES to determine if AOSR emissions are adversely changing the elemental composition of trembling aspen and white spruce trees located downwind, 2) to determine if elemental compositions differ between tree species; and 3) to determine if soil chemistry varies in areas located downwind.

4.3 Materials and Methods

4.3.1 Site description

The elemental composition of two tree species, trembling aspen and white spruce, were examined at three study sites (Figure 3.1). A Control site was selected approximately 190 km's (56º 73' 31.7" N, 114º 59' 27.3" W) upwind from the AOSR. Two sites were selected downwind approximately 50 km (Site 50 km – 56º 64' 35.3" N, 111º 06' 56.4" W) and at the edge of the AOSR (Site 0 km – 56º 88' 42.5" N, 111º 45' 21.0" W). The two downwind sites were selected in areas suspected to receive atmospheric fallout (within the 50 km zone airborne enrichment) from the AOSR, following regional prevailing winds. The Control site was located upwind from prevailing wind patterns, away from potential atmospheric fallout, so that it represented unspoiled and baseline tree chemistry. Trembling aspen and white spruce were sampled in June of 2015. A variety of tree components, including leaves, branches, stem wood, stem bark, and roots, were extracted from three white spruce and three trembling aspen trees per site. These tree components were extracted because they may contain remnants or enrichment from aerial fallout. Soil samples were also collected to outline any major differences in soil chemistry per site, potentially impacting pollutant uptake through tree roots. Selected sites were within a 200 km radius of one another ensuring that overall climate patterns remained consistent for each site. Climate conditions, within the region, are characterized by short warm summers (four month growing season), and long cold winters, with average temperatures ranging from +14.3ºC to -12.1 ºC (Government of Canada, 2010). Average-annual precipitation is relatively low, most prevalent in the summer months, at 418.6 mm (Government of Canada, 2010).

Each site contained dominantly similar site characteristics so that stand comparisons could be made. Results in Chapter three determined that pH, bulk density, organic carbon contents, and texture (sand, silt, and clay fractions) are similar throughout their soil profiles and

that intra-species growth is similar and comparable per site (Appendix D). All sites occurred on flat well-drained upland regions without the occurrence of standing water, to prevent pollution uptake from potentially contaminated underground aquifers and because upland trees are suspected to catch aerial fallout relative to trees situated in topographically lower regions. All stands grew in Luvisolic soils with similar horizon distributions, comprised of an LFH horizon, followed by an Ae horizon above a thick Bt horizon (Soil Classification Working Group, 1998; Appendix A). No effervescence and minor to moderate mottling (in the lower depths) occurred in soils at all sites (Appendix A). A loamy texture dominated in all soil profiles per site (Appendix A). All stands were selected at a minimum of 10 m away from the forest cut lines, roads, and highways, to avoid forest-edge effects and conflicting sources of forest disturbance.

4.3.2 Field sampling

Six 12 mm cores were extracted from three trembling aspen trees and three white spruce trees using an increment borer. The 12 mm cores allowed for a larger quantity of wood and stem bark tissue to be collected for chemical analyses. The 12 mm cores were extracted alongside of a 5.15 mm core to corroborate the two samples when a ring vs distance test was performed on the 5.15 mm cores. Branches and leaves were collected from the bottom of the canopy from three white spruce trees per site using clippers and were stored in brown paper bags. A section of mature lateral root was removed, within a one meter radius from the main stem at diameters ranging from 6 to 20 cm thick, from three trembling aspen and three white spruce trees per site with a reciprocating saw and stored in brown paper bags. Cores (stem wood/stem bark), branches, leaves, and roots were transferred to the University of Saskatchewan for additional processing and analysis.

Four soil pits were dug at representative locations per site. Representative locations were areas where flat topography dominated and native vegetation occurred. Five ≈ 60 g samples were obtained from each pit per depth increment. Depth increments were identified as: 1) leaf litter, 2) 0 to 5 cm, 3) 5 to 20 cm 4) 20 to 45 cm, and 5) 45 to 60 cm. Twenty soil samples were collected per site for a total of 60 soil samples. Soil samples were stored in plastic zip-lock bags and transported to the University of Saskatchewan.

4.3.3 Sample processing and analytical techniques

All tree media, inclusive of leaves, branches, stem wood, stem barks, roots, and soils were dried before XRF occurred. Leaves, branches, and subsets of soil were oven dried for 48

hours at 40º C. Oven temperature was kept low to reduce the potential volatility of certain elements that may have been present in leaf, branch, and soil material. Dried leaf material was separated from its branch, by hand, and deposited into separate paper bags. Twelve mm cores (stem wood) and roots were air-dried for one month prior to processing.

Dried leaves, branches, stem wood, stem bark, and root material were ground into fine powders by a Retch® Ultra Centrifuge Mill ZM 200 at a rotation speed of 14,000 rpm through a 0.25 mm sieve (Appendix F). Samples were ground to ensure adequate homogenization and representation of each tree's media chemistry. Dried 12 mm cores (stem wood) were sliced into 0.5 cm increments, in order from bark to pith, before grinding took place (Appendix F). The stem bark was sliced and removed first. The 5.15 mm partner core was sanded to a polish and its annual rings were measured to establish the number of rings present in each 0.5 core segment. Dried root sections were cut in half using a band saw. Three layers of root were extracted from each half of a root using a stainless steel hand-gouger. The three gouged layers included root bark, the outer rings of the root (immediately beneath the root bark), and the inner pith of the root (Appendix F). Root layers were extracted before grinding occurred. Dried soils were ground into fine powders using a ceramic mortar and pestle.

Twenty-five mg (±0.1) of ground tree material was placed into an ICL ® stainless steel KBr die set then pressed into a pellet using a Carver ® 4350 bench top laboratory manual press, at 7 tonnes of pressure for 2 minutes, resulting in a circular pellet with a radius of 6.35 mm (Appendix F). Pellets were created so that the thickness and density of the material remained relatively consistent per tree media, per site. Densities and thicknesses were not directly measured in this study, but it is assumed that similar tree media (ground needles vs. ground needles; ground cores vs. ground cores) have relatively similar densities and thicknesses since they were prepared in a consistent manner. Soils were placed into flat Teflon ® sample holders that contained an open horizontal slit, with dimensions that remained consistent per mould (Appendix F). Each sample holder was taped-over with Kapton ® pure, metal-free tape to ensure soil material remained in place for the chemical analysis.

` The elemental composition of each sample was assessed using XRF on the IDEAS beamline at the Canadian Light Source (CLS) in Saskatoon, Saskatchewan. The IDEAS beamline was capable of assessing 18 elements in the periodic table from Argon (Ar), to Bromine (Br), simultaneously. Fluorescence counts were measured for 180 s. This beamline was

chosen because it had the ability to scan for some of the major macro- and mirco- plant nutrients essential for proper tree growth. Each sample was scanned with consistent beam and instrument dimensions/parameters; a GE 220 (DCM) monochromator crystal; a sample slit width of 1.5 mm; a maximum sample slit height of ~ 3 mm; and a Ketek peaking time of 2 µs. The Ketek fluorescence detector was set to "highest resolution/low count rate" mode and oriented at a 90º angle to the main synchrotron beam, and the sample holder was placed at a 45º angle to minimize x-ray scattering (inelastic and elastic). Instrument position and angle remained consistent per sample.

Pellets were taped onto the automated sample holder and were assessed in vacuum. Individual pellets were scanned two or three times, over different relative positions (top, middle, or bottom), to account for localized elemental dispersion per sample and to obtain average relative amounts of elements per sample. Soil sample holders were only scanned once. A dead time between 10% - 40% was required for each scan. A silicon single-photon detector chip was used to assess fluorescence counts. Each sample's dead time-corrected fluorescence counts were normalized to the beamline's incoming X-ray intensity using an equation provided in Appendix F and code written in OriginPro ® by one of the CLS's beamline scientists (Chithra Karunakaran). Not all field-collected samples were scanned in our allotted time on the beamline. Individual elements are represented as peaks of fluorescence counts over time (fluorescence counts per energy Volt per time). Fluorescence counts are arbitrary values allowing for semi-quantitative observations to be made. Qualitatively, overlying peaks, with the same width and shape, were compared in this study. Quantitatively, relative fluorescence counts values at the top of each peak, corresponding to K-edge alpha 1 values for individual elements (maximum intensity values per peak), were also compared.

X-Ray Absorption Near Edge Structure (XANES) Spectroscopy provides information about the coordination environment and oxidation state (i.e., chemical speciation) of specific elements in a sample, which dictate properties such as toxicity. A XANES scan of K-edge manganese (Mn) was performed on six white spruce pellets from Site 0 km to assess Mn speciation; leaf litter, outer root, inner root, leaf, stem bark, and one core (stem wood) samples were scanned. Individual samples were scanned for 15 min 17 s on the same beam with equipment additions. A reference material (~5 µm Mn(II) oxide metal foil), provided by the CLS, was measured in series with each sample. All samples were scanned in vacuum. Beam and

equipment dimensions/parameters were held consistent and were specified as; Ketek mode: lowest resolution/highest count rate; I0 amplifier sensitivity: 100 nA/V; sample amplifier sensitivity: 20 nA/V, reference amplifier sensitivity: 100 pA/V; sample slit width: 1.5 mm; sample slit height: maximum (~ 3 mm); Monochromator crystal: GE 220 (DCM); and Ketek peaking time: 0.3 µs. Final XANES scans were normalized using program Athena by beamline scientists**.**

4.4 Results

4.4.1 Main elements observed

This study assessed trembling aspen and white spruce tree media and soils for 18 detectable elements using the IDEAS beamline. Eight out of the 18 elements were consistently identifiable in most tree media and soil samples. The eight elements identifiable in the samples were: K (potassium), Ca (calcium), Ti (titanium), Cr (chromium), Mn (manganese), Fe (iron), Zn (zinc), and Ni (nickel). The relative amounts of these elements (average fluorescence counts) varied per element, tree media, soil and site (Appendix G; Appendix H).

4.4.2 Elemental compositions of tree media per site

The elemental composition of white spruce leaves, branches, stem bark, a core (stem wood) segment, root bark, outer root, and inner root were assessed and compared per site. The elemental composition of trembling aspen's stem bark, a core (stem wood) segment, root bark, outer root, and inner root were also assessed and compared for one downwind site (Site 0 km) and the Control site. All tree media illustrated unique but relatively similar elemental compositions per site (Appendix H). A core segment's signature fluorescence is provided as a reference (Figure 4.1). In all white spruce and trembling aspen tree media, fluorescence was relatively greater for Ca and Fe, with moderate K, Zn, Mn, and Cr fluorescence, and traces of Ni and Ti fluorescence (Appendix G; Appendix H). Fluorescence counts were similar and comparable between tree species across sites.

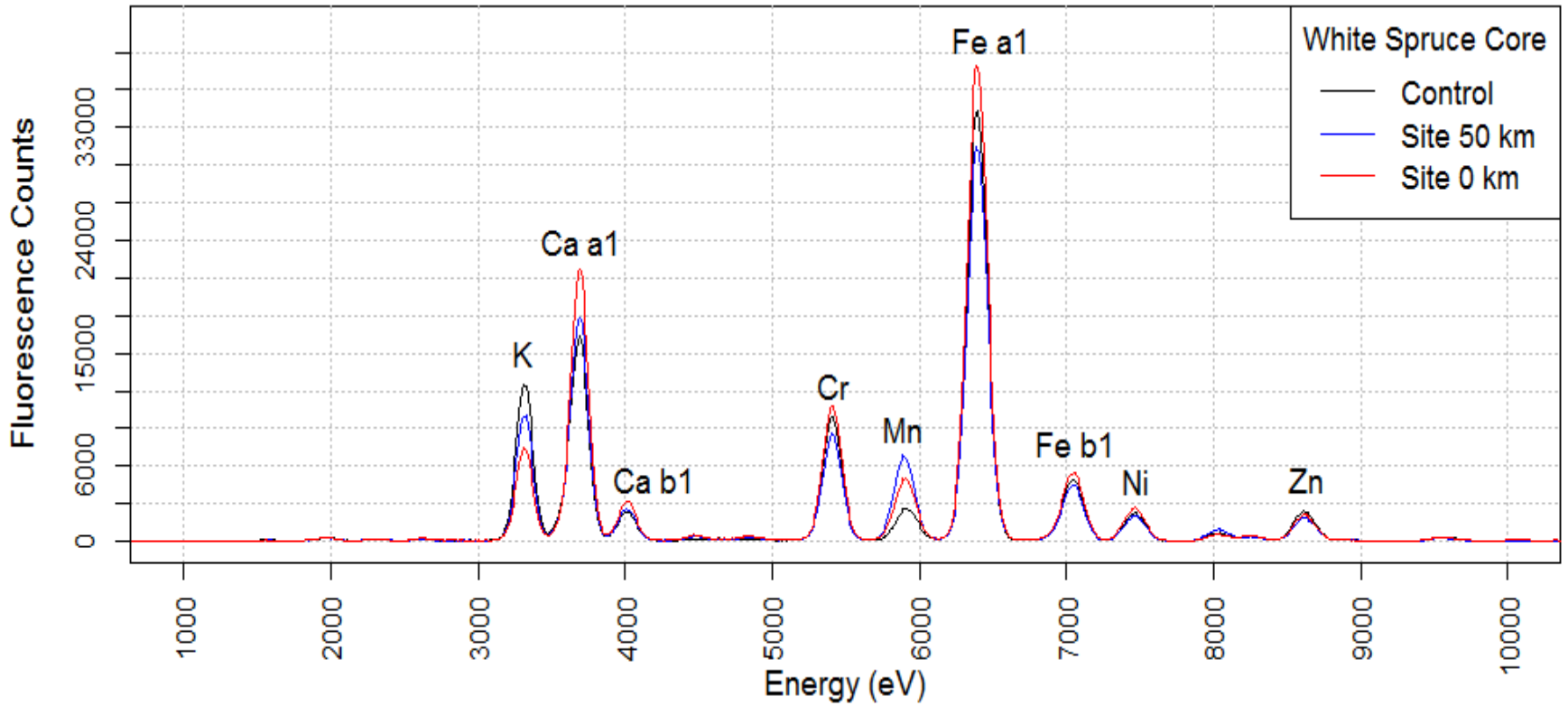

Figure 4.1 Average normalized fluorescence counts for a duration of 180 s illustrating distinct elements from the XRF scan on the IDEAS beamline for one white spruce's core (stem wood) segments (core seg. 1) per site; the Control site (black), Site 50 km (blue), Site 0 km (red). Each element corresponds to electron volt (eV) values. Fluorescence counts distinguish average relative amounts of each element per site. Note: a1 = K-edge alpha 1 eV values per element; b1 = K-edge beta 1 eV values per element.

All white spruce tree media were elevated in Mn at both downwind site's compared to the Control site, consistently illustrating greater fluorescence at Site 50 km compared to Site 0 km (Table 4.1; Appendix G). Manganese dominantly portrayed the greatest difference in fluorescence counts between sites in the majority of white spruce tree media, out of the eight identifiable elements (Appendix G). All trembling aspen tree media were elevated in Mn and K at Site 0 km compared to the Control site, except for core segment 1 (Table 4.2; Appendix G).

Table 4.1 Peak and average K-edge alpha 1 fluorescence counts comparisons between white spruce tree media per site (Control site vs. Site 50 km vs. Site 0 km) for eight identifiable elements derived from XRF using the IDEAS beamline. Elements were classified as elevated if their peaks exceeded and did not overlap the Control site's peak and K-edge alpha 1 fluorescence-count standard deviation (Appendix G; Appendix H). Elements were classified as not elevated if their peaks were below or overlapped the Control site's peak and K-edge alpha 1 fluorescence-count standard deviation.

White spruce tree media	Elements not elevated	Elements elevated at Site 50 km	Elements elevated at Site 0 km	Elements elevated at both downwind sites
Leaves	K, Ca, Fe, Ni, Cr, Zn	-	Ti,	Mn
Branches	K, Ca, Fe, Zn	-	Ti, Cr, Ni	Mn
Stem bark	K, Cr, Fe	Ca	-	Ti, Zn, Ni, Mn
Core seg.1	K, Cr, Fe, Zn	-	Ca, Ni	Ti, Mn
Root bark	Cr, Fe	-	K, Ti, Ni	Ca, Zn, Mn
Outer root	K, Ca, Fe, Zn, Ni, Ti, Cr	-	-	Mn
Inner root	K, Ca, Ti	Cr, Ni, Fe	-	Mn, Zn

Table 4.2 Peak and average K-edge alpha 1 fluorescence counts comparisons between trembling aspen tree media per site (Control site vs. Site 0 km) for eight identifiable elements derived from XRF using the IDEAS beamline. Elements were classified as elevated if their peaks exceeded and did not overlap the Control site's peak and K-edge alpha 1 fluorescence-count standard deviation (Appendix G; Appendix H). Elements were classified as not elevated if their peaks were below or overlapped the Control site's peak and K-edge alpha 1 fluorescence-count standard deviation.

Trembling aspen tree media	Elements not elevated	Elements elevated at Site 0 km
Stem bark	Ca, Ti, Cr, Fe, Zn, Ni	K, Mn
Core seg.1	K, Cr, Ti, Fe, Zn, Ni, Mn	Ca
Root bark	Ca, Ti, Cr, Fe, Zn, Ni	K, Mn
Outer root	Ca, Ti, Cr, Fe, Zn, Ni	K, Mn
Inner root	Ti	K, Ca, Cr, Fe, Zn, Ni, Mn

Species comparisons revealed consistently elevated Mn in all white spruce tree media at both sites (Site 0 km and the Control site) compared to trembling aspen, except in core segment 1 at the Control site and in inner root at Site 0 km (Table 4.3; Appendix G). Titanium fluorescence was consistently elevated in all white spruce tree media at Site 0 km compared to trembling aspen (Table 4.3; Appendix G). Trembling aspen appeared to contain greater K in all tree media at Site 0 km compared to white spruce (Table 4.3; Appendix G). No distinct pattern was identifiable for the remaining seven elements in all trembling aspen and white spruce tree media.

Table 4.3 Peak and average K-edge alpha 1 fluorescence counts comparisons between white spruce and trembling aspen tree media per site (Control site vs. Site 0 km) for eight identifiable elements derived from XRF using the IDEAS beamline. Elements were classified as elevated if one species peak exceeded and did not overlap the other species peak and K-edge alpha 1 fluorescence-count standard deviation (Appendix G; Appendix H). Elements were classified as similar if their peaks and K-edge alpha 1 fluorescence-count standard deviations did not exceed or overlap one another.

	Control			Site 0 km		
Tree media	Elements similar between species	Elements elevated in trembling aspen	Elements elevated in white spruce	Elements similar between species	Elements elevated in trembling aspen	Elements elevated in white spruce
Stem Bark	Ti	K, Ca, Cr, Fe, Ni, Zn	Mn	Cr, Fe, Ni	K, Ca	Zn, Ti, Mn
Core seg.1	Ca, Cr, Fe, Zn, Ni, Ti, Mn	-	K	Ca, Fe	K, Zn	Cr, Ni, Ti, Mn
Root bark	Cr, Ti	K, Ca, Fe, Ni, Zn	Mn	Cr, Fe	K	Ca, Ni, Zn, Ti, Mn
Outer root	K, Cr, Fe, Ni	Zn	Ca, Ti, Mn	Cr, Fe, Ni, Zn	K	Ca, Ti, Mn
Inner root	Ti	Zn	K, Ca, Cr, Fe, Ni, Mn	Cr, Fe, Ni, Mn	K, Ca, Zn	Ti

4.4.3 Elemental compositions of soil per site

The elemental composition of one pit with five soil depth increments including leaf litter, 0 to 5 cm, 5 to 20 cm, 20 to 45 cm, and 45 to 60 cm, were assessed and compared per site. All soil media illustrated unique but relatively similar elemental compositions per site, except for the leaf litter. Signature fluorescence for the 0 to 5 cm depth increment is provided as a reference (Figure 4.2). Leaf litter fluorescence counts were highest overall per element, for all eight

elements, and lowest overall fluorescence counts for the 45 to 60 cm depth increment per element. Manganese fluorescence appeared to be greater at both downwind sites in the topsoil (leaf litter and 0 to 5 cm depth increments) compared to the Control site, illustrating greater fluorescence at Site 0 km compared to Site 50 km (Table 4.4; Appendix G). No distinct pattern was identifiable for the remaining seven elements, as seen with Mn, in all soils.

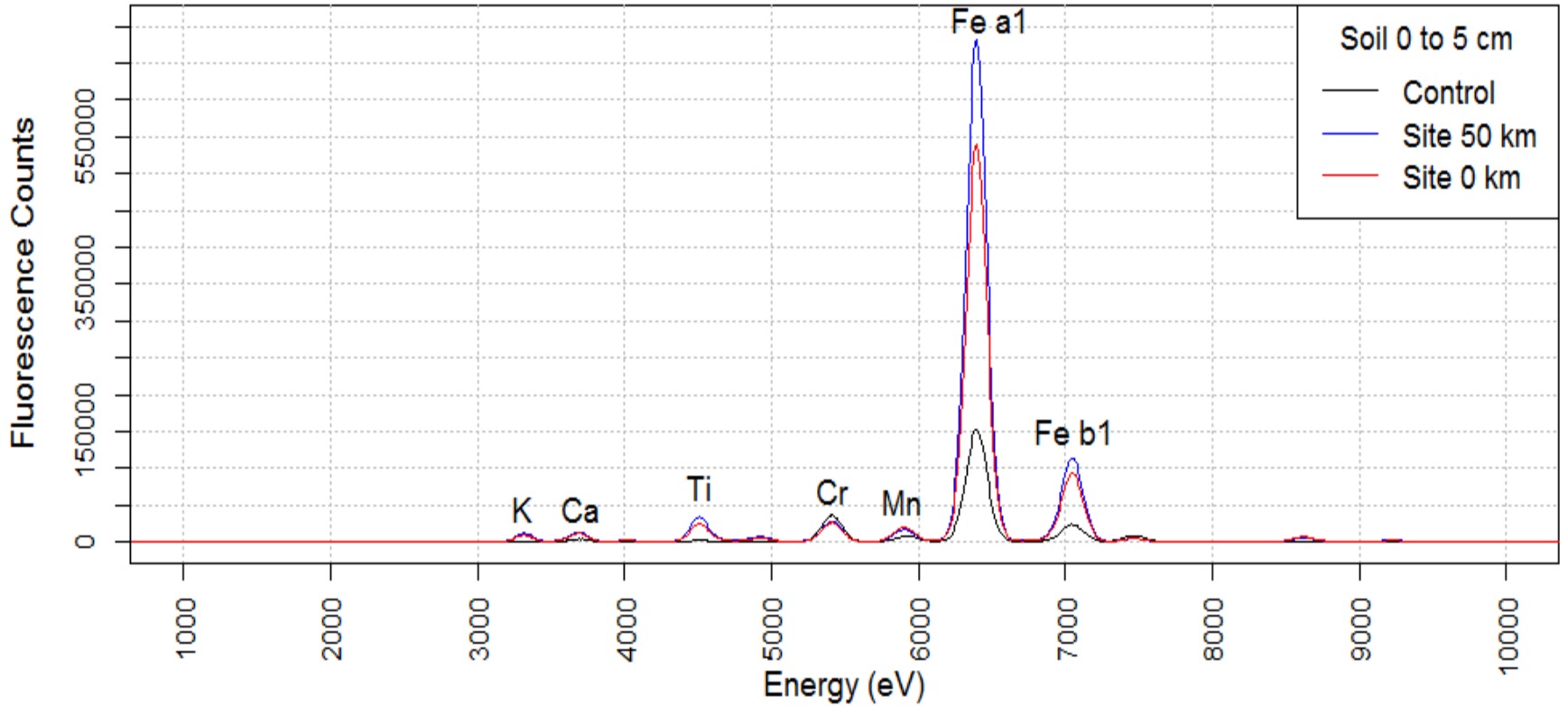

Figure 4.2 Normalized fluorescence counts for a duration of 180 s illustrating distinct elements from the XRF scan using the IDEAS beamline for the 0 to 5 cm soil depth increment per site; the Control site (black), Site 50 km (blue), Site 0 km (red). Each element corresponds to electron volt (eV) values. Fluorescence counts distinguish relative amounts of each element per site. Note: a1 = K-edge alpha 1 eV values per element; b1 = K-edge beta 1 eV values per element.

Table 4.4 Peak and K-edge alpha 1 fluorescence counts comparisons between soil depth increments per site (Control site vs. Site 50 km vs. Site 0 km) for eight identifiable elements derived from XRF using the IDEAS beamline. Elements were classified as elevated if their peaks exceeded and did not overlap the Control site's peak and K-edge alpha 1 fluorescence-count standard deviation (Appendix G; Appendix H). Elements were classified as not elevated if their peaks were below or overlapped the Control site's peak and K-edge alpha 1 fluorescence-count standard deviation.

Soil depth increments	Elements not elevated	Elements elevated at Site 50 km	Elements elevated at Site 0 km	Elements elevated at both downwind sites
Leaf litter	K, Cr, Fe, Ni, Zn	Ti	Ca	Mn
0 to 5 cm	Cr, Ni	-	-	K, Ca, Ti, Zn, Fe, Mn
5 to 20 cm	Fe, Ti, Ni, Mn, Cr	K, Ca	-	-
20 to 45 cm	-	Ni	K, Ca, Mn, Cr, Fe, Ti, Zn	-
45 to 60 cm	K, Ca, Fe, Ti, Cr	Ni, Zn, Mn	-	-

4.4.4 Manganese is consistently elevated at the downwind sites

Manganese fluorescence was elevated in the majority of tree media at the downwind sites compared to the Control site for both tree species, except in core segment 1 in trembling aspen at Site 0 km. Manganese was also elevated in all white spruce tree media at both sites (Control and Site 0 km) compared to trembling aspen, except for core segment 1 at the Control site and inner root at Site 0 km. Topsoil, including the leaf litter and the 0 to 5 cm depth increment, illustrated elevated Mn fluorescence at the downwind sites compared to the Control site. Manganese trends in the tree media differ from topsoil trends. Manganese fluorescence counts were greater at Site 0 km than Site 50 km for the topsoil, whereas Mn fluorescence counts were greater at Site 50 km than Site 0 km for white spruce tree media. Zoomed-in images of the Mn fluorescence peak is provided as reference for one white spruce (Figure 4.3) and trembling aspen (Figure 4.4) tree material, and one topsoil (Figure 4.5).

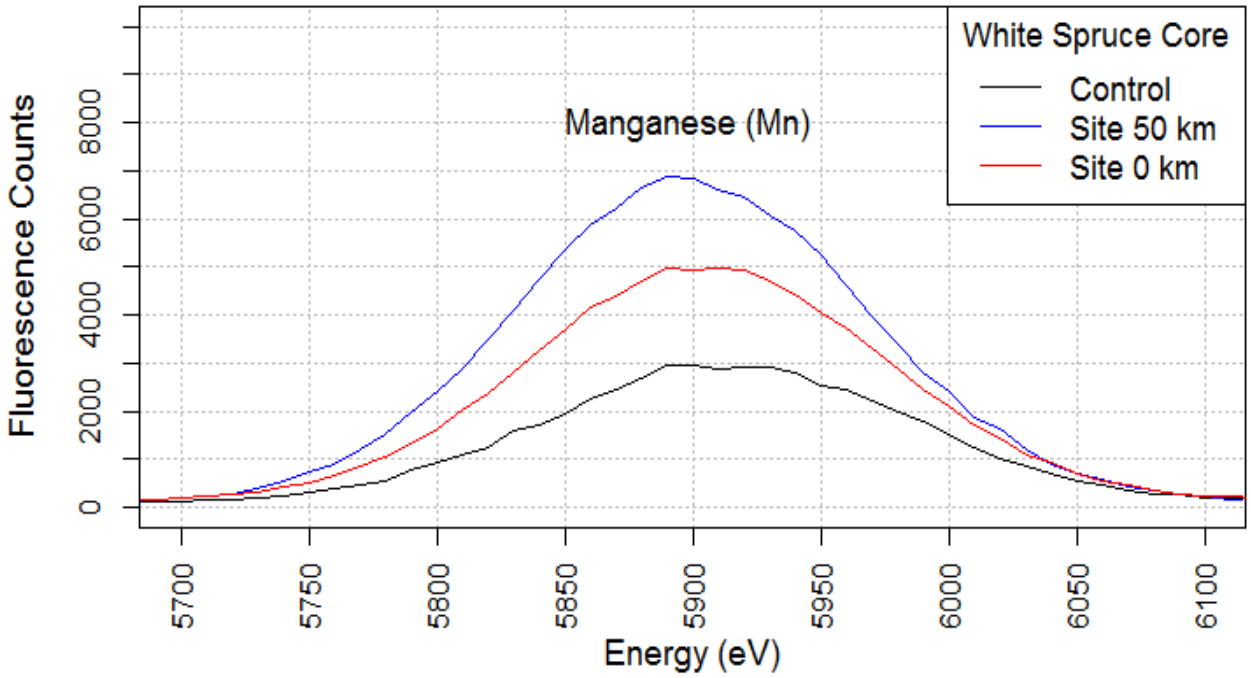

Figure 4.3 Zoomed-in view of average normalized fluorescence counts for 180 s illustrating Mn from XRF scan using the IDEAS beamline for one of white spruce's core (stem wood) segments per site; the Control site (black), Site 50 km (blue), Site 0 km (red). K-edge Mn corresponds to an electron volt (eV) value of 5900. Fluorescence counts distinguish average relative amounts of Mn per site.

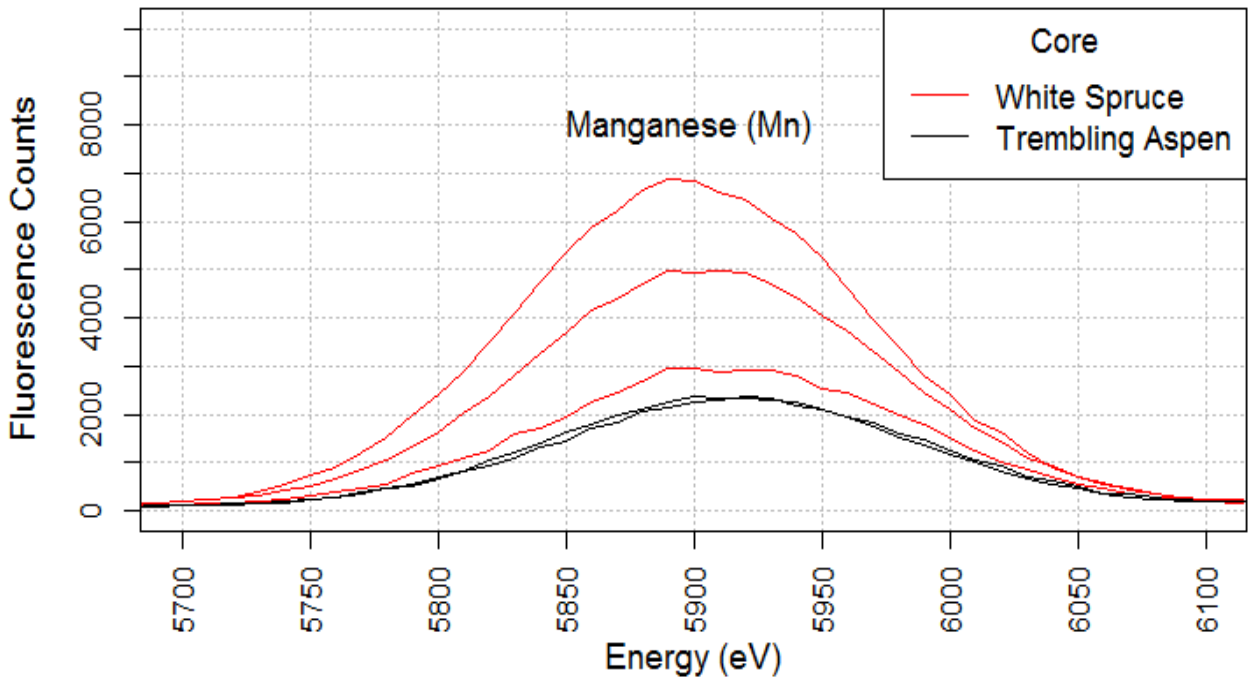

Figure 4.4 Zoomed-in view of average normalized fluorescence counts for a duration of 180 s illustrating Mn from the XRF scan using the IDEAS beamline comparing one of trembling aspen's and white spruce's core (stem wood) segments (core seg. 1) per site; white spruce (red), trembling aspen (black). Each red line represents white spruce fluorescence counts at the Control, Site 50 km and Site 0 km. Each black line represents trembling aspen fluorescence counts at the Control and Site 0 km. K-edge Mn corresponds to an electron volt (eV) value of 5900. Fluorescence counts distinguish average relative amounts of Mn per site.

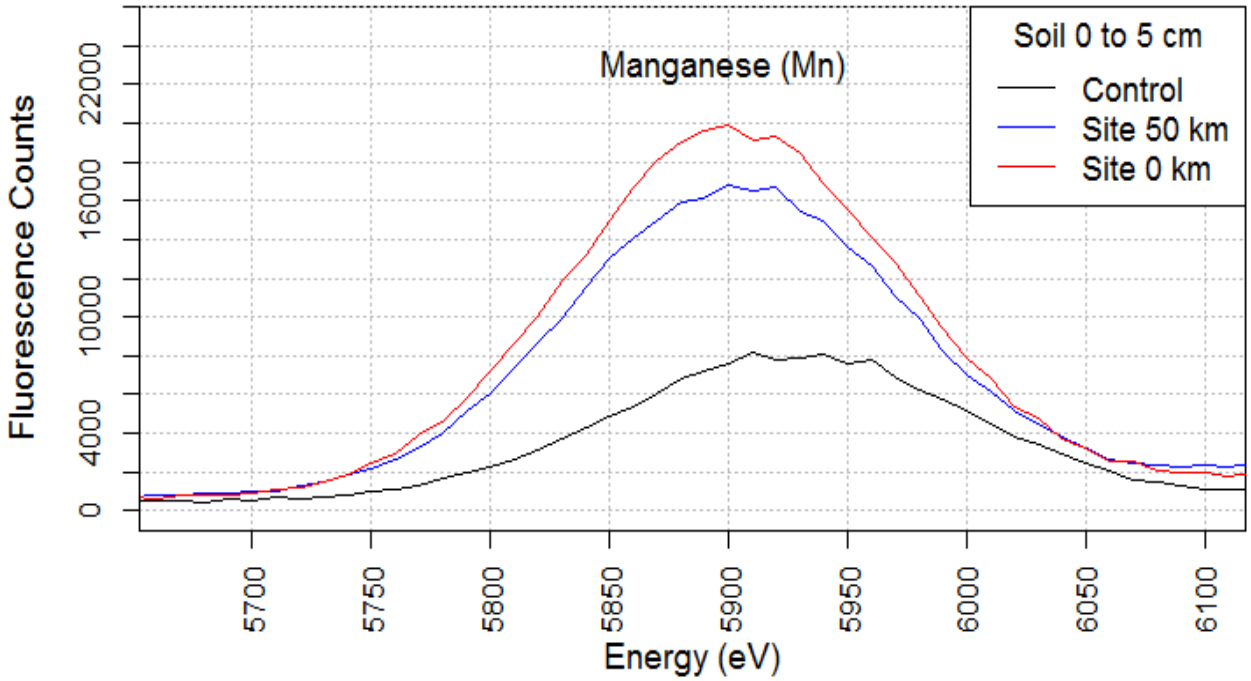

Figure 4.5 Zoomed-in view of normalized fluorescence counts for a duration of 180 s illustrating Mn from XRF scan using the IDEAS beamline for the 0 to 5 cm soil depth increment per site; the Control site (black), Site 50 km (blue), Site 0 km (red). K-edge Mn corresponds to an electron volt (eV) value of 5900. Fluorescence counts distinguish relative amounts of Mn per site

4.4.5 Trembling aspen and white spruce cores

K-edge Mn was traced over time through white spruce and trembling aspen cores (stem wood), sliced into 0.5 cm segments (Figure 4.6; Figure 4.7). White spruce Site 0 km and Control site cores illustrate relatively similar amounts of Mn through time until core segment 8 near the pith. Manganese fluorescence at Site 0 km surpasses Mn fluorescence at the Control site from core segment 8 onwards. The dendrochronological assessment revealed that core segment 8 corresponds to a time period of 1988-1992, depicting the approximate years when Mn amounts begin to change (Appendix I). Manganese fluorescence in cores at Site 50 km are anomalous to Site 0 km and Control site cores, illustrating elevated Mn fluorescence in all of its core segments. Manganese fluorescence is slightly elevated in all trembling aspen cores at Site 0 km compared to the Control site, except at core segment 1 where Mn fluorescence is similar per site. Trembling aspen's core segments, at Site 0 km and the Control site, date from 1992-2014 and 1997-2011, respectively (Appendix I). Species comparisons revealed that manganese fluorescence is greater in the majority of white spruce cores at both sites (Site 0 km and the Control site) compared to trembling aspen (Figure 4.8; Figure 4.9). All trembling aspen and

white spruce stem barks contain dramatically greater Mn fluorescence compared to their cores segments.

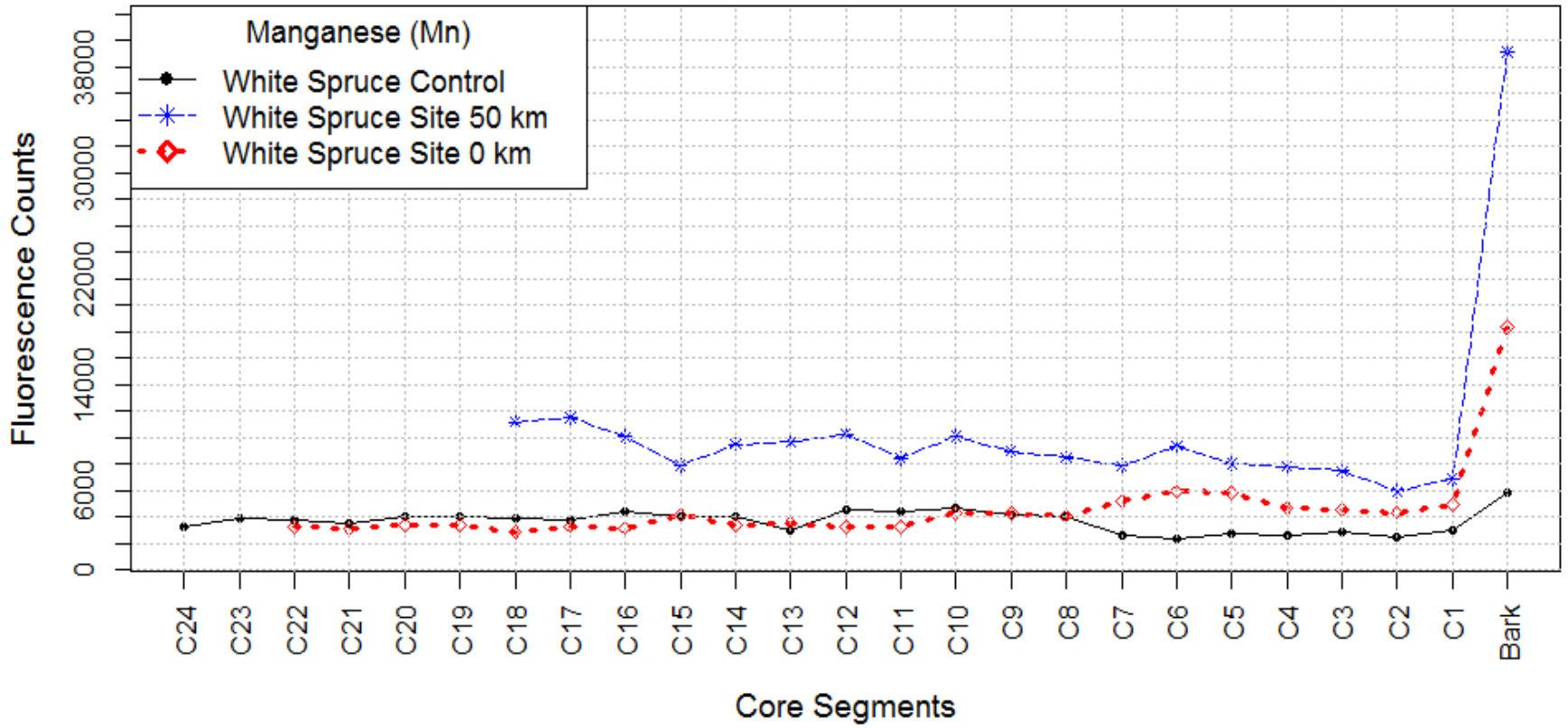

Figure 4.6 Average normalized fluorescence counts for a duration of 180 s illustrating K-edge Mn plotted over time for white spruce core (stem wood) segments per site; the Control site (solid line), Site 50 km (slashed line), Site 0 km (dotted line). K-edge Mn corresponds to an electron volt (eV) value of 5900. Fluorescence counts distinguish average relative amounts of Mn per core per site. Core segments represent tree rings from the pith to the bark.

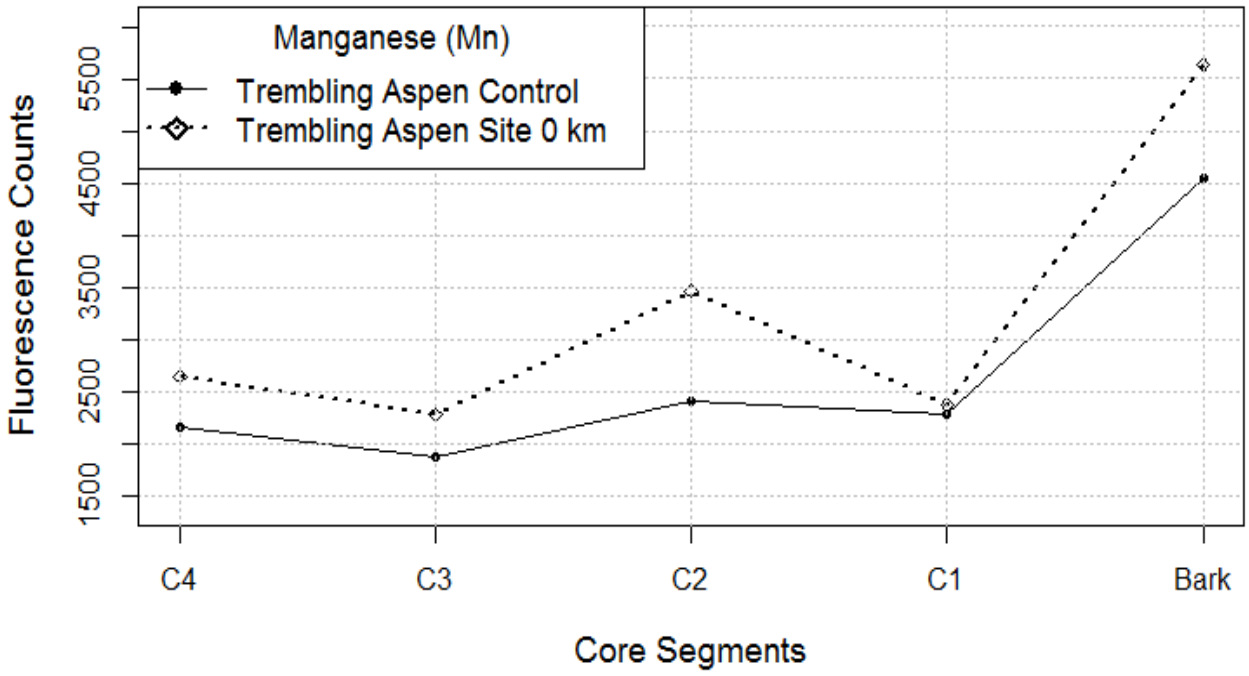

Figure 4.7 Average normalized fluorescence counts for a duration of 180 s illustrating K-edge Mn plotted over time for trembling aspen core (stem wood) segments per site; the Control site (solid line), Site 0 km (slashed line). K-edge Mn corresponds to an electron volt (eV) value of 5900. Fluorescence counts distinguish average relative amounts of Mn per core per site. Core segments represent tree rings from pith to bark.

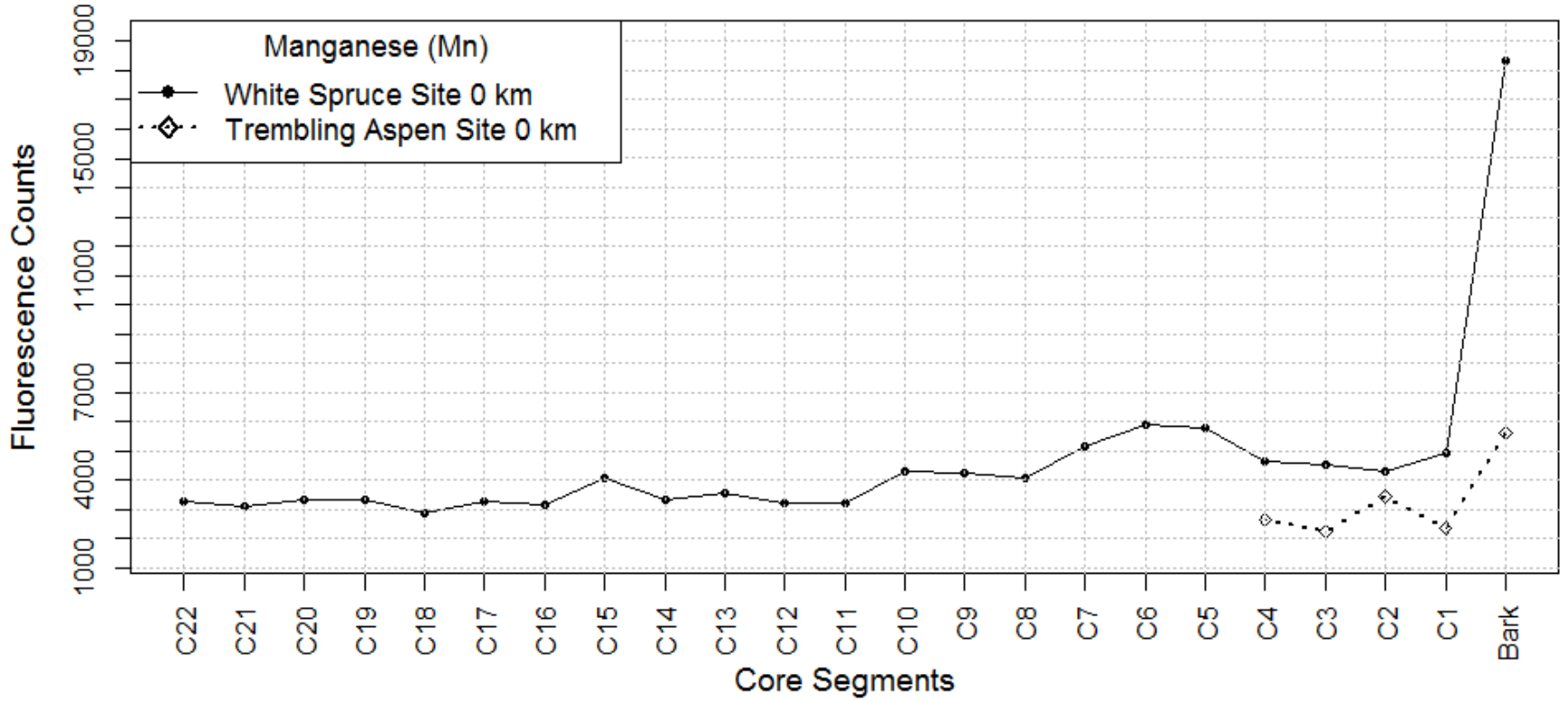

Figure 4.8 Average normalized fluorescence counts for a duration of 180 s illustrating K-edge Mn plotted over time for white spruce (solid line) and trembling aspen (dotted line) core (stem wood) segments for Site 0 km. K-edge Mn corresponds to an electron volt (eV) value of 5900. Fluorescence counts distinguish average relative amounts of Mn per core. Core segments represent tree rings from pith to bark.

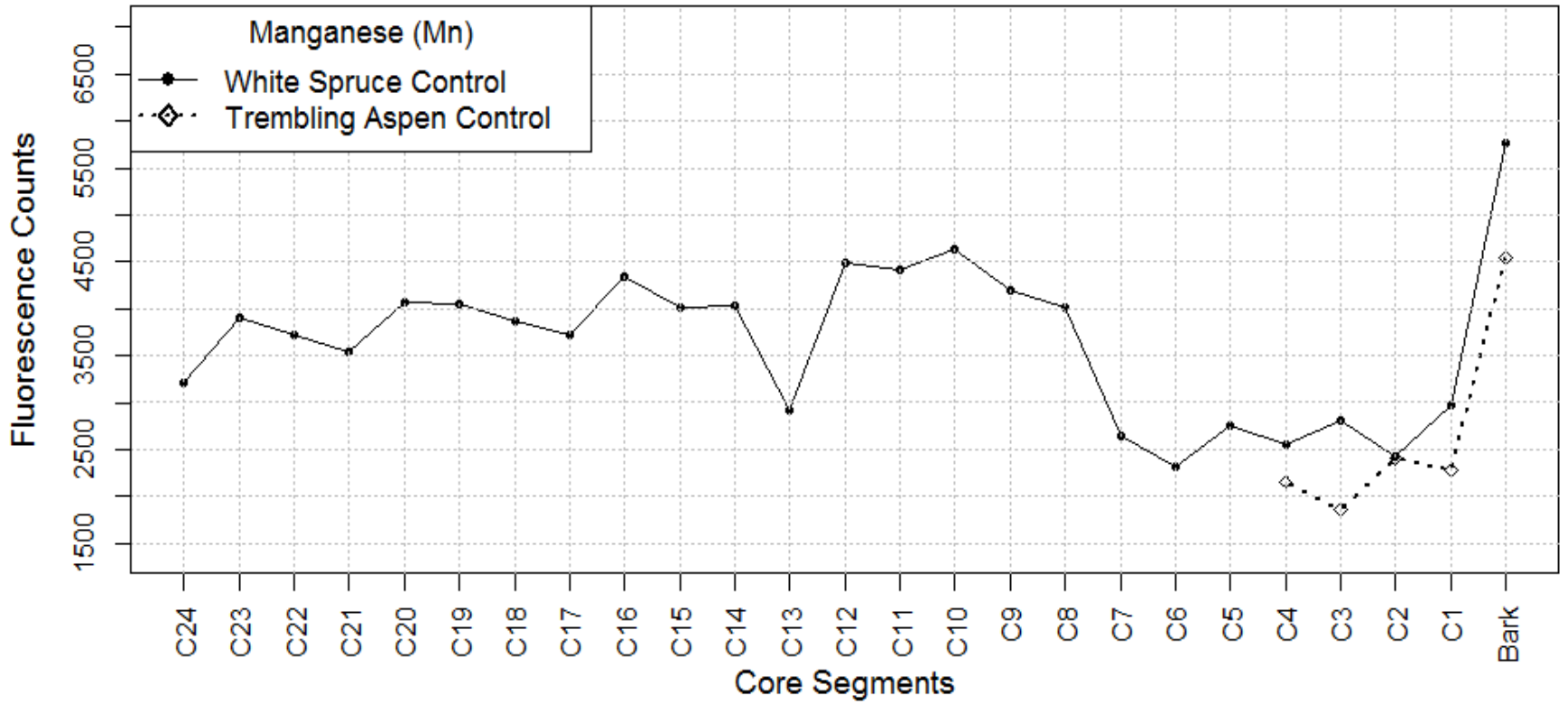

Figure 4.9 Average normalized fluorescence counts for a duration of 180 s illustrating K-edge Mn plotted over time for white spruce (solid line) and trembling aspen (dotted line) core (stem wood) segments for the Control site. K-edge Mn corresponds to an electron volt (eV) value of 5900. Fluorescence counts distinguish average relative amounts of Mn per core. Core segments represent tree rings from pith to bark.

4.4.6 XANES scans for K-edge Mn in white spruce tree media and the leaf litter

K-edge Mn XANES scans of five white spruce tree media; leaves, a sliced core (stem wood) segment, stem bark, inner root, and outer root, as well as leaf litter from Site 0 km were assessed and compared to determine the chemical speciation of Mn (Figure 4.10). The chemical speciation of Mn was the same for all white spruce tree components (leaves, core, stem bark, inner root, and outer root) corresponding to Mn (II). The speciation of Mn was different for the leaf litter corresponding to Mn (III/IV).

4.5 Discussion

4.5.1 Manganese enrichment occurring downwind from the AOSR

Manganese was elevated in the majority of tree media for trembling aspen and white spruce, as well as the topsoil, at both downwind sites compared to the Control site. The aerial deposition and enrichment of Mn in locations circumambient to AOSR facilities has been documented in previous literature (Graney et al., 2012; Bari et al., 2014; Lynam et al., 2015; Huang et al., 2016). Manganese deposition from emissions was determined to be 3 to 6 times higher at sites in close proximity to AOSR facilities compared to background concentrations (Lynam et al., 2015). Manganese deposition rates ranged from 20.3 to 70.6 µg/m^2/day around the AOSR depending on the distance of the site (Bari et al., 2015). Manganese concentrations were found to be greatest in sites immediately surrounding the AOSR but decreased exponentially with distances beyond 50 km from AOSR facilities (Bari et al., 2014; Lynam et al., 2015; Huang et al., 2016). Graney et al. (2012) found Mn to be greater in sites farther away from the AOSR. Previous spatial patterns of Mn deposition match topsoil Mn trends in this study, illustrating greater quantities of Mn in sites at the closest proximity to AOSR facilities (Site 0 km) and less Mn at distances further away from AOSR facilities (Site 50km > Control). Mn was elevated in white spruce cores (stem wood) at Site 0 km compared to the Control site from 1988 (core segment 8) onward. Trembling aspen's cores also illustrated an increase in Mn at Site 0 km compared to the Control site, from 1992 onward, except from 2002-2009 (core segment 2). The overall increase in Mn from the 1990's onward generally matches increasing production trends within the AOSR, occurring in 1979 and the 2000's (Gosselin et al., 2010; Jung et al., 2013a; Savard et al., 2014; Canadian Association of Petroleum Producers, 2015). The temporal

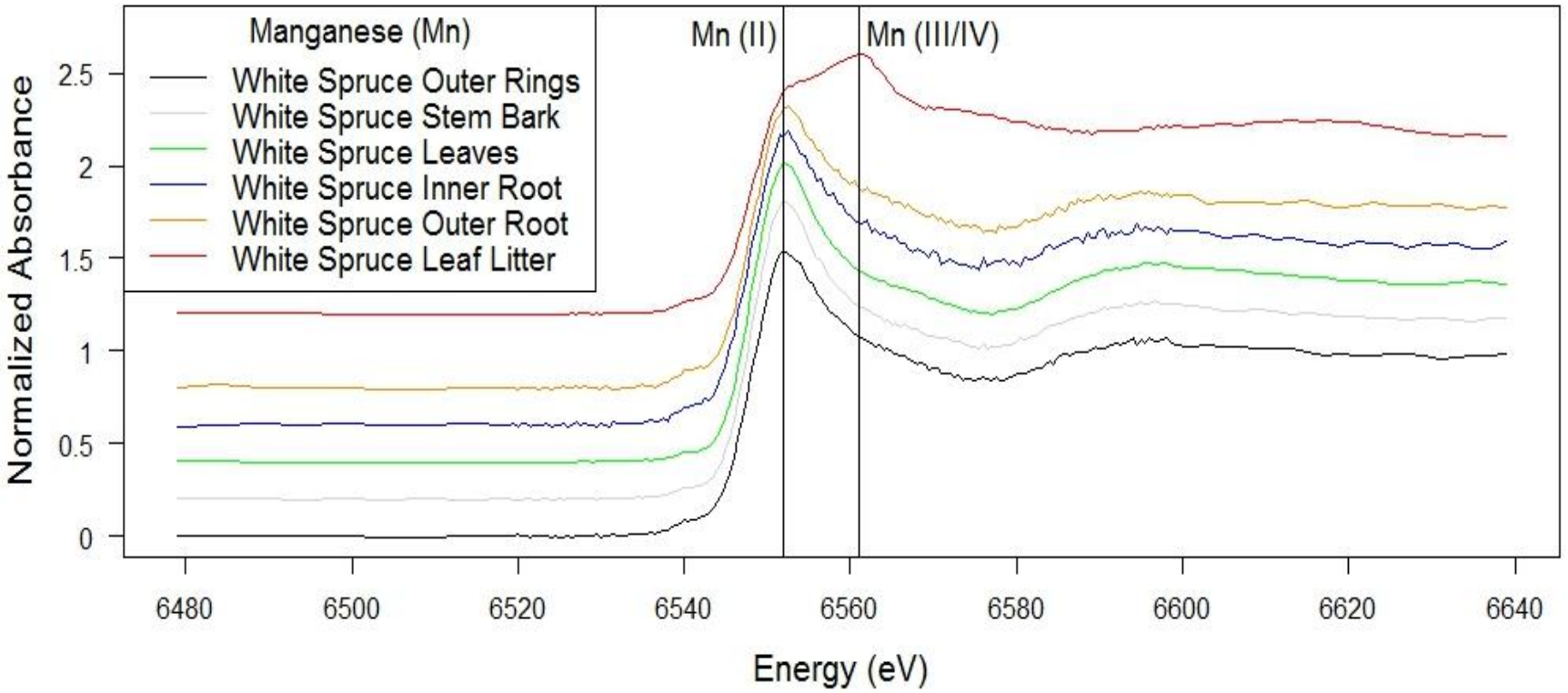

Figure 4.10 Offset normalized absorbance for a duration of 15 min illustrating K-edge Mn XANES scans for white spruce tree media at Site 0 km; a core (stem wood) segment (black), stem bark (gray), leaves (green), inner root (blue), outer root (orange), leaf litter (red).

accuracy of Mn may be skewed due to natural lateral and horizontal displacement (translocation) of Mn within its tree rings (Watmough, 1999; Watmough and Hutchinson, 2003; Siwik et al., 2010). In unpolluted coniferous trees, Mn remained unchanged or gradually decreased over time (Scharnweber et al., (in press), 2016), implying that elevated amounts of Mn in the outer stem wood (rings) of white spruce at Site 0 km is abnormal. Mn in white spruce and trembling aspen stem barks were elevated at the downwind sites compared to the Control site. Air contaminants directly deposit onto bark tissue and have recorded spatial patterns of aerial deposition in other studies, depicting greater concentrations of air contaminants in bark at closer proximity to industrial facilities, similar to bark patterns in this study (Huhn et al., 1995).

4.5.2 Combining findings: is Mn toxicity causing a decline in radial growth in white spruce?

In excess, Mn is known to be toxic to plants impairing photosynthesis and growth, interfering with plant metabolic process (absorption and utilization of specific elements; energy metabolism; increases in oxidative stress), creating visible brown spots, necrosis, and chlorosis on leaves, and flecking on stems (Kitao et al., 2001; Boojar and Goodarzi, 2008; Mou et al., 2011; Herndon et al., 2014). In Chapter three, white spruce illustrated a decline in radial growth at the downwind sites (Site 0 km and Site 50 km) during the last decade, but not at the Control site, with radial-growth declines more severe at Site 0 km compared to Site 50 km. Trembling aspen did not illustrate declines in radial growth at any site. Combining these two findings reveals a distinct pattern; Mn fluorescence increased in the topsoil's at sites closer to the AOSR and radial-growth declines became more severe in sites closer to the AOSR, suggesting that excess Mn (through roots and direct deposition onto tree components) may be causing phyto-toxicity in white spruce, resulting in their radial-growth declines. The cumulative impact of Mn accumulation through aerial deposition and decreased precipitation over the past decade, coupled with white spruce's shallower root system, may further contribute to radial-growth declines in white spruce. Sliced cores (stem wood) from Site 0 km and the Control site determined that Mn accumulation began in the late 1980's. White spruce tissues had greater Mn fluorescence than trembling aspen at all three sites, suggesting that white spruce accumulates Mn more readily than trembling aspen possibly making it more prone to Mn toxicity, resulting in radial-growth differences per species at the same sites. Evidence suggests that tolerance to Mn toxicity varies per tree species and for different genotypes (St. Clair and Lynch, 2005). It is possible that trembling aspen has cellular and metabolic mechanisms capable of removing Mn more

effectively than white spruce. Certain species of aspen have even been known to accumulate metals in their leaves (Hassinen et al., 2009; Nevel et al., 2011); in the fall, trembling aspens leaves shed annually, which would remove excess and localized Mn in its leaves from its system, preventing build up and toxicity.

Other elements (K, Ca, Ni, Cr, Ti, Fe, Zn) were elevated at some downwind sites in some tree media compared to the Control site, which are known to be aerially deposited within a 50 km radius of the AOSR (Kelly et al., 2010; Bari et al., 2014; Lynam et al., 2015; Huang et al., 2016). Excess amounts of these elements, especially metals (Nagajyoti et al., 2010; Yadav, 2010), may further contribute to radial-growth declines in white spruce at the downwind sites, meaning Mn may only be a part of any potential contamination problem.

4.5.3 Anomalies and unknowns

Mn exists naturally in the biosphere and is normally released into the atmosphere as dust from the earth's crust, volcanism, marine environments, and forest fires (Lynam et al., 2015). Activities that release Mn into the atmosphere, from the AOSR, are the burning of fossil fuels, re-suspended and windblown dust from near-field operations, such as mining (Bari et al., 2014; Lynam et al., 2015; Huang et al., 2016), and upgrading emissions. Mn exists as a trace impurity in bitumen (Filby, 1994) and coke and flyash materials (Jervis et al., 1982). XRF is unable to distinguish whether Mn is derived from anthropogenic sources or from natural causes. XANES revealed the chemical speciation of Mn to be the same for all white spruce tree media (inner root, outer root, core (stem wood) segment, stem bark, and leaves), except for the leaf litter. Leaf litter absorbance matches Mn (III or IV) oxides (Herndon et al., 2014). Mn-oxides are generally derived from plant decomposition or from industrial and anthropogenic sources (fossil fuel emissions) (U.S. Environmental Protection Agency, 1984; Zayed et al., 1999; Ressler et al., 2000; Herndon et al., 2014). XANES was unable to distinguish the source of Mn-oxides. Evidence suggests that other elements, besides the ones in this study, are being deposited in areas within a 50 km radius of the AOSR (Kelly et al., 2010; Bari et al., 2014; Lynam et al., 2015; Huang et al., 2016), which can additionally harm the growth the trees (Kurczynska et al., 1997; Watmough, 1999; Watmough and Hutchinson, 2003; Nagajyoti et al., 2010; Yadav, 2010). Other unstudied elements may be causing or contributing to the decline in radial growth occurring in white spruce downwind from the AOSR, alongside Mn, or may also be chemically assisting Mn in making the excess element bio-available.

Finally, Site 50 km contained greater Mn fluorescence in all white spruce tree media compared to Site 0 km, opposite to the reduced radial-growth severity and aerial deposition trends that depict a gradual increase in severity and pollutant enrichment in areas at closer proximity to the AOSR. The long-term trends in the core (stem wood) segments suggest Mn enrichment predated and remained the same prior to aerial deposition increases within the AOSR. The cause of this anomaly can be speculated by: other forms of disturbance that occurred in the area before the AOSR existed (such as gravel road construction and activity), greater Mn input from increased soil acidity around the selected tree either through disturbance or a natural causes (Markovic et al., 2013), or natural variations in Mn within white spruce tree components. In terms of this study, Mn amounts at Site 50 km cannot be directly compared to Site 0 km and the Control site, because it exhibits a shift in baseline Mn fluorescence alluding to gaps in our knowledge of baseline Mn fluorescence in white spruce cores (i.e., we don't know what the normal range of variation is within different trees, since we were only able to test one tree at each site).

4.6 Conclusions

Eight elements were consistently identified in most tree and soil media inclusive to K, Ca, Cr, Mn, Fe, Ti, Ni, and Zn. Findings illustrate consistent enrichment of Mn in the downwind sites for the majority of trembling aspen and white spruce tree media, including cores (stem wood). The dendrochemical assessment revealed elevated amounts of Mn occurring from 1988 onward at Site 0 km. Previously determined spatial patterns of air pollution around the AOSR, depicted a gradual increase in pollutant deposition in areas closer to the AOSR. Mn enrichment in the topsoil's of the downwind sites showed similar patterns, illustrating a gradual increase in Mn at sites closer to the AOSR. Mn fluorescence was greater in all white spruce materials compared to trembling aspen materials at each site, meaning white spruce more readily incorporates and accumulates Mn into its tissues than trembling aspen. Other random elements appeared to be elevated in some trembling aspen and white spruce tree media at some of the downwind sites compared to the Control site, but no distinct pattern such as what was seen with Mn, was observed. Multi-element enrichment, through aerial deposition remains a possibility, meaning Mn enrichment may only be part of a bigger toxicity problem.

A K-edge Mn XANES scan revealed that the speciation of Mn was the same for all white spruce tree media (leaves, inner roots, outer root, stem bark, core (stem wood) segment), except for the leaf litter. Aqueous and organic Mn (II) comprises white spruce tree media but become oxidized and transformed to Mn (III/IV) in the leaf litter and soil. Mn-oxides exist naturally in the soil through decomposition processes or they can be derived from anthropogenic and industrial activities.

Excess Mn is known to be toxic to trees and plants and can disrupt major cellular, metabolic, and physiological processes. Accumulation of Mn over time to toxic levels, from aerial deposition, may be one factor leading to radial-growth declines in white spruce at the downwind sites. Other elements elevated in the downwind sites compared to the Control site, such as various metals, could enhance or contribute to radial-growth declines in white spruce, alongside Mn. As well, Mn accumulates more readily in white spruce tissue than trembling aspen tissue (especially their leaves), and as a result, white spruce may be more prone to Mn toxicity than trembling aspen, since aspen lose their leaves every year, and spruce keep their needles for 4-5 years. The translocation and accumulation of Mn into trembling aspen's leaves and their loss every autumn, relieves aspen of Mn build-ups and subsequent toxicity, contrary to white spruce, possibly explaining species-different radial-growth responses at the downwind sites. The cumulative impact of decreased precipitation, shallow root systems, and the aerial deposition of Mn could more fully explain radial-growth declines occurring in white spruce at the downwind sites.

Aerial fallout from the AOSR is a probable contributor to the local enrichment of Mn and a possible contaminant of concern causing radial-growth declines in white spruce, at the downwind sites. It should be noted that many anomalies and unknowns remain regarding Mn accumulation in tree components downwind from the AOSR and more detailed research and sampling is needed before any definitive conclusions regarding Mn toxicity can be made. Thus this study puts forth a possible starting point for future research projects, regarding radial-growth declines in white spruce. It is recommended that those forests, and other ecosystem components, downwind from the AOSR or at least within the 50 km zone of enrichment, be monitored long-term while Alberta's oil sand production continues to expand. Aerial deposition and accumulation within the AOSR is ongoing, meaning adverse impacts to surrounding ecosystem

components will continue to occur at a later date as elements build up to potentially toxic levels, as what is seen in the radial growth of white spruce.

4.7 References

Aznar, J., M. Richer-Lafleche, C. Begin, and Y. Begin. 2009. Lead exclusion and copper translocation in black spruce needles. Water Air Soil Pollt. 203: 139-145.

Bari, M., W. Kindzierski, and S. Cho. 2014. A wintertime investigation of atmospheric deposition of metals and polycyclic aromatic hydrocarbons in the Athabasca Oils Sands Region, Canada. Sci. Tot. Environ. 485-486: 180-192.

Boojar, M.M.A., and F. Goodarzi. 2008. Comparative evaluation of oxidative stress status and manganese availability in plants growing on manganese mine. Ecotoxicol. Environ. Saf. 71: 692-699.

Canadian Association of Petroleum Producers. 2015. Oil Sands History and Milestones [Online]. Available at http://www.canadasoilsands.ca/en/what-are-the-oil-sands/oil-sands-history-and-milestones (accessed June 2016).

Cheng, Z., B. Buckley, B. Katz, W. Wright, R. Bailey, K. Smith, J. Li, A. Curtis, and A. van Green. 2007. Arsenic in tree rings at a highly contaminated site. Sci. Tot. Environ. 376: 324-334.

Esri Canada Ed. 2001. Provinces and Territories of Canada [Online]. Available at ArcGIS.

Fenn, M.E., A. Bytnerowicz, S.L. Schilling, and C.S. Ross. 2015. Atmospheric deposition of nitrogen, sulfur and base cation sin jack pine stands in the Athabasca Oil Sands Region, Alberta, Canada. Environ. Pollut. 196: 497-510.

Filby, R. 1994. Origin and nature of trace element species in crude oils, bitumens, and kerogens: implications for correlation and other geochemical studies. *In* Edition by J. Parnell, from Geofluids: Origin, Migration and Evolution of Fluids in Sedimentary Basins. Geol. Soc. Spec. Publ. 78: 203-219.

Fittschen, U., and G. Falkenberg. 2011. Trends in environmental science using microscopic x-ray fluorescence. Spectrochimica Acta Part B 66: 567-580.

Gosselin, P., S. Hrudey, A. Naeth, A. Plourde, R. Therrien, G. Van Der Kraak, and Z. Xu. 2010. Environmental and health impacts of Canada's oil industry. The Royal Society of Canada. Ottawa, Ontario.

Government of Alberta, Alberta Environment and Parks. 2015. Shapefiles for Oil Sands Project Boundaries and Points: 1985 to 2013 [Online]. Available at http://osip.alberta.ca/library/Browser#SearchByKeyword=shapefile&Location=ATHAB&Location=AB&Page=3&Sort=Title (accessed June 2016).

Government of Canada. 2010. Canadian Climate Normals 1981 – 2010 Station Data [Online]. Available at http://climate.weather.gc.ca/climate_normals/results_1981_2010_e.html?searchType=stnProv&lstProvince=AB&txtCentralLatMin=0&txtCentralLatSec=0&txtCentralLongMin=0&txtCentralLongSec=0&stnID=2467&dispBack=0 (accessed June 2016).

Government of Canada, Agriculture and Agri-Food Canada. 2016. Ecozones of Canada [Online]. Available at ArcGIS.

Graney, J.R., M.S. Grandis, and S. Krupa. 2012. Coupling lead isotopes and element concentrations in epiphytic lichens to track sources of air emissions in the Athabasca Oil Sands Region. Dev. Environ. Sci. 11: 343-372.

Hassinen, V., V-M. Vallinkoski, S. Issakainen, A. Tervahauta, S. K. Renlampi, and K. Servomaa. 2009. Correlation of foliar MT2b expression with Cd and Zn concentrations in hybrid aspen (*Populus tremula* x *tremuloides*) grown in contaminated soil. Environ. Pollut. 157: 922-930.

Helmisaari, H-S., J. Derome, H. Fritze, T. Nieminem, K. Palmgren, M. Salemaa, and I. Vanha-majamaa. 1995. Copper in Scots pine forests around a heavy-metal smelter in south-western Finland. Water, Air & Soil Pollut. 85: 1727-1732.

Herndon, E.M., C.E., Martınez, and S.L. Brantley. 2014. Spectroscopic (XANES/XRF) characterization of contaminant manganese cycling in a temperate watershed. Biogeochem. 121: 505-517.

Hodson, P.V. 2013. History of environmental contamination by oil sands extraction. Proc. Natl. Acad. Sci. 110: 1569-1570.

Hojdova, M., T. Navratil, J. Rohovec, K. Zak, A. Vanek, V. Chrastny, R. Bace, and M. WSvoboda. 2011. Changes in mercury deposition in mining and smelting region as recorded in tree rings. Water Air Soil Pollut. 216: 73-82.

Hu, Y., K. Jung, D. Zeng, and S. Chang. 2013. Nitrogen-and-sulphur-deposition-altered soil microbial community functions and enzyme activities in a boreal mixedwood forest in western Canada. Can. J. For. Res. 43: 777-784.

Huang, R., K.N. McPhedran, L. Yang, and M.G. El-Din. 2016. Characterization and distribution of metal and nonmetal elements in the Alberta oil sands region of Canada. Chemosphere 147: 218-229.

Huhn, G., H. Schultz, H-J. Stark, R. Tolle, and G. Schurrmann. 1995. Evaluation of regional heavy metal deposition by multivariate analysis of element contents in pine tree barks. Water Air Soil Pollut. 84: 367-383.

Jervis, R., K. Richard Ho, and B. Tiefenbach. 1982. Trace impurities in Canadian oil-sands, coals and petroleum products and their fate during extraction, up-grading and combustion. J. Radioanal. Chem. 71: 225-241.

Jung, K., W-J. Choi, S.X. Chang, and M.A. Arshad. 2013. Soil and tree ring chemistry of *Pinus banksiana* and *Populus tremuloides* stands as indicators of changes in atmospheric environments in the oil sands region of Alberta, Canada. Ecol. Indic. 25: 256-265.

Kelly, E., D. Schindler, P. Hodson, J. Short, R. Radmanovich, and C. Nielson. 2010. Oil sands development contributes elements toxic at low concentrations to the Athabasca River and its tributaries. Proc. Natl. Acad. Sci. 107: 16178-16183.

Kershaw, G. 2013. Talking to trees: A dendrochronological assessment of the atmospheric pollution effects of Athabasca bitumen mining downwind from the industry. MS Thesis. University of Dalhousie. Halifax, Nova Scotia.

Kitao, M., T.T. Lei, T. Nakamura, and T. Koike. 2001. Manganese toxicity as indicated by visible foliar symptoms of Japanese white birch (*Betula platyphylla* var. *japonica*). Environ. Pollut. 111: 89-94.

Kurczynska, E., W. Dmuchowski, W. Wloch, and A. Bytnerowicz. 1997. The influence of air pollutants on needles and stems of scots pine (*Pinus sylvestris L.*) trees. Environ. Pollut. 98: 325-334.

Lageard, J., J. Howell, J. Rothwell, and I. Drew. 2008. The utility of *Pinus sylvestris* L. in dendrochemical investigations: pollution impact of lead mining and smelting in Darley Dale, Derbyshire, UK. Environ. Pollut. 153: 284-294.

Laxton, D., S. Watmough, and J. Aherne. 2012. Nitrogen cycling in *Pinus banksiana* and *Populous tremuloides* stands in the Athabasca oil sands region, Alberta, Canada. Water Air Soil Pollut. 223: 1-13.

Liggio, J., S-M. Li, K. Hayden, Y. M. Taha, C. Stroud, A. Darlington, B. D. Drollette, M. Gordon, P. Lee, P. Liu, A. Leithead, S. G. Moussa, D. Wang, J. O'Brien, R. L. Mittermeier, J. R. Brook, G. Lu, R. M. Staebler, Y. Han, T. W. Tokarek, H. D. Osthoff, P. A. Makar, J. Zhang, D. L. Plata, and D. R. Gentner. 2016. Oil sands operations as a large source of secondary organic aerosols. Nature 534: 91 – 94.

Lombi, E., M. Jonge, E. Donner, C. Ryan, and D. Paterson. 2011. Trends in hard x-ray fluorescence mapping: environmental applications in the age of fast detectors. Anal. Bioanal. Chem. 400: 1637-1634.

Lynam, M.M., J.T. Dvonch, J.A. Barres, M. Morishita, A. Legge, and K. Percy. 2015. Oil sands development and its impact on atmospheric wet deposition of air pollutants to the Athabasca Oil Sands Region, Alberta, Canada. Environ. Pollut. 206: 469-478.

Majumdar, S., J. Peralta-Videa, H. Castillo-Michel, J. Hong, C. Rico, and J. Gardea-Torresdey. 2012. Applications of synchrotron μ-XRF to study the distribution of biologically important elements in different environmental matrices: A review. Analytica Chemica Acta 755: 1-16.

MapCruzin. 2016. Download Free Canada Alberta ArcGIS GIS Shapefile Map Layers: Location GIS Shapefile. Available at <http://www.mapcruzin.com/free-canada-alberta-arcgis-maps-shapefiles.htm> (accessed June 2016).

Markovic, D.M., I.R. Milosevic, and D. Vilotic. 2013. Accumulation of Mn and Pb in linden (*Tilia platyphyllos* Scop.) bark and wood. Environ. Sci. Pollut. *Research* 20: 136-145.

Mou, D., Y. Yao, Y. Yang, Y. Zhang, C. Tian, V. Achal. 2011. Plant high tolerance to excess manganese related with root growth, manganese distribution and antioxidative enzyme activity in three grape cultivars. Ecotoxicol. Environ. Saf. 74: 776-786.

Nagajyoti, P.C., K.D. Lee, and T.V.M. Sreekanth. Heavy metals, occurrence and toxicity for plants: a review. 2010. Environ. Chem. Lett. 8: 199-216.

Nevel, L.V., J. Mertens, J. Staelens, A. D. Schrijver, F. M.G. Tack, S. D. Neve, E. Meers, and K. Verheyen. 2011. Elevated Cd and Zn uptake by aspen limits the phytostabilization potential compared to five other tree species. Ecol. Eng. 37: 1072-1080.

Oleksyn, J., K. Oleksynowa, E. Kozlowska, and L. Rachwal. 1987. Mineral content and sensitivity of black pine (*Pinus nigra*) of various provenances to industrial air pollution. For. Ecol. Manage. 21: 237-247.

Proemse, B., B. Mayer, and M. Fenn. 2012. Tracing industrial sulfur contributions to atmospheric sulfate deposition in the Athabasca oil sands region, Alberta, Canada. Appl. Geochem. 27: 2425-2434.

Proemse, B., B. Mayer, M. Fenn, and C. Ross. 2013. A multi-isotope approach for estimating industrial contributions to atmospheric nitrogen deposition in the Athabasca oil sands region in Alberta, Canada. Atmos. Environ. 60: 555-563.

Ressler, T., J. Wong, J. Roos, and I.L. Smith. 2000. Quantitative speciation of mn-bearing particulates emitted from autos burning (methylcyclopentadienyl) manganese tricarbonyl-added gasolines using xanes spectroscopy. Environ. Sci. Tech. 34:950–958

Roberts, T. 1984. Effects of air pollution on agriculture and forestry. Atmos. Environ. 18: 629-652.

Savard, M.M., C. Begin, and J. Marion. 2014. Modelling carbon isotopes in spruce trees reproduces air quality changes due to oil sands operations. Ecol. Indic. 45: 1-8.

Scharnweber, T., A. Hevia, A. Buras, E. van der Maaten, and M. Wilmking (in press). 2016. Common trends in elements? Within- and between-tree variations of wood-chemistry measured by X-ray fluorescence — A dendrochemical study. Sci. Tot. Environ.

Schindler, D. 2010. Tar sands needs solid science. Nature 468: 499 – 501.

Schindler, D.W. 2014. Unravelling the complexity of pollution by the oil sands industry. Proc. Natl. Acad. Sci. 111: 3209-3210.

Shparyk, P., and V. Parpan. 2004. Heavy metal pollution and forest health in the Ukrainian Carpathians. Environ. Pollut. 130: 55-63.

Simpson, I., N. Blake, B. Barletta, D. Diskin, H. Fuelberg, K. Gorham, L. Huey, S. Meinardi, F. Rowland, S. Vay, A. Weinheimer, M. Yang, and D. Blake. 2010. Characterization of trace gases measured over Alberta oil sands mining operations: 76 speciated C2 – C10 volatile organic compounds (VOCs), CO_2, CH_4, CO, NO, NO_2, NO_Y, and SO_2. Atmos. Chem. Phys. 10: 11931-11954.

Siwik, E., L. Campbell, and G. Mierle. 2010. Distributions and trends of mercury in deciduous tree cores. Environ. Pollut. 158: 2067-2073.

Smith, W. 1974. Air pollution- effects on the structure and function of the temperate forest ecosystem. Environ. Pollut. 6: 111-129.

Soil Classification Working Group. 1998. The Canadian System of Soil Classification, p. 187. Third Edition. Agriculture and Agri-Food Canada Publication 1646.

St. Clair, S.B., and J.P. Lynch. 2005. Element accumulation patterns of deciduous and evergreen tree seedlings on acid soils: implications for sensitivity to manganese toxicity. Tree Physiol. 25: 85-92.

U.S. Environmental Protection Agency. 1984. Health assessment document for manganese. Cincinatti, Ohio

Watmough, S. 1999. Monitoring historical changes in soil and atmospheric trace metal levels by dendrochemcial analysis. Environ. Pollut. 106: 391-403.

Watmough, S., and T. Hutchinson. 2003. A comparison of temporal patterns in trace metal concentration in tree rings of four common European tree species adjacent to a Cu-Cd refinery. Water Air Soil Pollut. 146: 225-241.

Yadav, S. 2010. Heavy metals toxicity in plants: an overview on the role of glutathione and phytochelatins in heavy metal stress tolerance of plants. S. Afr. J. Bot. 76: 167-179.

Zayed, J., B. Hong, and G. L'esperance. 1999. Characterization of manganese-containing particles collected from the exhaust emissions of automobiles running with MMT additive. Environ. Sci. Tech. 33:3341–3346

Zhang, C., B. Huang, J.D.A. Piper, and R. Luo. 2008. Biomonitoring of atmospheric particulate matter using magnetic properties of *Salix matsudana* tree ring cores. Sci. Tot. Environ. 393: *177-190.*

5. SYNTHESIS AND CONCLUSIONS

Trembling aspen and white spruce tree components (leaves, branches, roots, and cores) were extracted from three study locations circumambient to the AOSR. Soil samples were also collected from five different depth increments (leaf litter, 0 to 5 cm, 5 to 20 cm, 20 to 45 cm, and 45 to 60 cm) at these same locations. An upwind Control site was selected to represent baseline radial growth and baseline tree/soil elemental composition, within the region. Two downwind sites (Site 0 km and Site 50 km), were selected in areas suspected to receive aerial fallout from the AOSR, and were aligned with regional wind patterns. Site 0 km was located in closest proximity to the AOSR, whereas Site 50 km was located further downwind, approximately 50 km SE from the AOSR. All study locations contained dominantly similar site characteristics. Trembling aspen and white spruce stands at these sites were exposed to similar climate conditions, had similar soil-horizon distributions and qualitative (effervescence, coarse fragments, mottling) soil properties, similar topographies, grew in areas resistant to forest edge effects, and were sampled consistently at each site. Similar site characteristics and sampling regimes allowed for stand comparisons to be made.

Chapter three compared the radial growth of trembling aspen and white spruce trees at each site. More quantitative soil properties; including pH, soil organic carbon content, bulk density, and pH, were also assessed per depth increment per site. The aim of the dendrochronological assessment was to determine if aerial fallout from the AOSR was impacting the radial growth of trembling aspen and white spruce at the downwind sites. Physical soil properties were assessed to determine if soil properties varied per site, which can influence the radial growth of trembling aspen and white spruce trees, contrasting with potential influences derived from AOSR airborne contamination. Results illustrated a decline in radial growth occurring in white spruce stands near the last decade of growth at the downwind sites, but not at the Control site. My results complement Kershaw's (2013) findings illustrating a decline in radial growth in white spruce downwind from the AOSR that is more severe in sites in closer proximity to the AOSR. The radial-growth declines occurring in white spruce at Site 0 km were more severe and occurred earlier compared to Site 50 km's radial-growth declines. These results were generated from the broken-stick model and master chronologies, representative of the average growth at each site over time for each species. The severity of radial-growth declines at

the downwind sites in white spruce, match previously proposed patterns of aerial fallout, which found airborne pollutants concentrations to increase at sites closer to the AOSR. My dendrochronological assessment suggests that long-term aerial deposition accumulated to a threshold point, and thereafter caused a decline in radial growth in white spruce at the downwind sites. The severity of radial-growth declines appear to be spatially dependent on the concentration of aerial deposition in the atmosphere. Radial-growth declines cannot be attributed to varying soil properties because pH, organic carbon content, bulk density, and texture were similar per depth increment per site. Other factors that can cause radial-growth declines, including fire out breaks, insect infestations, pathogens, climate and topography variations, age, competition, and nutrient deficiencies or toxicities were discussed, concluding that nutrient deficiencies or toxicities are the most probable factor causing radial-growth declines in white spruce at the downwind sites. A drier climate manifesting over the past decade may also attribute to radial-growth declines in white spruce.

Chapter four compared the elemental composition of soils, and trembling aspen and white spruce tree media, per site. Aerial deposition, from the AOSR, could potentially input greater quantities of elements, and/or pollutants, into surrounding ecosystems altering ambient nutrient cycles in tree media and soils, leading to nutrient toxicities or deficiencies. Enrichment of particular elements (if any) in the downwind sites compared to the Control site was sought out. Enrichment of element(s) in the downwind sites could potentially explain the decline in radial growth occurring in white spruce at these sites. The elemental assessment could also explain species-different radial-growth responses occurring between trembling aspen and white spruce. Eight elements were consistently identified through an XRF analysis, in all soil and tree media including K, Ni, Ca, Mn, Cr, Fe, Zn, and Ti. The XRF assessment revealed elevated amounts of Mn in the majority of white spruce and trembling aspen tree components at the downwind sites compared to the Control site. Mn was also elevated in the topsoil's (leaf litter and 0 to 5 cm depth increment) at the downwind sites compared to the Control site. Tree species comparisons revealed elevated amounts of Mn in the majority of white spruce tree materials at all sites (Site 0 km, Site 50 km, and the Control site) compared to trembling aspen. In other studies, the aerial deposition of Mn, attributed to AOSR activities, followed previously-mentioned spatial patterns; Mn increased in sites closer to the AOSR. The topsoil's Mn distribution in this study complements previous research and illustrates increasing Mn amounts

at sites in closer proximity to the AOSR. The dendrochemical assessment determined an increase in Mn from 1988 onward, in Site 0 km cores compared to the Control site cores, a trend not normally found in unpolluted cores of the same genus. The accumulation of Mn in white spruce cores generally follows increasing production trends within the AOSR, with translocation between tree rings possibly skewing some temporal accuracy. Site 50 km's cores were anomalous to Site 0 km and the Control site's cores, illustrating greater Mn baseline fluorescence overall predating AOSR commercial production.

Excess Mn is known to be toxic to trees at cellular to physiological levels, suggesting that excess Mn in white spruce tree media and cores at the downwind sites may be causing the decline in their radial growth. Findings from chapter four suggest that Mn deposition dominantly follows previously-described patterns of AOSR aerial deposition and that Mn enrichment at the downwind sites may be causing a decline in radial growth in white spruce. Mn accumulated more in white spruce tissues compared to trembling aspen tissues, suggesting that white spruce is more prone to Mn toxicity, possibly explaining species-different radial-growth responses. The cumulative impact of a drier climate, shallow root systems, the aerial deposition of Mn and/or other toxic metals, and genetic variations between tree species may more fully explain radial-growth declines occurring in white spruce, compared to trembling aspen, at the downwind sites.

XANES revealed that Mn is the same in white spruce tree media and exists as aqueous and organic Mn (II). Leaf litter Mn is different and likely exists as Mn (III/IV)-oxides a change attributed to natural plant-soil processes, industrial pollutants, or anthropogenic sources. The remaining seven elements did not show a distinct pattern, as was seen with Mn. Enrichment of these elements did occur in some tree media at some downwind sites, which complements previous studies that have found enrichment of these elements within a 50 km radius of the AOSR. These other enriched elements may also contribute to radial-growth declines in white spruce at the downwind sites, alongside Mn, and Mn contamination may only be part of the problem.

In general, this study has some inherent limitations. XRF was only able to assess 18 elements. The aerial deposition of other elements, not assessed in this study, has occurred within a 50 km radius of the AOSR. Other elements, such as heavy metals, are known to hinder tree growth and function. This study was unable to distinguish if radial-growth declines were caused by Mn alone, or by other unstudied elements. Future research should assess the relative

fluorescence counts of other elements using the same beamline parameters as in this study to better understand radial-growth declines that are occurring. XRF results portray elemental information at very small scale (molecular), and were only able to determine relative fluorescence counts of elements per sample, which were not correlated to particular concentrations, a chemical parameter more commonly used in other research. Future studies should determine the relative concentrations of Mn and other elements in white spruce tree media and soils downwind from the AOSR. Future studies should also correlate fluorescence counts to concentrations using a calibration curve in white spruce tree media and soils downwind from the AOSR. These research contributions will to allow for better research comparisons to be made.

Another major limitation of this study is that only three sites were chosen and only one tree from each site was assessed using XRF. Expanding my dendrochronological assessment and synchrotron (XRF, XANES) assessment to include more study sites, within the 50 km zone of airborne pollutant enrichment and beyond the 50 km zone of enrichment, will increase our understanding of AOSR pollution extent and long-term impacts on the surrounding forests. Increasing the sample size of trees assessed through XRF will also increase our understanding of the relative variations of Mn (or other elements) fluorescence that exists within trembling aspen and white spruce tree components, possibly explaining the apparent anomalies in the dendrochemcial assessment at Site 50 km. The dendrochemical variation of elemental fluorescence of boreal forest trees species, including trembling aspen and white spruce, is unknown to date and remains a large area of potential future research.

XRF is prone to some types of error, as with any tool used to assess the chemical properties of environmental media. Error, in this study, may result from absorbing and scattering effects of synchrotron light onto a sample, potentially skewing fluorescence count accuracy to some extent. Minor inconsistencies in thickness and density may exist between ground pellets and soil samples, which may further skew fluorescence count accuracy to some extent. Future studies should directly measure thicknesses and densities of their samples to quantify potential errors.

This study provides potentially useful information to Alberta's oil sands reclamation teams and local forestry companies. Aerial deposition from Alberta's oil sands activities may be contaminating white spruce trees downwind, and at minimum within a 50 km radius, of the

AOSR. Mn release, from the AOSR, may be a potential contaminant causing radial-growth declines in white spruce, although only speculations of Mn toxicity can be made at this time since anomalies and unknowns still exists within these hypotheses. Alberta's oil sands are required to reclaim land and any associated forest species that have been impacted by their activities. Trembling aspen appears to be more tolerant to aerial fallout than white spruce. The installation of air-pollution-control technologies, such as smoke-stack filters, and dust-collecting fences or more enclosed mining areas are other possible solutions.

In terms of forestry, aerial deposition may be reducing the value of merchantable timber, meaning a loss in resources and profits. Forestry companies should be cautious in their management strategies of forests areas near oil refineries or industrial areas that emit similar air pollution.

Finally, it is important to note that time is an important factor when considering pollutant accumulation of any kind. In the AOSR, air emissions, and subsequent deposition, is ongoing and, over time, may accumulate to levels that become toxic to other forest species and ecosystem components, at a minimum of a 50 km radius from the AOSR. It is therefore recommended that forests and other ecosystem components surrounding the AOSR be monitored over the long term, especially while oil sands production continues to expand.

APPENDIX A:

SOIL PIT DESCRIPTIONS

Table A.1 Soil pit descriptions for the Control site following the Canadian System of Soil Classification. Pit depth ranged from 55 to 65 cm and widths of 45 to 60 cm. R = Rounded; S = Sub-rounded; A = Angular. vw = very weak; w = weak; m = moderate; s = strong.

Pit	Horizon Desig.	Horizon Depth	Hand-Texture	Color	Mottle Color	Coarse Fragments	Effervescence	Notes
		cm		(Value/ Chroma)	(Value /Chroma)	% + (R, S, A)	(vw, w, m, s)	
1	LFH	6 – 0	-	-	-	1% + S	none	-
	Ah	0 – 4	loam	4/2 10 YR	none	1% + S	none	-
	Ae	4 – 10	clay loam	6/2 10 YR	none	none	none	-
	Bt1	10 – 23	clay	4/3 10 YR	none	none	vw	Mottled sand pocket present
	Bt2	23 +	clay	4/2 10YR	4/6 7.5 YR	none	none	-
2	LFH	6 – 0	-	-	-	none	none	-
	Ah	0 – 2	loam	4/2 10YR	none	none	none	-
	Ae	2 – 8	clay loam	6/2 10 YR	none	none	m	-
	Bt	8 – 51	clay	4/3 10 YR	4/6 10 YR	none	w	-
	C	51 +	clay	3/3 10 YR	none	none	none	-
3	LFH	14 – 0	-	-	-	none	none	-
	Ah	0 – 5	loam	4/2 10 YR	none	none	none	-
	Ae	5 – 23	clay loam	6/2 10 YR	none	none	vw	-
	Bm	23 – 35	sandy clay loam	5/3 10 YR	none	none	vw	-
	Bt	35 +	clay	4/2 10 YR	5/6 5 YR	none	none	-
4	LFH	7 – 0	-	-	-	none	none	-
	Ah	0 – 7	loam	4/2 10YR	none	none	none	-
	Ae	7 – 13	clay loam	3/1 10 YR	none	1% + S	vw	-
	BC	13+	clay	3/2 10 YR	3/4 5 YR	1% + S	vw	-

Table A.2 Soil pit descriptions for Site 50 km following the Canadian System of Soil Classification. Pit depth ranged from 55 to 65 cm and widths of 45 to 60 cm. R = Rounded; S = Sub-rounded; A = Angular. vw = very weak; w = weak; m = moderate; s = strong.

Pit	Horizon Desig.	Horizon Depth	Hand-Texture	Color	Mottle Color*	Coarse Fragments	Effervescence	Notes
		cm		(Value/ Chroma)	(Value /Chroma)	% + (R, S, A)	(vw, w, m, s)	
1	LFH	5 – 0	-	-	-	none	none	-
	Ah	0 – 5	loam	4/2 10 YR	none	none	none	-
	Ae	5 – 15	clay loam	5/4 10 YR	none	5% + S	vw	Buried organic horizon
	Bt	15 – 45	clay	4/4 10 YR	none	10% + S	none	-
	C	45 +	clay	4/2 10YR	4/6 7.5 YR	5% + S	none	-
2	LFH	4 – 0	-	-	-	none	none	-
	Ah	0 – 4	loam	4/2 10YR	none	none	none	-
	Ae	4 – 15	clay loam	7/2 10 YR	none	none	vw	-
	Bt	15 – 50	clay	4/4 10 YR	none	2% + S	none	-
	C	50 +	clay	3/3 10 YR	4/6 7.5 YR	none	none	-
3	LFH	4 – 0	-	-	-	none	none	-
	Ah	0 – 2	loam	4/2 10 YR	none	none	none	-
	Ae	2 – 12	clay loam	6/3 10 YR	none	25% + S	none	Large rocks present
	Bt	12 – 31	clay	4/6 10 YR	none	25% + S	none	-
	C	31 +	clay	4/3 2.5 YR	4/6 7.5 YR	10% + S	none	-
4	LFH	6 – 0	-	-	-	none	none	-
	Ah	0 – 3	loam	4/2 10YR	none	none	none	-
	Ae	3 – 14	clay loam	4/3 10 YR	none	1% + S	vw	-
	Bt	14+	clay	5/3 10 YR	none	1% + S	none	-

Table A.3 Soil pit descriptions for Site 0 km following the Canadian System of Soil Classification. Pit depth ranged from 55 to 65 cm and widths of 45 to 60 cm. R = Rounded; S = Sub-rounded; A = Angular. vw = very weak; w = weak; m = moderate; s = strong.

Pit	Horizon Desig.	Horizon Depth	Hand-Texture	Color	Mottle Color*	Coarse Fragments	Effervescence	Notes
		cm		(Value/ Chroma)	(Value /Chroma)	% + (R, S, A)	(vw, w, m, s)	
1	LFH	10 – 0	-	-	-	none	none	-
	Ah	0 – 5	loam	4/2 10 YR	none	none	none	-
	Ae	5 – 20	clay loam	7/2 10 YR	none	2% + S	vw	-
	Bt	20 +	clay	4/4 10 YR	6/8 10 YR	2% + S	none	-
2	LFH	5 – 0	-	-	-	none	none	-
	Ah	0 – 4	loam	4/2 10YR	none	none	none	-
	Ae	4 – 17	clay loam	6/2 10 YR	none	none	vw	-
	Bt1	17 – 41	clay loam	5/4 10 YR	none	none	vw	-
	Bt2	41 +	clay	4/4 10 YR	none	none	none	-
3	LFH	11 – 0	-	-	-	none	none	-
	Ah	0 – 5	loam	4/2 10 YR	none	none	none	-
	Ae	5 – 23	clay loam	6/2 10 YR	none	5% + S	vw	-
	Bt1	23 – 32	clay loam	5/3 10 YR	none	5% + S	vw	-
	Bt2	32 +	clay	4/4 10 YR	none	5% + S	none	-
4	LFH	5 – 0	-	-	-	none	none	-
	Ah	0 – 5	loam	4/2 10YR	none	none	none	-
	Ae	5 – 17	clay loam	6/2 10 YR	none	2% + S	vw	-
	Bt	17 +	clay	4/3 10 YR	none	2% + S	none	-

APPENDIX B:

RAW AND STANDARDIZED RING-WIDTHS PER SITE

Table B.1 Master Chronologies depicting average annual-radial growth per site. Raw = raw average ring-widths measured with a microscope and J2X staging system; Std = average ring-widths standardized with ARSTAN.

	Spruce Control		Aspen Control		Spruce Site 50 km		Aspen Site 50 km		Spruce Site 0 km		Aspen Site 0 km	
Year	Raw	Std	Raw	Std	Raw	Std	Raw	Std	Raw	Std	Raw	Std
1904							1.401	0.937				
1905							1.427	0.83				
1906							1.677	1.221				
1907							1.642	0.955				
1908							1.874	1.041				
1909							2.328	1.131				
1910			1.038	0.491			1.693	0.912				
1911			1.99	0.979			1.945	0.975				
1912			1.457	0.712			2.073	0.993				
1913			1.979	1.015			1.413	0.771				
1914			2.023	0.835			2.112	1.093				
1915			2.663	1.173			2.374	1.292				
1916			2.545	1.123			1.67	0.755				
1917			1.983	0.892			1.46	0.716				
1918			2.143	0.995	2.282	0.783	2.024	1.067				
1919			2.106	0.987	1.931	1.301	1.695	0.943				
1920			1.964	0.942	2.291	1.034	1.857	1.042				
1921			1.292	0.646	1.957	1.015	1.845	1.056				
1922			1.411	0.7	2.079	0.959	1.868	1.125				
1923			2.368	1.102	2.084	0.983	1.493	0.904				
1924			1.809	0.831	1.959	0.943	1.494	0.881				
1925	9.36	1.122	2.189	1.018	1.721	0.847	1.317	0.823				
1926	5.056	0.798	2.182	1.007	1.118	0.561	1.472	0.917				

1927	4.32	0.872	2.456	1.102	1.958	0.985	0.961	0.617			2.654	0.926
1928	3.853	0.966	2.553	1.149	2.034	1.004	1.196	0.754			1.98	0.697
1929	2.68	0.974	2.38	1.101	2.324	1.08	1.819	1.195			3.575	1.186
1930	2.686	1.026	2.673	1.194	2.187	0.949	1.725	1.165			4.501	1.378
1931	2.163	0.936	2.641	1.189	2.402	1.139	1.898	1.297			2.937	0.978
1932	2.262	1.399	2.779	1.285	2.137	1.011	1.918	1.307			2.978	1.029
1933	1.99	1.253	2.739	1.353	1.95	0.918	1.907	1.356			2.56	0.893
1934	2.296	1.092	2.388	1.139	2.137	1.018	1.634	1.171			2.42	0.879
1935	2.026	1.064	2.258	1.107	2.537	1.191	2.086	1.442			1.987	0.714
1936	1.819	0.982	2.328	1.176	2.397	1.158	1.799	1.323			2.614	0.917
1937	2.053	1.129	2.087	1.051	1.7	0.824	2.243	1.684			1.73	0.665
1938	1.972	0.917	2.55	1.349	1.479	0.709	1.152	0.872			1.444	0.577
1939	1.908	0.929	1.662	0.972	1.604	0.79	1.096	0.845			1.37	0.558
1940	1.928	0.983	1.639	0.961	1.632	0.817	1.325	1.018			1.669	0.675
1941	1.455	0.685	1.284	0.779	1.399	0.684	1.43	1.135			0.218	0.071
1942	2.14	0.946	1.474	0.89	1.709	0.823	0.655	0.526			0.608	0.268
1943	1.936	0.932	0.581	0.358	1.39	0.669	0.622	0.538			1.789	0.795
1944	2.587	1.14	0.294	0.19	1.779	0.88	0.454	0.374			2.053	0.934
1945	2.497	1.098	0.769	0.503	1.977	0.99	0.49	0.413			3.153	1.345
1946	2.467	1.091	1.385	0.9	2.357	1.158	0.99	0.852			3.211	1.499
1947	2.293	1.08	1.759	1.15	2.335	1.223	1.118	0.977			3.685	1.62
1948	1.88	0.845	1.676	1.089	1.68	0.887	1.483	1.308			2.781	1.375
1949	2.327	1.052	1.797	1.174	2.074	1.133	1.177	1.04			3.563	1.628
1950	2.709	1.045	1.672	1.141	1.892	1.011	1.007	0.952			2.568	1.226
1951	2.27	1.013	1.549	1.037	2.01	1.072	1.175	1.069			2.672	1.086
1952	1.757	0.812	1.822	1.264	1.693	0.871	1.078	1.03			3.058	1.182
1953	2.248	0.933	1.408	0.985	1.866	0.95	1.049	0.979	1.676	0.516	2.545	0.926
1954	2.301	0.973	1.349	0.954	2.03	1.047	0.542	0.517	2.723	0.904	2.495	0.927
1955	2.555	1.09	1.305	0.917	2.266	1.166	1.023	0.959	2.674	0.91	2.321	0.875
1956	2.461	1.01	1.799	1.297	1.988	1.052	1.083	1.026	2.004	0.686	3.296	1.368

1957	1.739	0.687	1.592	1.161	2.06	1.127	1.383	1.37	2.486	0.869	3.057	1.293
1958	2.339	0.97	1.471	1.066	1.738	0.958	1.682	1.635	2.071	0.746	2.052	0.876
1959	2.153	0.889	1.605	1.173	1.687	0.916	1.059	1.04	2.158	0.767	2.398	1.012
1960	2.24	0.891	1.834	1.385	1.931	1.07	0.906	0.922	2.656	0.984	3.147	1.32
1961	1.822	0.72	1.489	1.083	1.346	0.749	1.361	1.336	2.488	0.901	1.528	0.679
1962	2.744	1.139	1.586	1.162	1.643	0.915	1.534	1.572	2.575	0.949	2.597	1.129
1963	2.767	1.109	1.989	1.489	1.974	1.084	1.106	1.138	2.48	0.943	2.444	1.097
1964	2.837	1.165	0.476	0.381	1.493	0.854	0.39	0.397	2.678	1.052	2.326	1.051
1965	2.903	1.253	0.861	0.758	1.963	1.075	0.539	0.558	2.31	0.941	2.31	1.053
1966	2.399	1.023	1.5	1.187	1.99	1.108	0.878	0.937	2.173	0.837	1.978	0.958
1967	2.115	0.885	1.602	1.253	1.771	1.019	0.891	0.939	2.173	0.862	2.132	1.088
1968	2.111	0.911	1.55	1.232	1.798	1.038	1.053	1.128	2.305	0.894	1.974	1.044
1969	2.389	0.962	1.379	1.103	1.651	0.988	1.039	1.094	2.09	0.874	1.546	0.774
1970	2.122	0.846	1.166	0.899	1.766	1.042	0.678	0.727	2.214	0.902	1.643	0.99
1971	2.266	0.927	1.294	1.017	1.904	1.139	0.882	0.97	2.294	1.016	2.287	1.257
1972	2.133	0.859	1.389	1.146	1.561	0.969	1.07	1.221	2.281	1.042	1.822	1.043
1973	2.123	0.864	1.642	1.297	1.817	1.088	0.971	1.081	2.721	1.203	2.034	1.165
1974	2.452	0.975	1.387	1.111	1.944	1.216	0.802	0.925	2.718	1.228	1.794	1.046
1975	2.518	1.027	1.488	1.19	2.218	1.385	0.969	1.088	3.162	1.438	2.207	1.311
1976	2.962	1.213	1.549	1.244	2.294	1.451	1.293	1.482	3.306	1.562	2.279	1.415
1977	3.04	1.252	1.82	1.485	1.81	1.145	1.411	1.743	2.735	1.284	2.021	1.281
1978	2.777	1.133	1.682	1.388	1.56	1.001	1.327	1.478	2.518	1.272	1.599	1.035
1979	2.351	0.98	0.298	0.244	1.567	1.032	0.885	1.017	2.523	1.219	1.265	0.836
1980	1.968	0.823	0.155	0.155	1.328	0.861	0.788	0.863	2.177	1.072	1.214	0.796
1981	2.626	1.088	0.151	0.173	1.34	0.886	0.805	0.897	2.235	1.092	0.757	0.512
1982	1.832	0.762	0.268	0.324	1.184	0.789	0.593	0.675	1.535	0.806	0.323	0.228
1983	1.962	0.808	0.373	0.331	1.169	0.791	0.382	0.429	1.551	0.829	0.414	0.293
1984	3.107	1.292	0.586	0.466	1.239	0.839	0.395	0.466	1.896	1.013	0.859	0.636
1985	2.815	1.194	0.503	0.499	1.315	0.932	0.73	0.888	1.929	1.053	1.276	0.94
1986	2.896	1.24	1.017	0.853	1.226	0.878	0.894	1.057	2.003	1.11	1.285	1.002

1987	2.525	1.078	1.385	1.171	1.044	0.758	1.019	1.195	1.784	1.027	1.267	0.962
1988	2.846	1.212	1.208	0.991	1.322	0.969	0.707	0.869	1.875	1.12	1.518	1.179
1989	3.003	1.295	1.554	1.278	1.573	1.176	0.788	0.983	1.984	1.212	1.188	0.96
1990	2.699	1.164	1.315	1.107	1.642	1.296	0.84	1.014	1.841	1.127	1.174	0.968
1991	2.897	1.243	1.388	1.226	1.787	1.385	0.887	1.089	1.988	1.245	1.327	1.09
1992	2.669	1.15	1.499	1.312	1.776	1.363	0.901	1.098	1.854	1.223	1.269	1.08
1993	2.598	1.128	1.296	1.157	1.83	1.408	0.907	1.124	1.966	1.308	1.352	1.192
1994	2.668	1.177	1.375	1.225	1.577	1.267	1.018	1.339	1.984	1.353	1.053	0.953
1995	2.028	0.89	1.241	1.104	0.947	0.757	0.823	1.017	1.214	0.931	0.887	0.82
1996	2.334	1.054	1.024	0.954	1.604	1.308	0.672	0.827	1.657	1.234	1.204	1.125
1997	2.339	1.077	0.837	0.793	1.761	1.502	0.884	1.168	1.602	1.225	1.259	1.213
1998	2.351	1.065	1.206	1.158	1.369	1.194	0.856	1.123	1.541	1.218	1.065	1.034
1999	1.515	0.675	1.317	1.278	0.88	0.772	0.632	0.854	0.874	0.737	0.558	0.565
2000	1.769	0.798	0.847	0.785	1.058	0.917	0.504	0.664	1.055	0.88	0.844	0.837
2001	2.037	0.912	0.582	0.602	0.966	0.866	0.665	0.882	0.965	0.845	1.161	1.24
2002	1.412	0.643	0.425	0.441	0.718	0.617	0.725	0.975	0.742	0.704	1.016	1.129
2003	2.102	0.942	0.35	0.384	1.149	1.01	0.603	0.8	1.022	0.966	1.436	1.573
2004	1.707	0.804	0.567	0.658	0.974	0.916	0.517	0.697	0.842	0.841	0.822	0.914
2005	1.789	0.826	0.736	0.69	0.942	0.92	0.519	0.735	0.774	0.813	0.759	0.856
2006	1.949	0.928	0.749	0.675	0.93	0.922	0.551	0.741	0.65	0.729	0.907	1.019
2007	2.011	0.948	1.008	1.002	0.826	0.872	0.483	0.683	0.654	0.745	0.292	0.357
2008	2.064	1.005	0.904	0.98	0.706	0.77	0.186	0.286	0.561	0.682	0.188	0.218
2009	1.857	0.914	0.944	1.123	0.622	0.702	0.298	0.445	0.377	0.48	0.509	0.607
2010	2.102	1.004	0.697	0.778	0.613	0.693	0.628	0.917	0.358	0.494	0.909	1.106
2011	2.174	1.023	0.711	0.793	0.428	0.508	0.954	1.393	0.159	0.258	0.914	1.128
2012	2.102	1.022	0.58	0.726	0.43	0.504	1.007	1.524	0.199	0.332	0.846	1.052
2013	1.451	0.713	0.932	0.973	0.524	0.537	0.678	1.012	0.219	0.432	0.497	0.728
2014	1.846	0.912	0.681	0.774	0.599	0.651	0.857	1.093	0.268	0.477	0.624	0.891

APPENDIX C:

BROKEN-STICK MODEL RESULTS FOR TREMBLING ASPEN

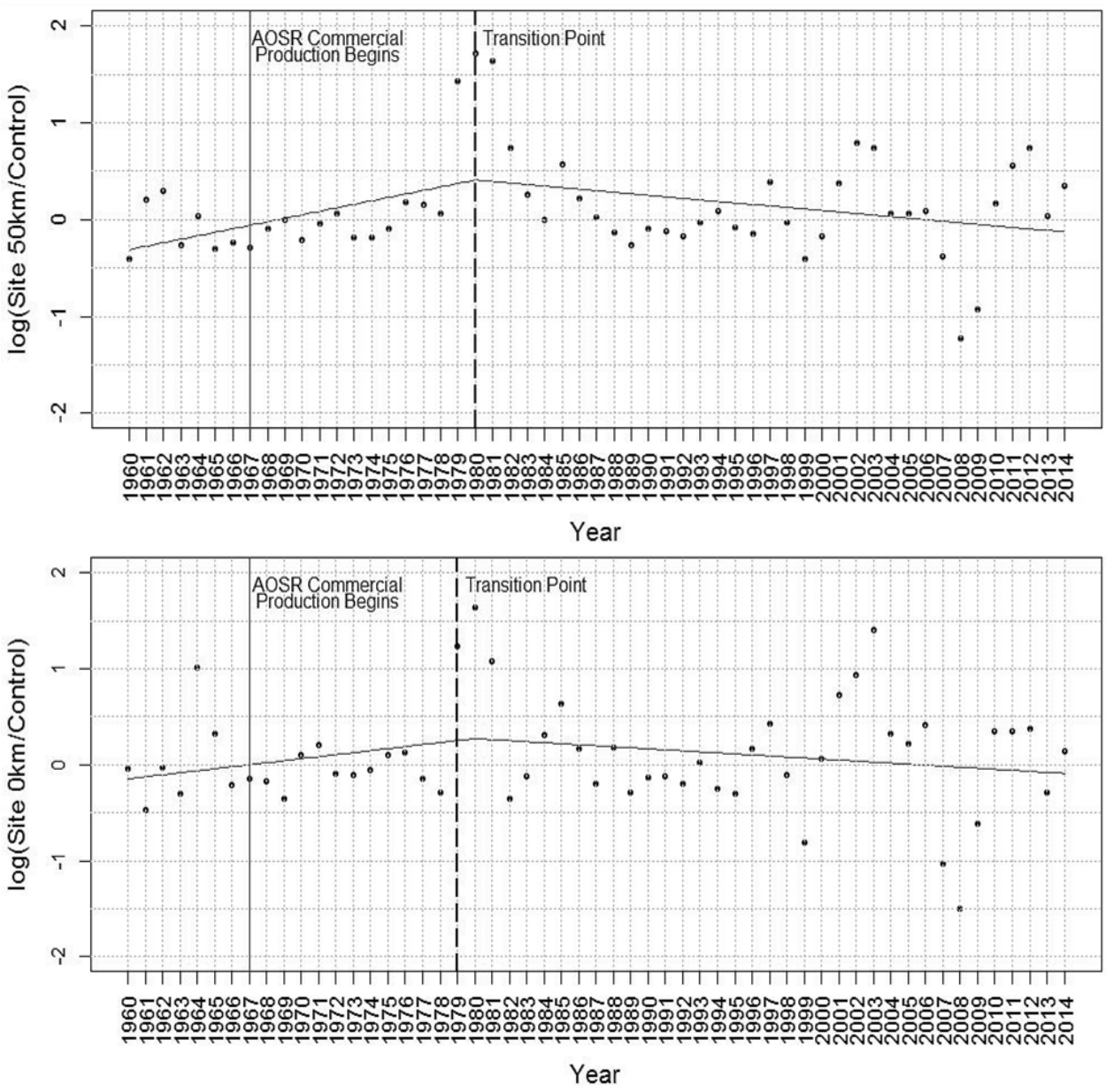

Figure C.1 Broken-stick model results for trembling aspen Site 50 km and Site 0 km. The black dots represent individual change points per year. The top graph illustrates change points for trembling aspen at Site 50 km. The bottom graph illustrates change points for trembling aspen at Site 0 km. The slashed-black vertical line indicates the transition or threshold point and the beginning of the second slope.

APPENDIX D:

KRUSKAL-WALLIS STATISTICAL RESULTS

Table D.1 Kruskal-Wallis rank sum test for each soil parameter (pH, bulk density, organic carbon, sand, silt, and clay) by site (Site 0 km vs Site 50 km vs the Control site). Bolded values represent statistically significant results (p-value < 0.05).

Soil Parameter	Degrees of freedom	Chi-squared	Significance (p-value)
Bulk Density	2	2.4876	0.2883
% Organic Carbon (Leaf Litter)	2	1.3846	0.5004
% Organic Carbon (0 to 5 cm)	2	7.0385	**0.02962**
% Organic Carbon (5 to 20 cm)	2	5.8077	0.05481
% Organic Carbon (20 to 45 cm)	2	4.2842	0.1174
% Organic Carbon (45 to 60 cm)	2	0.2692	0.8741
pH (0 to 5 cm)	2	0.9939	0.6084
pH (5 to 20 cm)	2	1.4231	0.4909
pH (20 to 45 cm)	2	1.0769	0.5836
pH (45 to 60 cm)	2	2.3462	0.3094
% Sand (0 to 5 cm)	2	8.3462	**0.0154**
% Sand (5 to 20 cm)	2	2.1923	0.3342
% Sand (20 to 45 cm)	2	0.4615	0.7939
% Sand (45 to 60 cm)	2	0.4615	0.7939
% Clay (0 to 5 cm)	2	9.8462	**0.007277**
% Clay (5 to 20 cm)	2	7.7308	**0.02095**
% Clay (20 to 45 cm)	2	0.4615	0.7939
% Clay (45 to 60 cm)	2	2.5769	0.2757
% Silt (0 to 5 cm)	2	6.2692	**0.04352**
% Silt (5 to 20 cm)	2	0.7308	0.6939
% Silt (20 to 45 cm)	2	2.4615	0.2921
% Silt (45 to 60 cm)	2	1.8846	0.3897

Table D.2 Post-hoc test (Dunn test) results of soil parameters by site that are statistically significant in the Kruskal-Wallis rank sum test; **a)** % Silt (0 to 5 cm), **b)** % Clay (0 to 5 cm), **c)** % Clay (5 to 20 cm), **d)** % Sand (0 to 5 cm), and **e)** % Organic carbon (0 to 5 cm). Bolded values represent statistically significant results (p-values < 0.05).

a)	p – value
Site 0 km vs Control	**0.0071**
Site 50 km vs Control	0.2164
Site 50 km vs Site 0 km	**0.0478**
b)	
Site 0 km vs Control	**0.0009**
Site 50 km vs Control	0.0583
Site 50 km vs Site 0 km	0.0583
c)	
Site 0 km vs Control	**0.0041**
Site 50 km vs Control	**0.0197**
Site 50 km vs Site 0 km	0.2781
d)	
Site 0 km vs Control	**0.0022**
Site 50 km vs Control	0.1634
Site 50 km vs Site 0 km	**0.0312**
e)	
Site 0 km vs Control	**0.0041**
Site 50 km vs Control	0.0707
Site 50 km vs Site 0 km	0.1197

APPENDIX E:

ANNUAL PRECIPITATION IN FORT MCMURRAY, AB

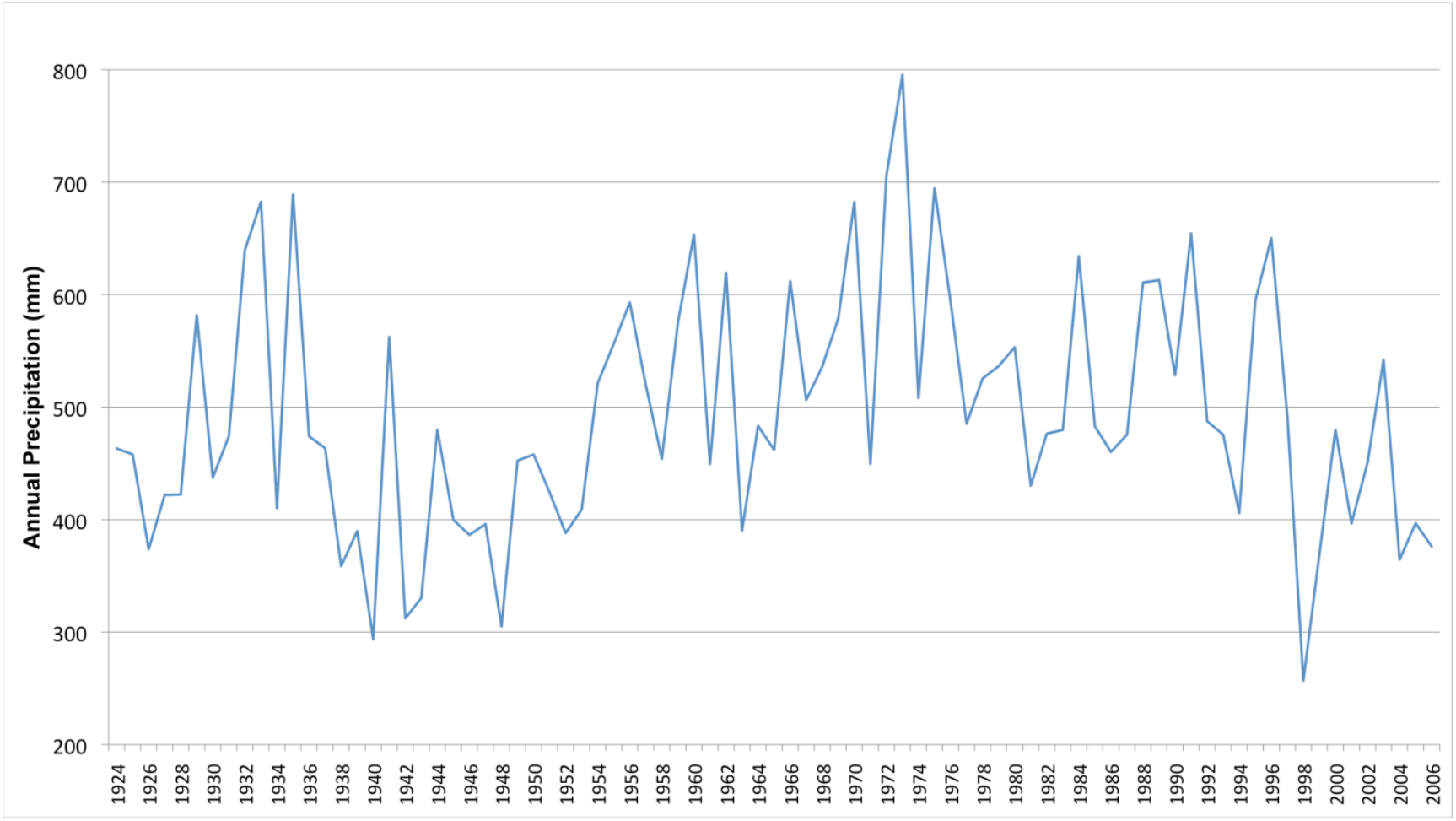

Figure E.1 Average annual precipitation in Fort McMurray, Alberta from 1924 to 2006.

APPENDIX F:

PROTOCOL TO MAKE PELLETS AND SOILS FOR SYNCHROTRON (XRF, XANES) ANALYSIS WITH IMAGES

1. Dry samples

- Dry leaves, branches, and subsets of soil in brown paper bags in an oven for 48 hours at 40ºC.
- Separate leaves from branches after drying
- Air-dry 12 mm cores, and roots for one month

***2.* Process 12 mm cores and roots**

- Slice 12 mm core into 0.5 cm increments using a stainless steel blade. We used a mini guillotine to assist with core placement and cutting (Figure C.1)
- Slice core from bark to pith and place each core section into separate plastic-capped vials with appropriate labels (CB0, CB1, CB2… etc).
- Saw root section in half with table saw (or other)
- Hand-gouge roots into three sections; first remove root bark, then inner root, then the pith (Figure C.2)
- Place shavings into plastic-capped vials with appropriate labels

3. Grind tree media

- Change the Retch® Ultra Centrifuge Mill ZM 200 ring sieve to 0.25mm (Figure C.3)
- Set Retch® to an rpm of 14,000 then start spinning the machine's blades
- After rpm maximum is reached, drop root shavings, leaves, braches, and individual core segments into Retch® chamber, individually
- Stop the machine and remove its contents into plastic-capped vials. I used a paint brush to transfer powders from the Retch® sample chamber into vials
- Clean machine blades and sieve (or other parts if necessary) with high-pressure air
- Clean machine blades per site with soap, water, and paper towel
- Repeat until all sites and samples are ground

4. Grind soil

- Remove rocks from dried soil with a 2 mm mesh sieve
- Grind dried soil, by hand or automated, using a ceramic mortar and pestle
- Grind soil into a very fine powder until it can visibly become no smaller
- Transfer soil into plastic-capped vial

5. Creating pellets out of ground tree media

- Weigh 25 mg (±.1) of ground tree material into plastic weigh boat (Figure C.4)
- Transfer material into ICL ® 13mm KBr stainless steel die set and manipulate tree material by hand so that tree material is evenly spread over the die
- Press into pellet using a Carver ® 4350 bench top laboratory manual press (or other) for 7 tonnes of pressure for 2 minutes (or a consistent time and pressure period)
- Measure densities of pellets or ground material if possible
- Place pellet back into plastic weight boat until XRF analysis (Figure C.4)

6. Place soils into sample holders

- Obtain Teflon ® sample holders with consistent horizontal slit dimensions (Figure C.5)
- Tape one side of slit with Kapton ® pure, metal-free tape
- Place soil into sample holder over tape
- Tape other side of slit to enclose the soil sample

7. Scan pellets and soils using XRF and XANES on the IDEAS beamline

- Set IDEAS beamline to parameters specified in this study before scanning, to allow for study comparisons

- Carefully tape (masking tape) an edge of a pellet and soil holders onto automated sample holder into a flat position
- Scan bottom, middle, and top of pellet (do not scan too close to the edge of a pellet to avoid scanning the tape)

7. 1. Beamline parameters:

XRF:

- Scan time: 180 s
- Dead time: between 10% - 40%
- Sample slit width: 1.5 mm
- Sample slit height: maximum (~3 mm)
- Ketek mode: highest resolution/low count rate
- Monochromator crystal: GE 220 (DCM)
- Ketek peaking time: 2 µs

XANES:

- Scan time: 15 min 17 s
- Dead time: between 10% - 40%
- I0 amplifier sensitivity: 100 nA/V
- Sample amplifier sensitivity: 20 nA/V
- Reference amplifier sensitivity: 100 pA/V
- Sample slit width: 1.5 mm
- Sample slit height: maximum (~3 mm)
- Ketek mode: lowest resolution/highest count rate
- Monochromator crystal: GE 220 (DCM)
- Ketek peaking time: 0.3 µs

8. Normalize and average XRF and XANES data

- XRF was normalized to the incoming beamline intensity (I0) per sample in OriginPro (with help from experts) following the equation:
- Normalized XRF values were averaged per tree media per site

$$Dead\ time\ Corrected\ Sample\ Fluorescence\ Counts\ \times \left[\frac{Maximum\ I0}{Sample\ I0}\right] = Normalized\ Fluorescence$$

$$I0 = the\ ion\ chamber\ current\ (flux\ intensity)$$

- XANES was normalized using a program called Athena (with help from experts)

F**igure F.1** Image of 0.5 cm sliced 12 mm cores using constructed guillotine and razor blade.

Figure F.2 Image of half of a mature root sliced with a stainless-steel hand gouger into three root layers. From left to right are half a root, root bark, outer root, and inner root materials.

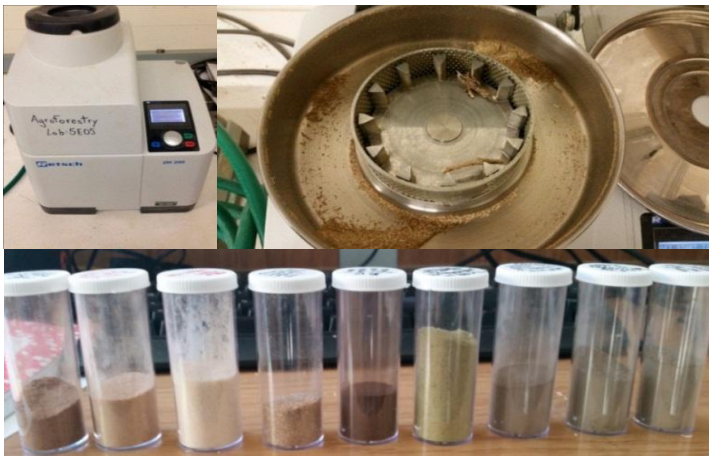

Figure F.3 The topleft image is the Retch® Ultra Centrifuge Mill ZM 200. The topright image is the Retch® stainless steel blades, ring sieve, and sample chamber. The bottom image is resulting ground tree and soil materials in plastic-capped vials.

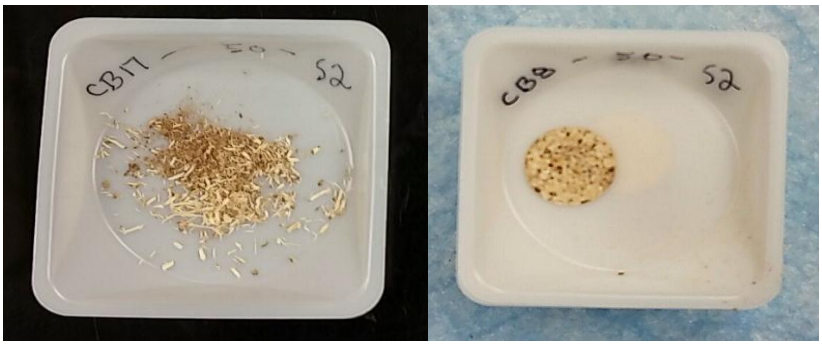

Figure F.4 Image of 25 mg of ground tree material (left) and resulting pellet after pressing (right).

Figure F.5 Image of Teflon ® soil holders with slits and Kapton ® pure tape (yellow) over the slits, holding the soil in place.

APPENDIX G:

AVERAGE K-EDGE FLUORESCENCE COUNTS FOR EIGHT ELEMENTS PER SITE

Table G.1 Average normalized fluorescence counts (± standard deviations) over 180 s for eight elements consistently identifiable in all samples using XRF on the IDEAS beamline. Averages and standard deviations were only available whenever samples were scanned more than once (duplicates or triplicates). Only approximate K-edge alpha 1 fluorescence counts (values at the top of a fluorescence peak) were shown for each element in this table (K = 3310 eV; Ca = 3690 eV; Ti = 4510 eV; Cr = 5410 eV; Mn = 5900 eV; Fe = 6400 eV; Ni = 7480 eV; Zn = 8640 eV). WS = White spruce; TA = Trembling aspen; N/A = not applicable.

Tree Species	Tree Component	Depth Increment (cm)	Site	K	Ca	Ti	Cr	Mn	Fe	Ni	Zn
WS	Leaves	N/A	0 km	54,459 ± 1,010	322,024± 12,091	3,909 ± 425	9,346 ± 278	50,539± 6,368	62,346 ± 962	2,894 ± 108	17,001 ± 1,970
WS	Leaves	N/A	50 km	65,963 ± 6	245,923± 7,242	1,139 ± 236	9,847 ± 257	68,148 ± 4,503	41,324 ± 476	2,635 ± 104	5,369 ± 21
WS	Leaves	N/A	Control	68,176 ± 2,256	416,560 ± 11,015	2,608 ± 10	10,018 ± 14	39,352 ± 806	86,769 ± 1,028	3,300 ± 146	19,198 ± 1,000
WS	Branches	N/A	0 km	57,187 ± 17,086	226,122 ± 29,104	5,225 ± 860	14,630 ± 328	21,219± 2,220	173,565 ± 18,437	3,816 ± 177	19,928 ± 2,602
WS	Branches	N/A	50 km	52,402 ± 31,139	130,081± 47,938	1,492 ± 558	9,609 ±1,070	23,779± 6,569	50,209 ± 12,515	2,265 ± 509	9,102 ± 3,514
WS	Branches	N/A	Control	57,708 ± 23,472	191,854 ± 40,988	3,627 ± 150	11,736 ± 561	16,134 ± 558	166,098 ± 1,180	2,943 ± 16	17,536 ± 406
TA	Stem Bark	N/A	0 km	57,701 ± 2,244	325,945 ± 20,402	844 ± 73	10,563 ±1,495	5,632 ± 1	43,354 ± 4,564	3,498 ± 691	23,974 ± 1.556
TA	Stem Bark	N/A	Control	40,228 ± 408	412,986 ± 8,957	1,097 ± 49	11,516 ± 649	4,542 ± 107	50,997 ± 3,293	4,422 ± 369	42,922 ± 2,390
WS	Stem Bark	N/A	0 km	36,363 ± 3,283	206,379 ± 4,882	4,424 ± 160	9,284, ± 396	18,362 ± 243	55,076 ± 14,202	2,641 ± 129	29,474 ± 194
WS	Stem Bark	N/A	50 km	30,199 ± 473	322,955 ± 1,418	2,738 ± 35	9,627 ± 512	39,120 ± 2,177	34,281 ± 405	2,834 ± 95	20,812 ± 1,024
WS	Stem Bark	N/A	Control	29,826 ± 5,702	174,125 ± 39,490	1,031 ± 189	8,549 ± 366	5,769 ± 5	30,585 ± 3,362	2,204 ± 70	13,607 ± 320
TA	Core seg.1	N/A	0 km	17,828 ± 302	21,916 ± 213	190 ± 8	8,090 ± 504	2,365 ± 122	36,544 ± 1,717	1,845 ± 97	2,744 ± 90
TA	Core seg.1	N/A	Control	12,514 ±	16,431 ±	220	9,869	2,593 ±	34,387 ±	2,249	2,369

				5,503	2,013	± 53	± 421	366	4,766	± 7	± 597
WS	Core seg.1	N/A	0 km	7,489 ± 642	21,647 ± 679	458 ± 22	10,820 ±1,326	4,952 ± 476	37,857 ± 2,948	2,678 ± 252	1,960 ± 176
WS	Core seg.1	N/A	50 km	9,919 ± 659	17,790 ± 207	351 ± 96	8,655 ±1,486	6,843 ± 843	31,137 ± 2,018	2,055 ± 344	1,833 ± 379
WS	Core seg.1	N/A	Control	16,738 ± 470	15,948 ± 1,329	246 ± 17	10,029 ± 194	2,977 ± 175	36,903 ± 1,209	2,304 ± 71	2,219 ± 385
TA	Root Bark	N/A	0 km	72,904 ± 4,833	301,674 ±24,628	1,810 ± 32	9,233 ± 944	8,468 ± 868	38,411 ± 1,923	3,132 ± 461	18,050 ± 4,832
TA	Root Bark	N/A	Control	36,684 ± 784	355,101 ±10,824	2,137 ± 198	10,988 ± 168	6,526 ± 280	59,812 ± 3,459	3,765 ± 169	40,366 ± 661
WS	Root Bark	N/A	0 km	47,000 ± 1,583	618,488 ±46,752	5,544 ± 503	9,962 ± 276	22,669 ± 655	37,040 ± 7,112	4,527 ± 302	32,631 ± 601
WS	Root Bark	N/A	50 km	29,338 ± 218	351,031 ±26,748	2,898 ± 152	10,272 ±1,133	25,379 ± 456	39,693 ± 6,043	3,188 ± 408	13,450 ± 1,671
WS	Root Bark	N/A	Control	28,502 ± 3,463	244,688 ± 27,422	2,599 ± 450	10,644 ±1,628	10,152 ± 358	39,665 ± 10,094	2,845 ± 167	20,447 ± 1,273
TA	Outer Root	N/A	0 km	35,296 ± 4,940	14,340 ± 602	241 ± 55	10,757 ±1,505	2,821 ± 55	32,945 ± 6,303	2,219 ± 264	2,285 ± 652
TA	Outer Root	N/A	Control	28,670 ± 10,277	29,761 ± 6,200	327 ± 17	10,063 ± 825	2,504 ± 208	31,101 ± 4,082	2,590 ± 291	6,724 ± 1,938
WS	Outer Root	N/A	0 km	12,684 ± 1,640	18,208 ± 691	512 ± 48	10,012 ± 722	4,204 ± 364	29,572 ± 2,373	2,411 ± 157	2,307 ± 287
WS	Outer Root	N/A	50 km	10,095 ± 300	20,072 ± 661	353 ± 0.8	9,737 ± 799	4,816 ± 237	30,023 ± 2.722	2,155 ± 133	1,576 ± 64
WS	Outer Root	N/A	Control	16,341 ± 3,697	41,830 ± 2,685	618 ± 116	9,198 ± 188	3,556 ± 237	27,778 ± 634	2,422 ± 313	2,963 ± 204
TA	Inner Root	N/A	0 km	14,699 ± 927	32,314 ± 1,121	270 ± 56	9,451 ±1,445	3,124 ± 594	26,919 ± 4,251	2,311 ± 354	4,551 ± 834
TA	Inner Root	N/A	Control	6,237 ± 1,287	22,836 ± 1,250	324 ± 99	6,923 ± 418	1,671 ± 122	21,511 ± 203	1,606 ± 83	3,173 ± 138
WS	Inner Root	N/A	0 km	3,928 ± 117	21,671 ± 722	485 ± 32	8,857 ± 549	3,881 ± 265	25,224 ± 1,532	1,964 ± 174	1,820 ± 74

WS	Inner Root	N/A	50 km	6,929 ± 336	22,495 ± 672	365 ± 19	10,028 ± 279	5,473 ± 48	30,290 ± 12	2,302 ± 9	1,123 ± 124
WS	Inner Root	N/A	Control	8,862 ± 627	24,816 ± 578	405 ± 17	9,065 ± 387	3,159 ± 211	27,354 ± 1,252	2,174 ± 107	1,732 ± 0.3
N/A	Leaf Litter	N/A	0 km	34,530 ± 3,037	418,987 ± 11,807	9,897 ±1,394	19,254 ±1,263	80,461 ± 2,903	343,270 ± 47,916	6,230 ± 297	23,473 ±3,783
N/A	Leaf Litter	N/A	50 km	31,185 ± 2,832	172,671 ± 9,509	30,720 ±2,814	33,505 ±4,429	39,900 ± 7,479	812,590 ±138,483	9,369 ±1,802	5,409 ±1,348
N/A	Leaf Litter	N/A	Control	38,445	286,661	23,753	32,122	27,818	862,989	8,253	27,257
N/A	Soil	0 to 5	0 km	9,302	11,842	24,124	26,901	19,995	539,261	4,704	6,566
N/A	Soil	0 to 5	50 km	11,651	13,041	33,569	28,381	16,853	681,203	4,756	5,527
N/A	Soil	0 to 5	Control	645	4,182	2,089	35,969	7,559	152,186	8,616	1,302
N/A	Soil	5 to 20	0 km	757	3,604	1,333	33,961	7,328	135,109	8,011	858
N/A	Soil	5 to 20	50 km	1,328	4,482	3,509	34,123	7,691	177,644	8,238	905
N/A	Soil	5 to 20	Control	974	4,338	3,844	35,617	7,865	199,447	8,334	1,256
N/A	Soil	20 to 45	0 km	6,936	9,256	12,838	35,367	9,856	625,283	6,928	4,006
N/A	Soil	20 to 45	50 km	586	3,580	1,227	34,172	7,378	148,054	8,119	518
N/A	Soil	20 to 45	Control	1,906	5,352	4,136	34,789	7,908	271,591	7,924	1,502
N/A	Soil	45 to 60	0 km	280	3,466	340	31,395	6,383	92,721	7,651	343
N/A	Soil	45 to 60	50 km	860	3,760	1,626	35,364	8,075	163,099	8,234	1,338
N/A	Soil	45 to 60	Control	1,167	4,148	2,108	35,372	7,502	190,944	7,865	818

APPENDIX H:

SUPPLEMENTARY XRF GRAPHS

NOTE: Shortened figure captions were used in this section because all XRF graphs depict the same concepts. Graphs illustrate fluorescence spectra for the remainder of all individual tree and soil media not illustrated in this thesis (white spruce materials; trembling aspen materials, trembling aspen vs. white spruce materials, and soil depth increments). A full figure caption is provided below. Italicized words vary per graph.

Figure H. *Average* normalized fluorescence counts for a duration of 180 s illustrating distinct elements from the XRF scan using the IDEAS beamline for *white spruce or trembling aspen, or trembling aspen versus white spruce leaves, branches, cores, root bark, outer root, or inner root, or soil leaf litter, 5 to 20 cm, 20 to 45 cm, or 45 to 60 cm per site or at Site 0 km versus the Control site*; the Control site (black), Site 50 km (blue), and Site 0 km (red) *or trembling aspen (black) and white spruce (black)* Each element corresponds to electron volt (eV) values. Fluorescence counts distinguish *(average)* relative amounts of each element per site. Note: a1 = K-edge alpha 1 eV values per element; b1 = K-edge beta 1 eV values per element.

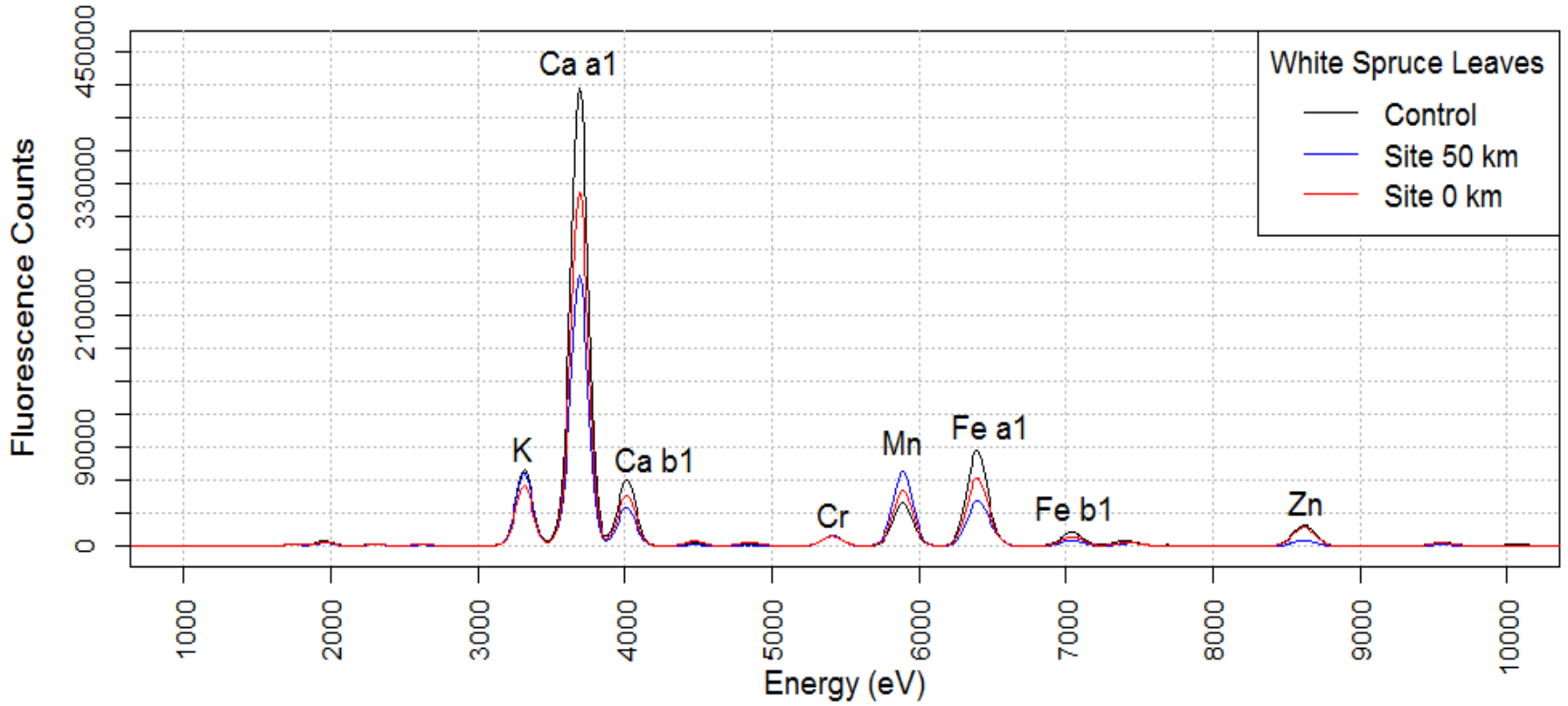

Figure H.1 Average normalized fluorescence counts illustrating distinct elements present in white spruce leaves per site.

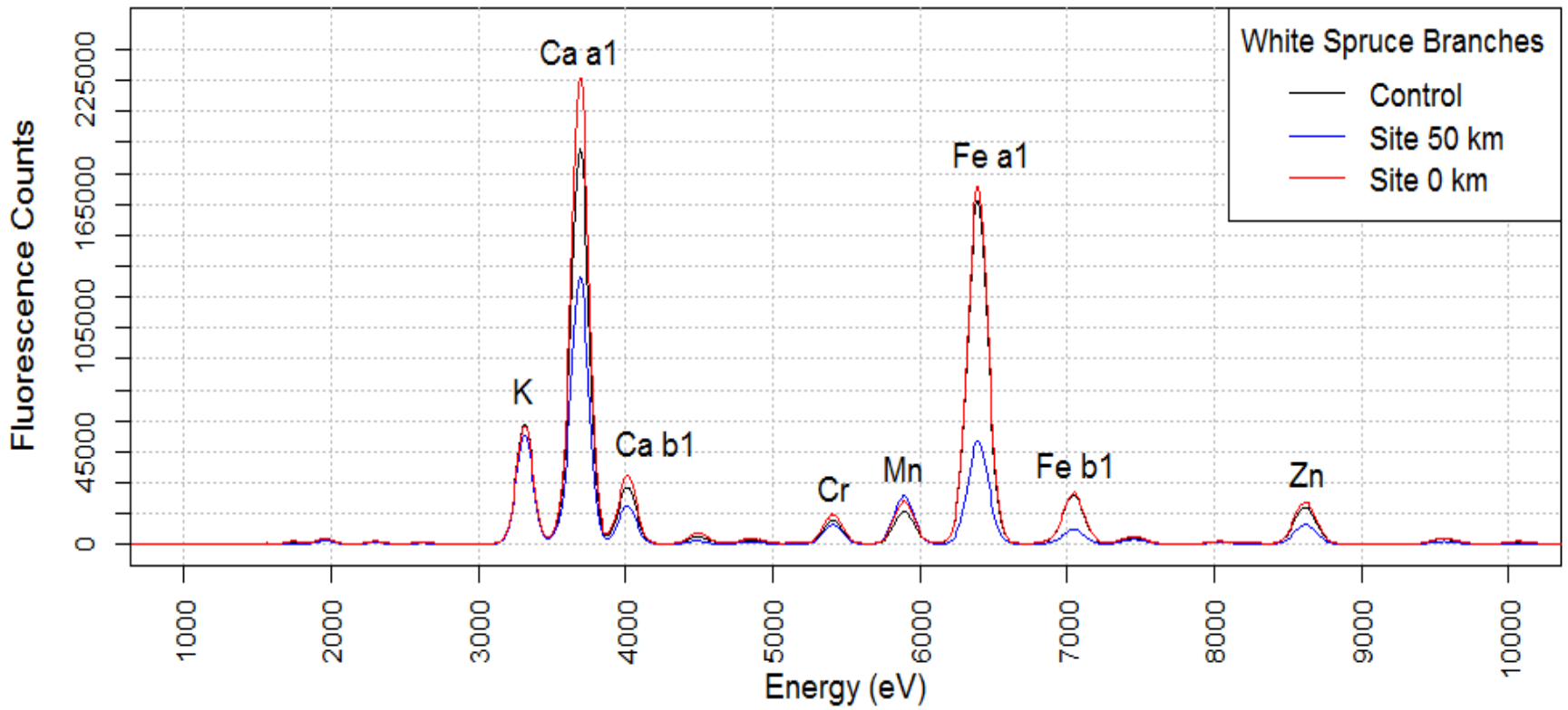

Figure H.2 Average normalized fluorescence counts illustrating distinct elements in white spruce's branches per site.

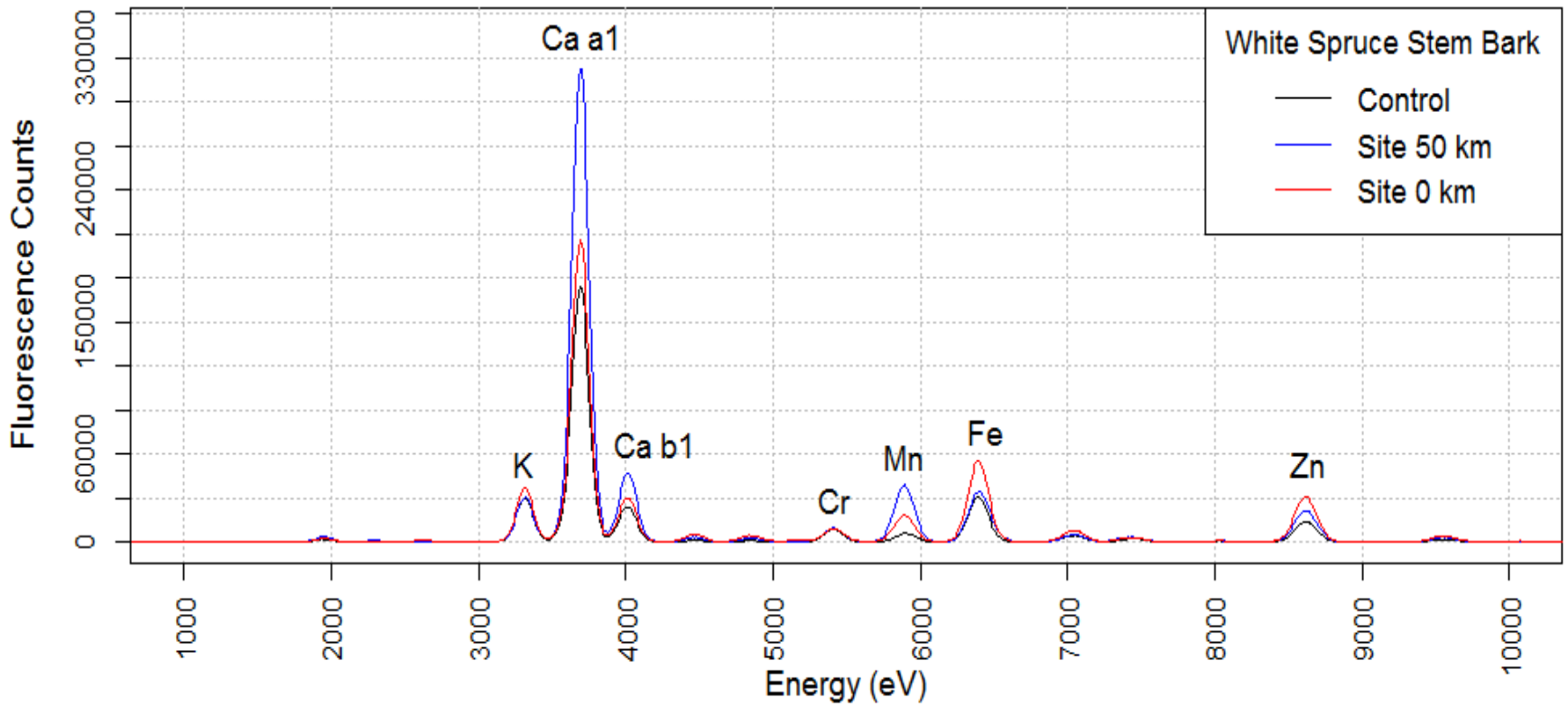

Figure H.3 Average normalized fluorescence counts illustrating distinct elements in white spruce's stem bark per site.

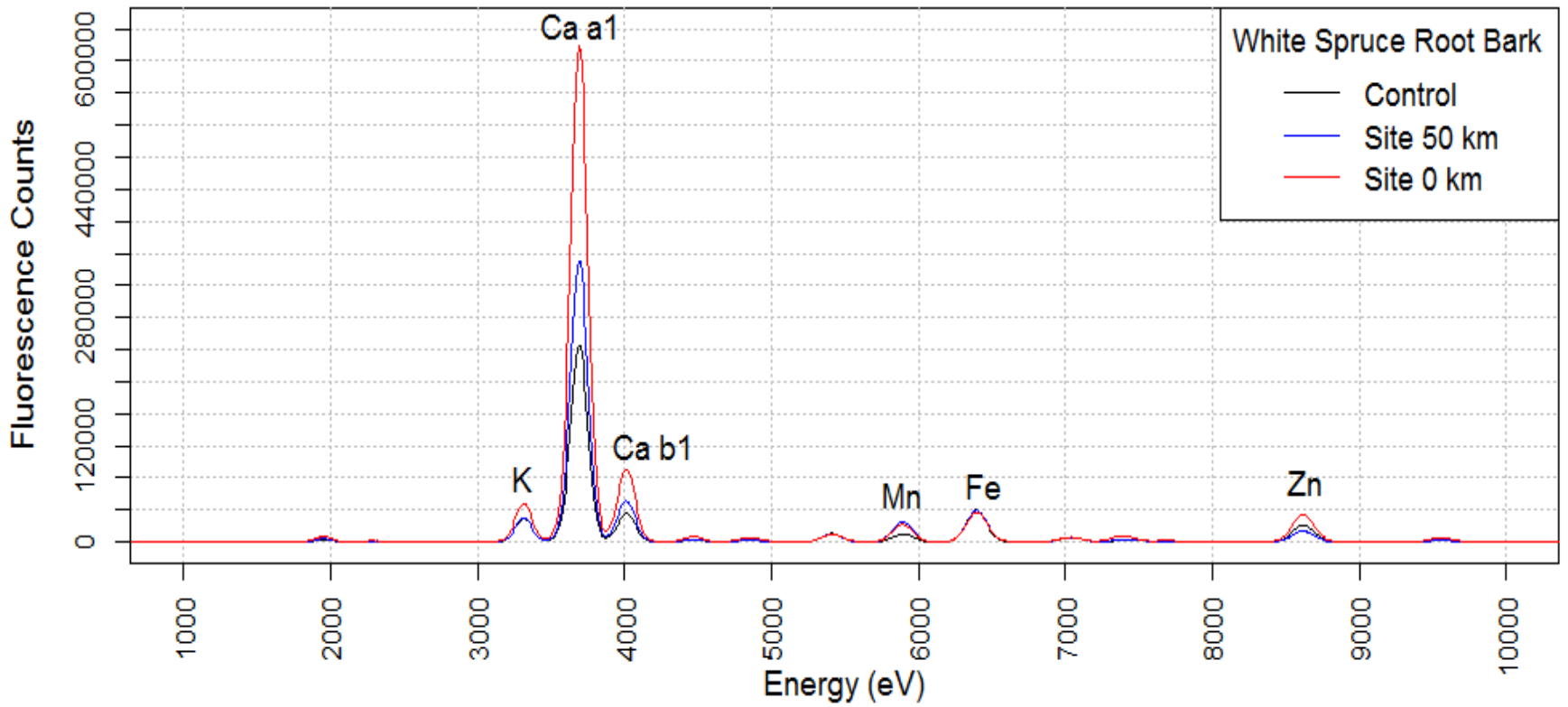

Figure H.4 Average normalized fluorescence counts illustrating distinct elements in white spruce's root bark per site.

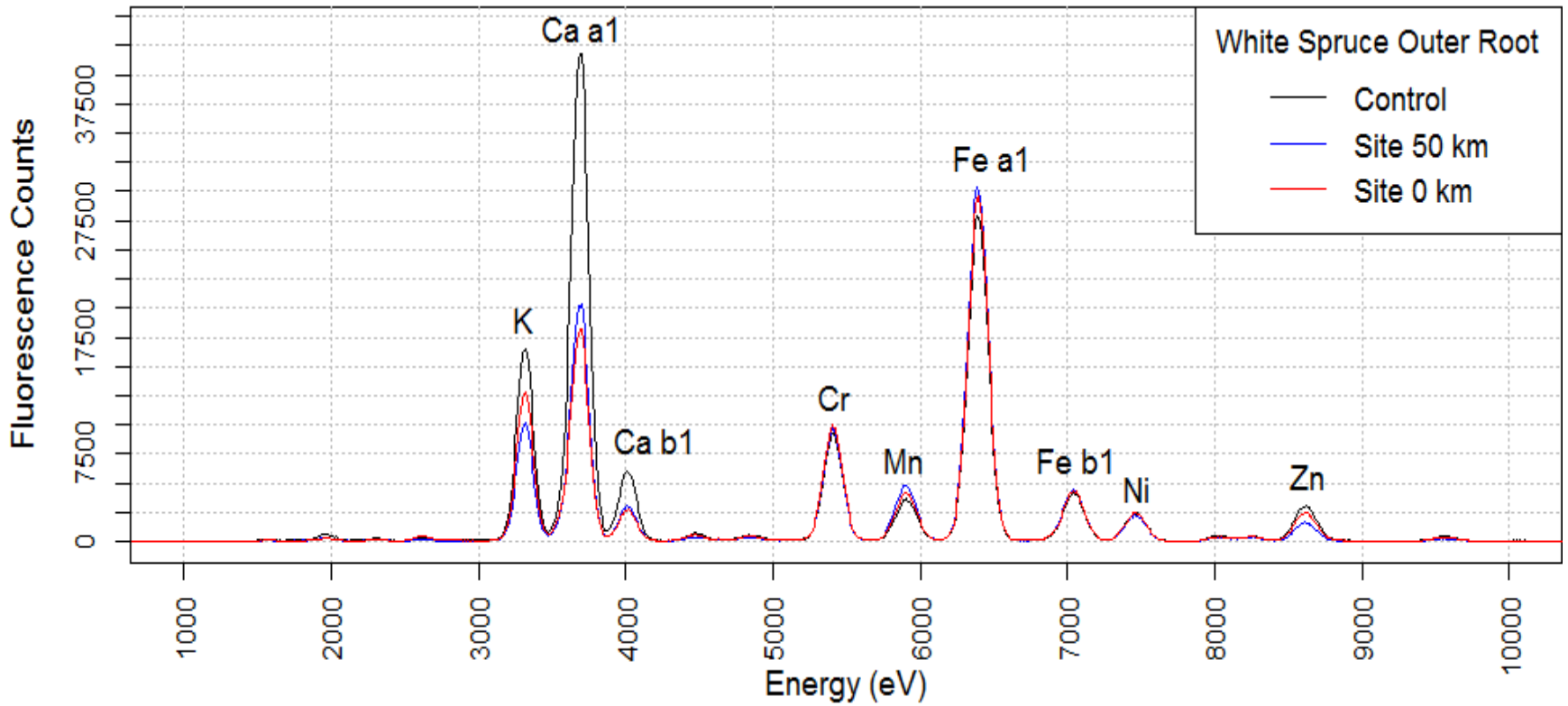

Figure H.5 Average normalized fluorescence counts illustrating distinct elements in white spruce's outer root per site.

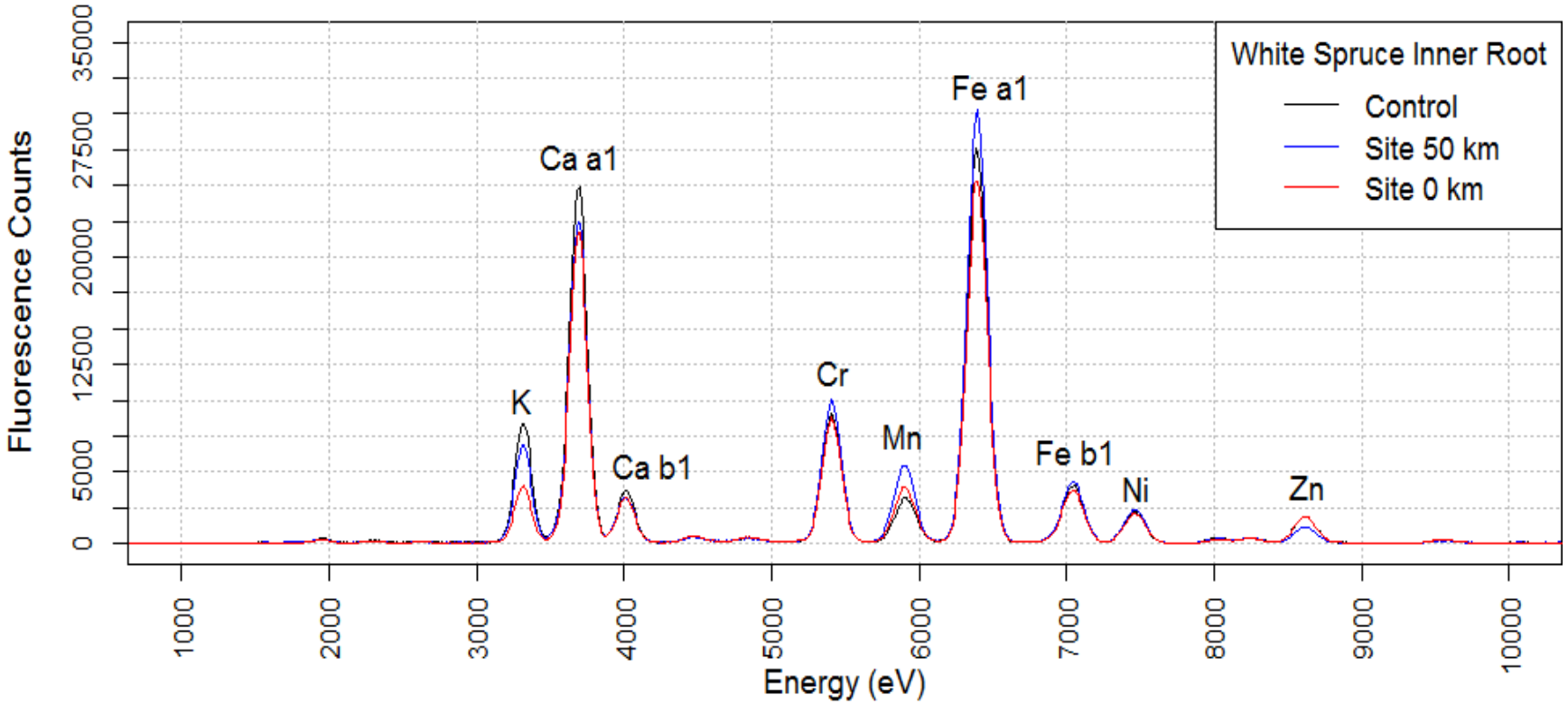

Figure H.6 Average normalized fluorescence counts illustrating distinct elements in white spruce's inner root per site.

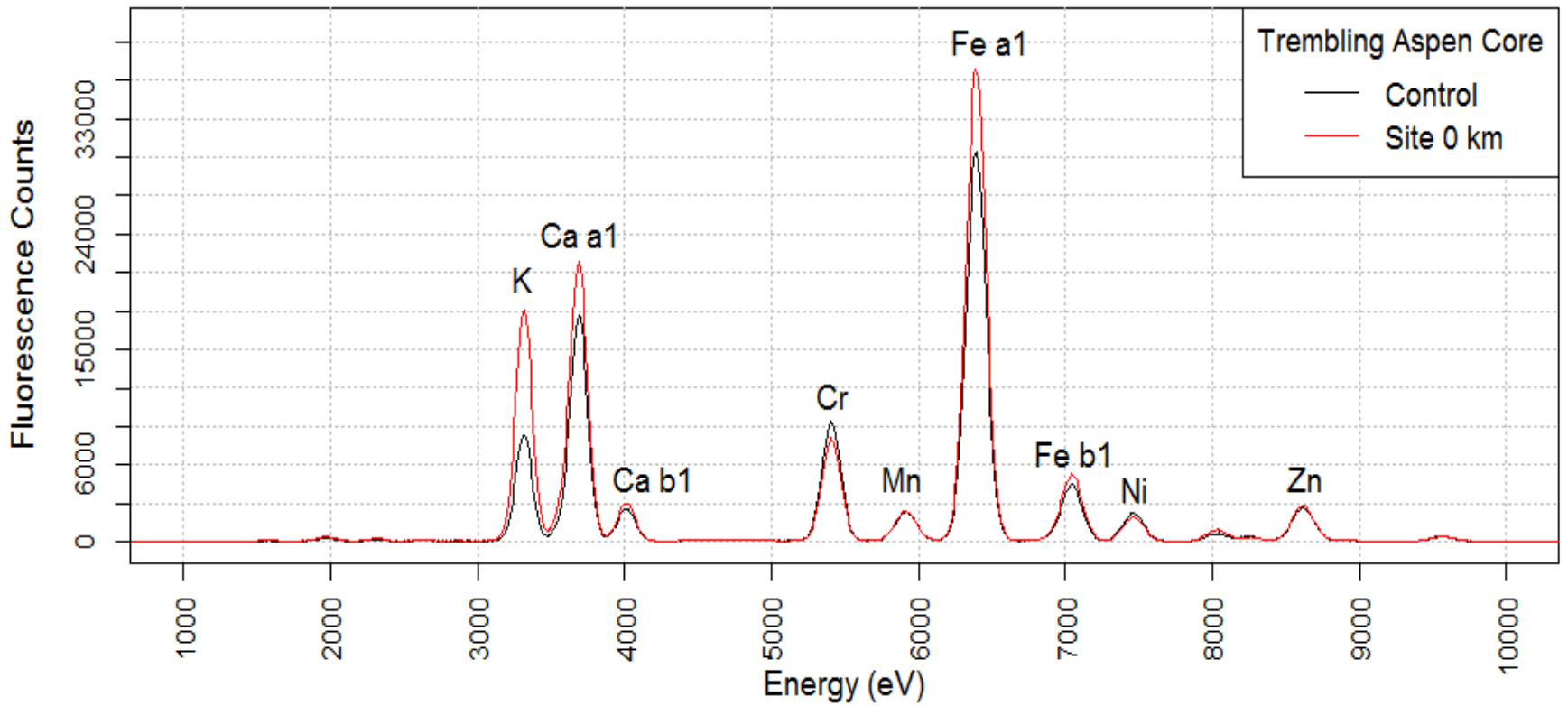

Figure H.7 Average normalized fluorescence counts illustrating distinct elements in trembling aspen's core (stem wood) segment for Site 0 km versus the Control site.

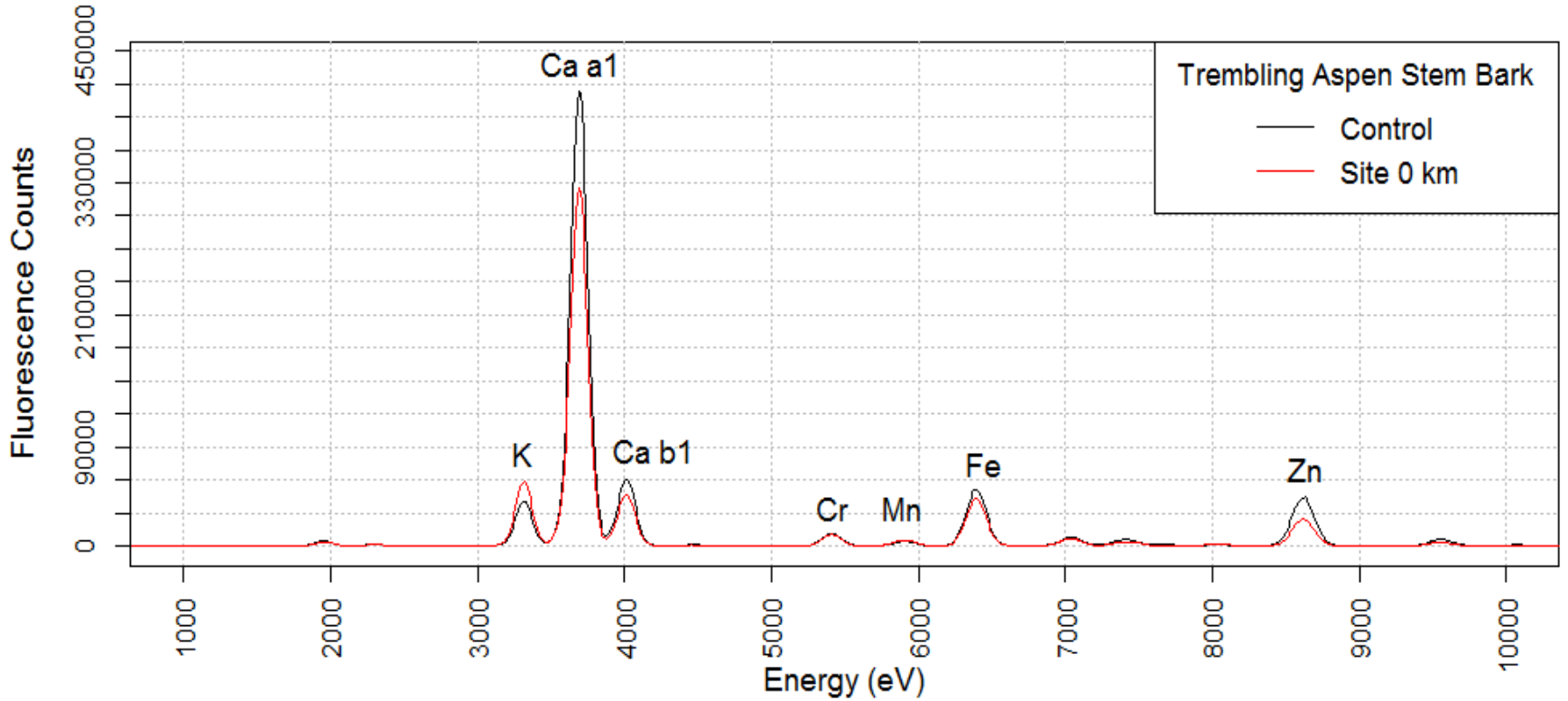

Figure H.8 Average normalized fluorescence counts illustrating distinct elements in trembling aspen's stem bark for Site 0 km versus the Control site.

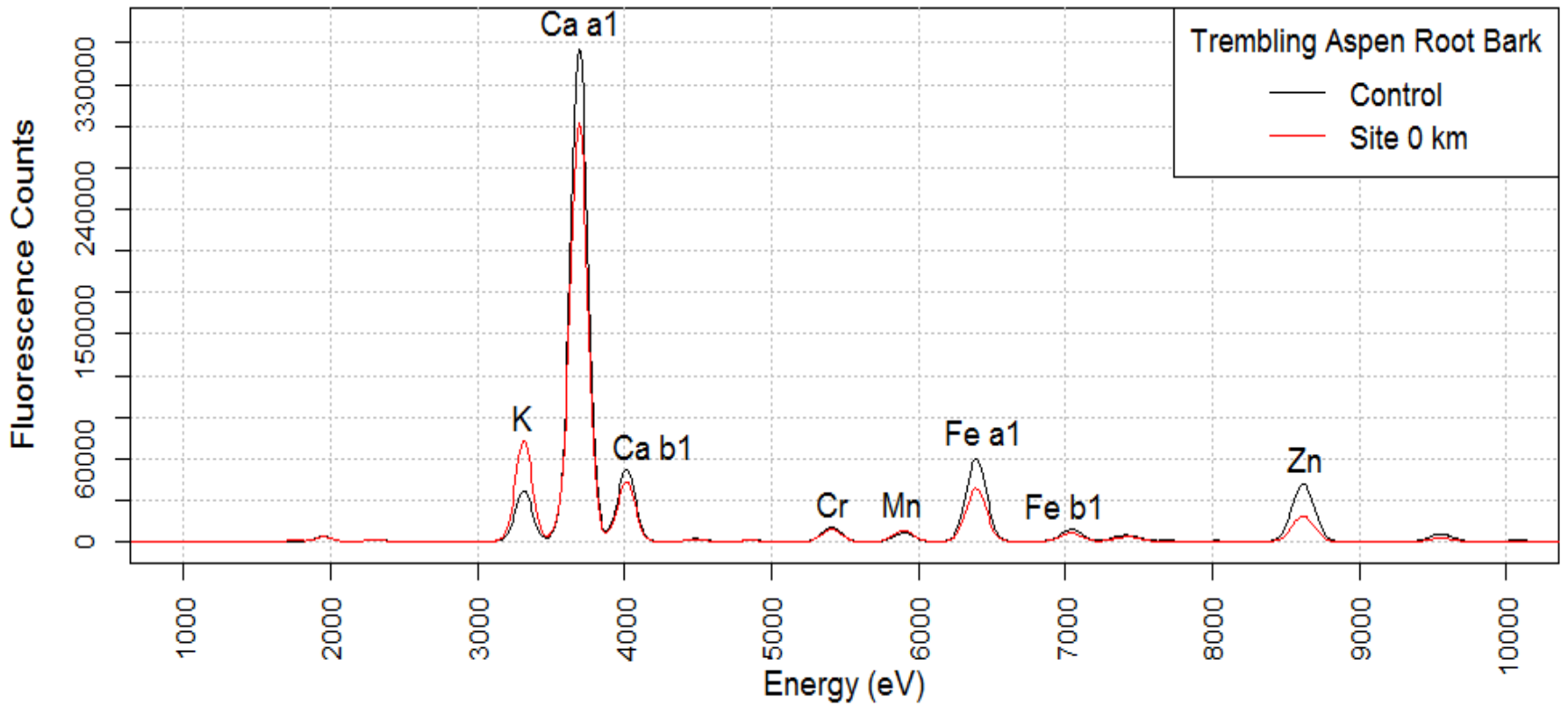

Figure H.9 Average normalized fluorescence counts illustrating distinct elements in trembling aspen's root bark for Site 0 km versus the Control site.

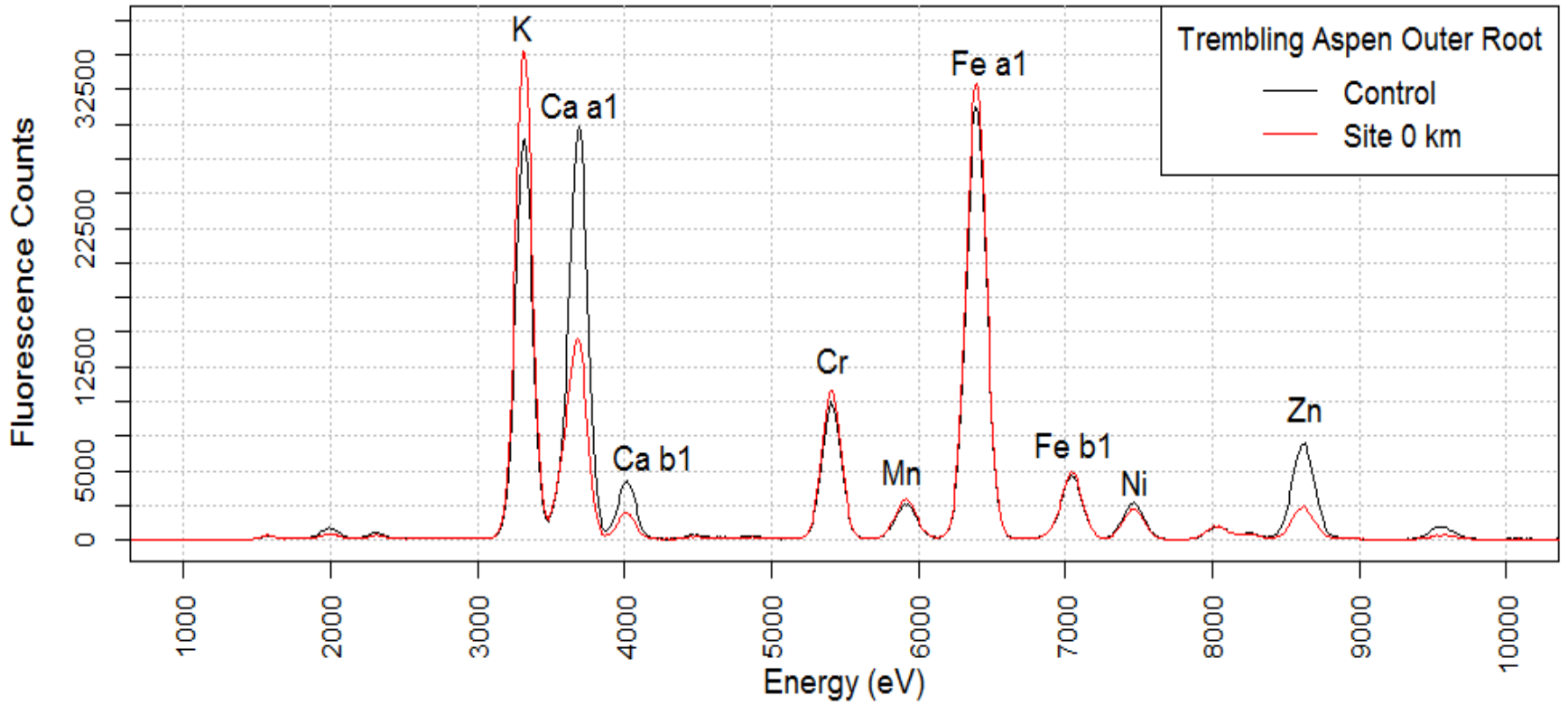

Figure H.10 Average normalized fluorescence counts illustrating distinct elements in trembling aspen's outer root for Site 0 km versus the Control site.

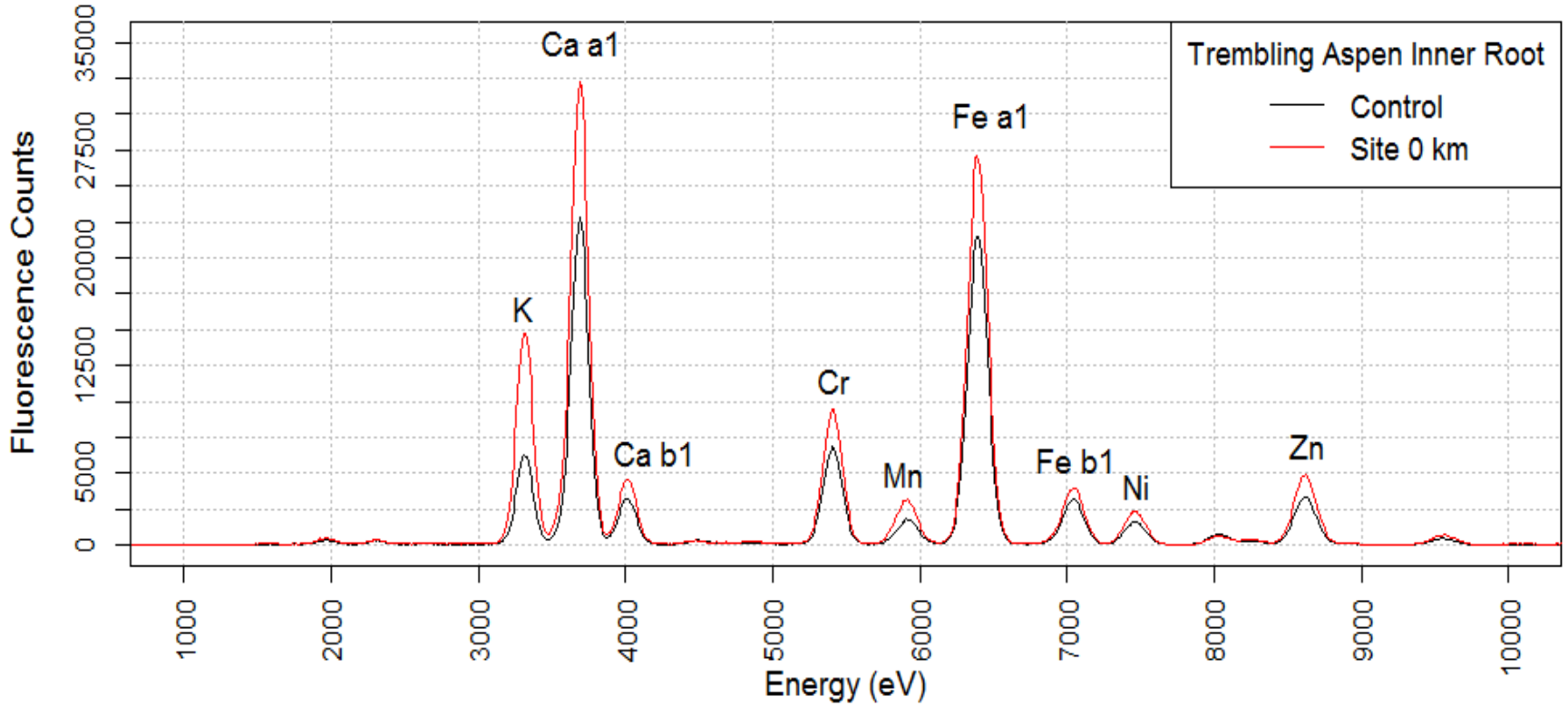

Figure H.11 Average normalized fluorescence counts illustrating distinct elements in trembling aspen's inner root for Site 0 km versus the Control site.

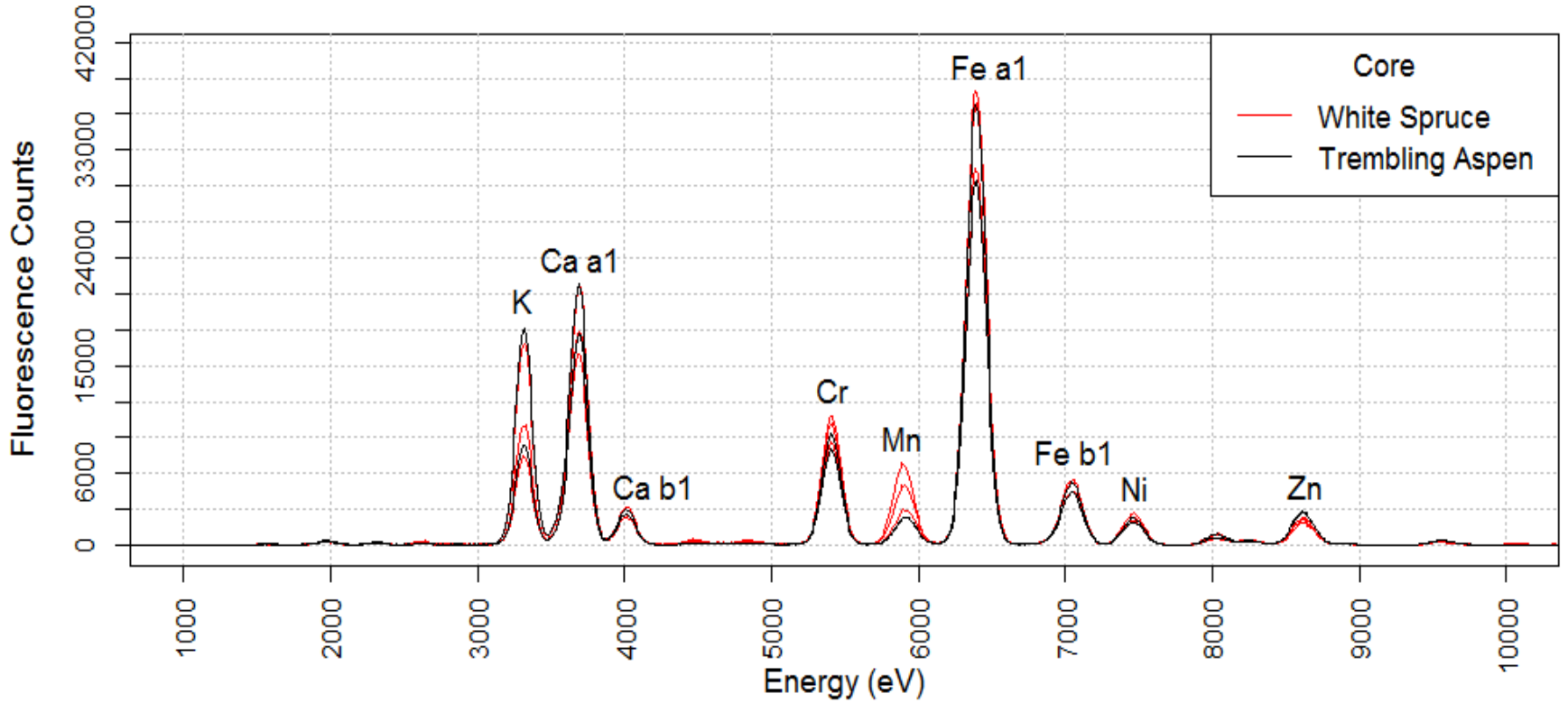

Figure H.12 Average normalized fluorescence counts illustrating distinct elements in trembling aspen's versus white spruce's core (stem wood) segment per site.

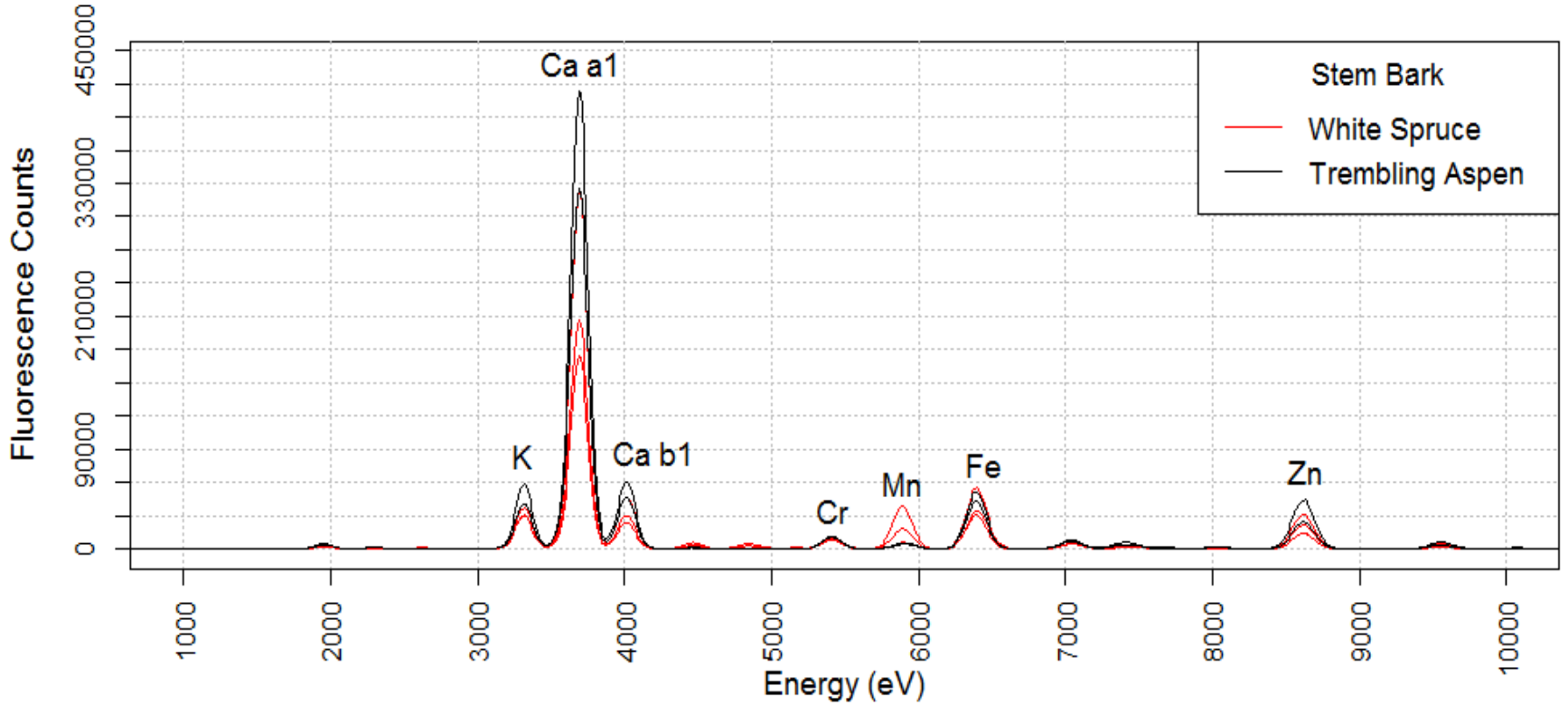

Figure H.13 Average normalized fluorescence counts illustrating distinct elements in trembling aspen's versus white spruce's stem bark per site.

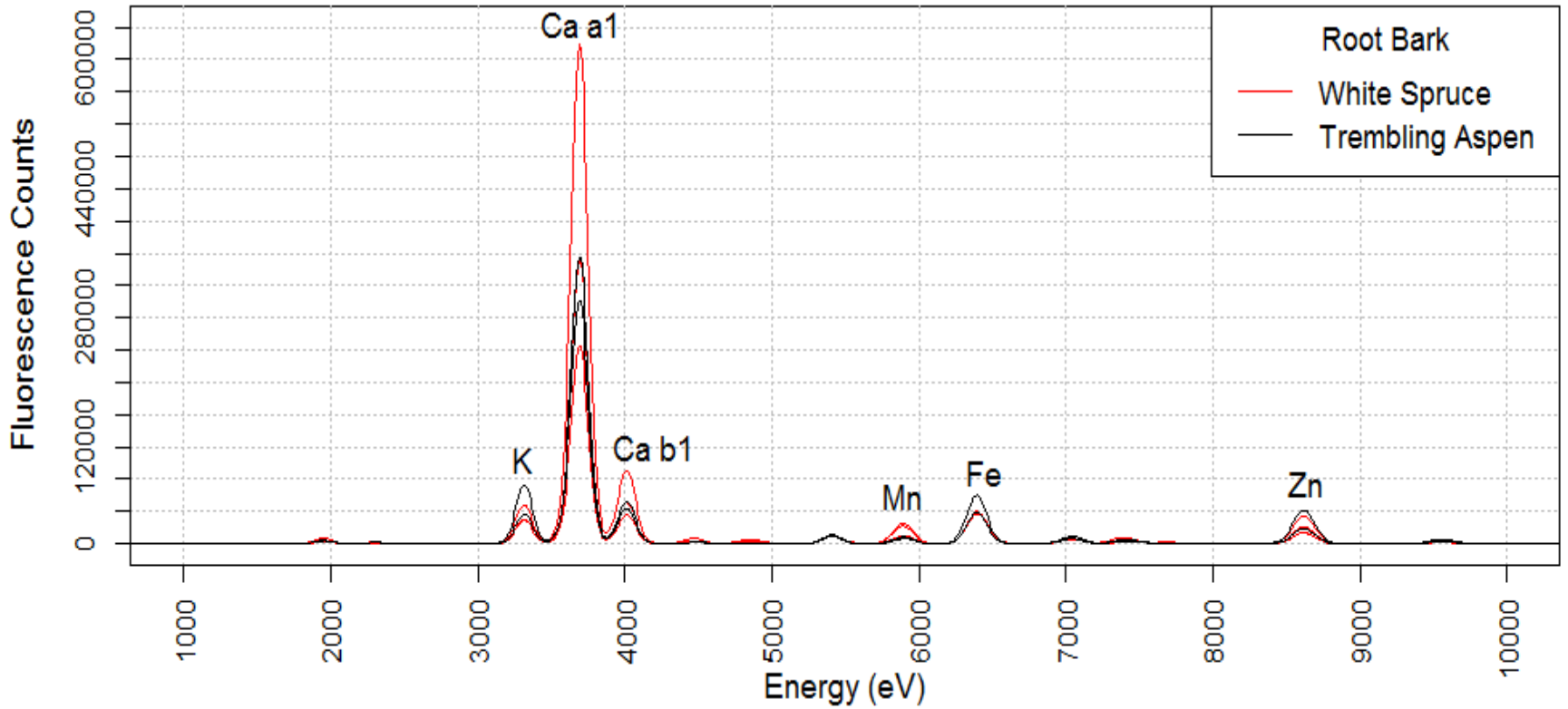

Figure H.14 Average normalized fluorescence counts illustrating distinct elements in trembling aspen's versus white spruce's root bark for per site.

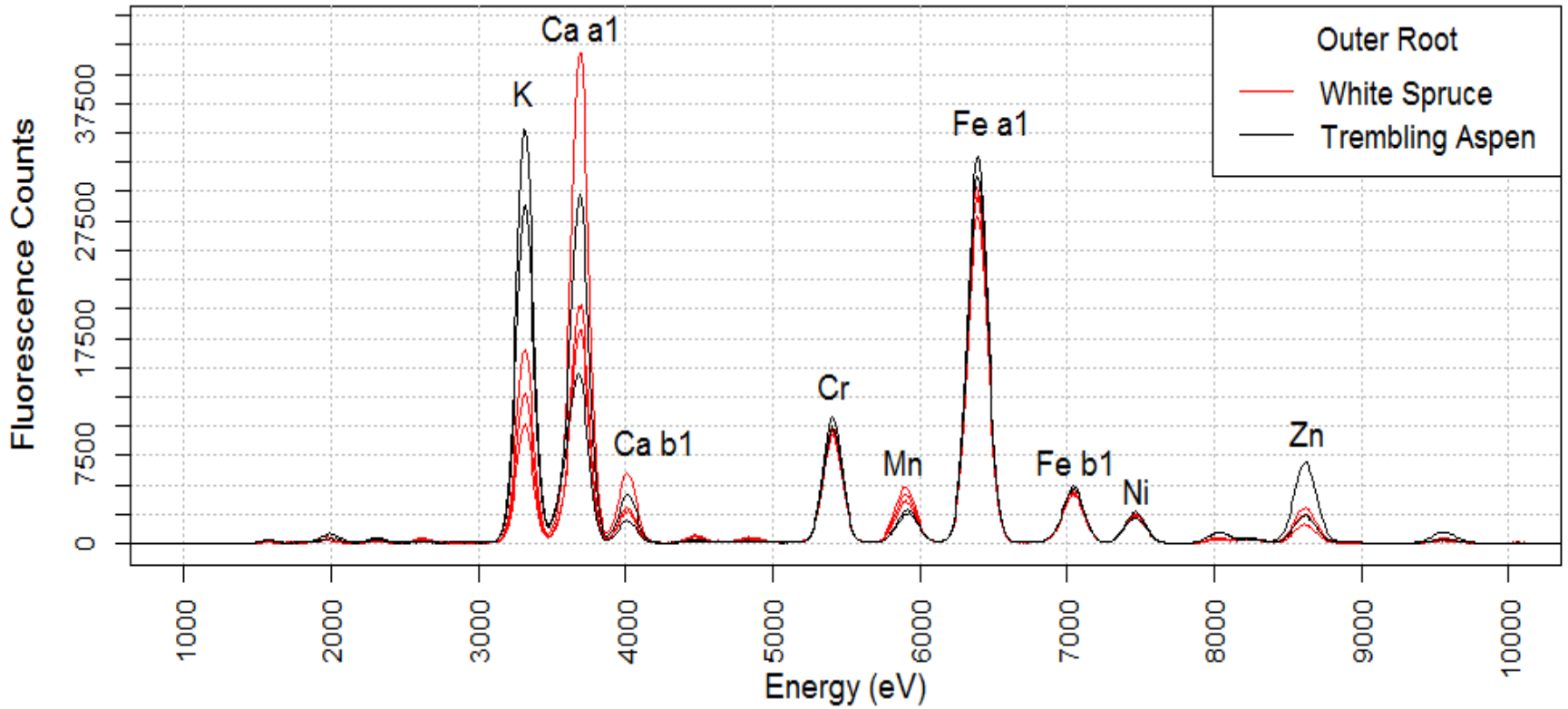

Figure H.15 Average normalized fluorescence counts illustrating distinct elements in trembling aspen's versus white spruce's outer root per site.

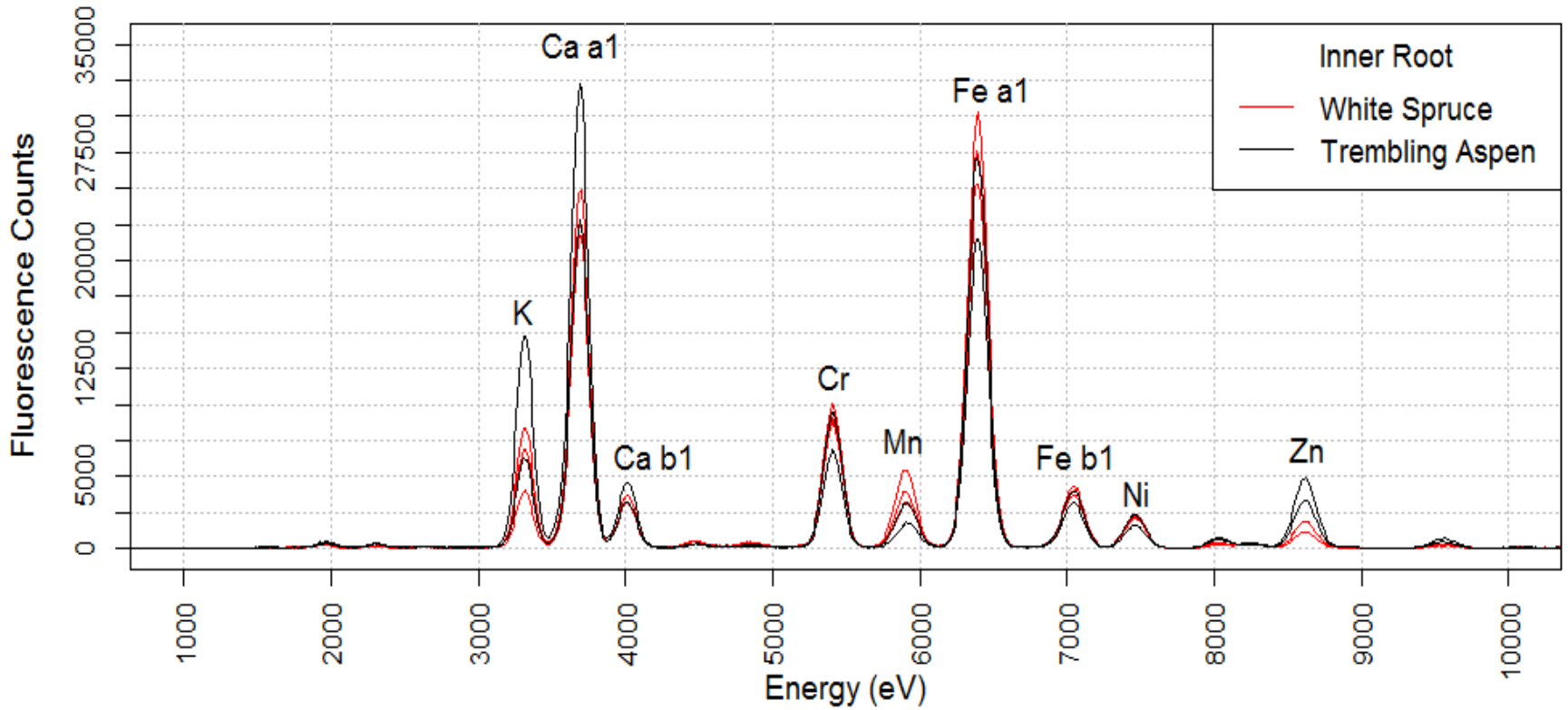

Figure H.16 Average normalized fluorescence counts illustrating distinct elements in trembling aspen's versus white spruce's inner root per site.

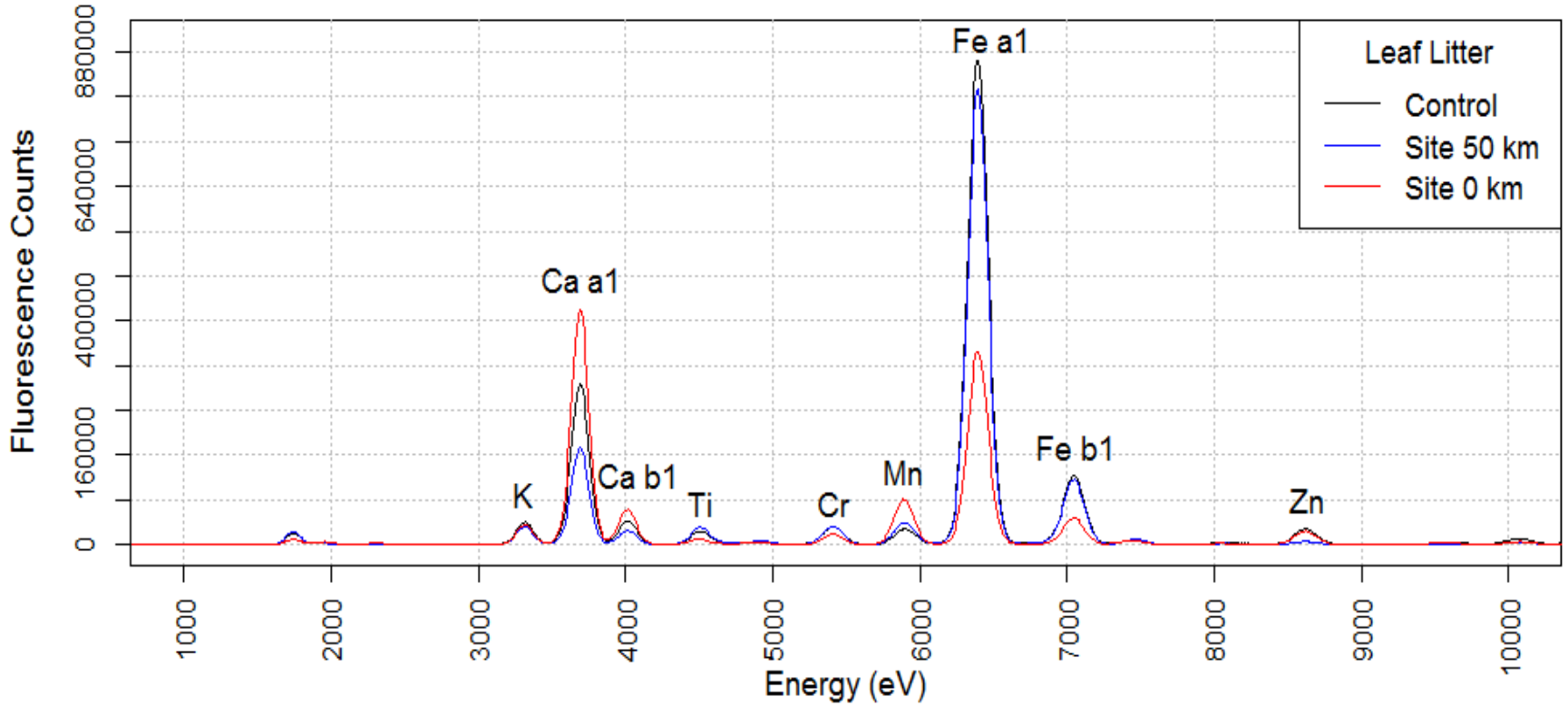

Figure H.17 Average normalized fluorescence counts illustrating distinct elements in the leaf litter per site.

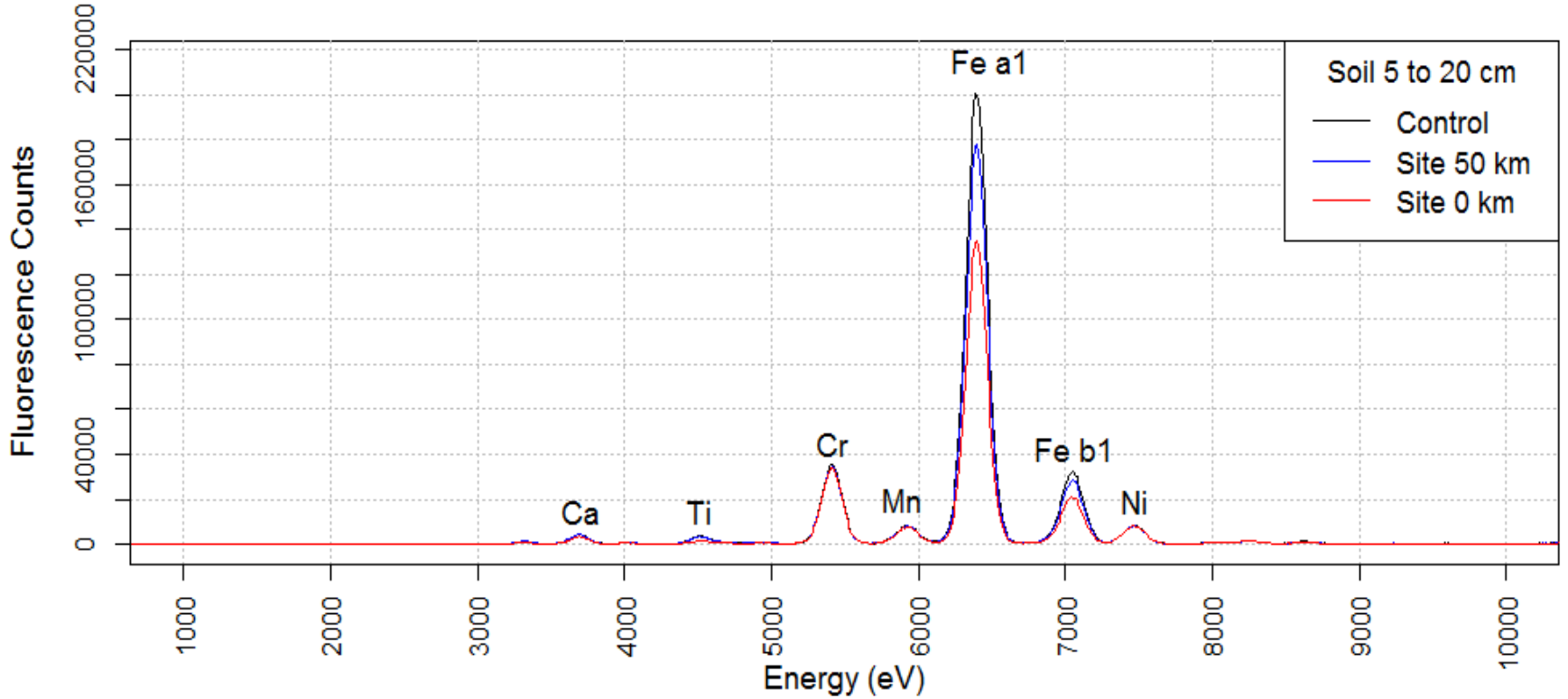

Figure H.18 Normalized fluorescence counts illustrating distinct elements in the soil's 5 to 20 cm depth increment per site. Note: Site 50 km did not scan properly

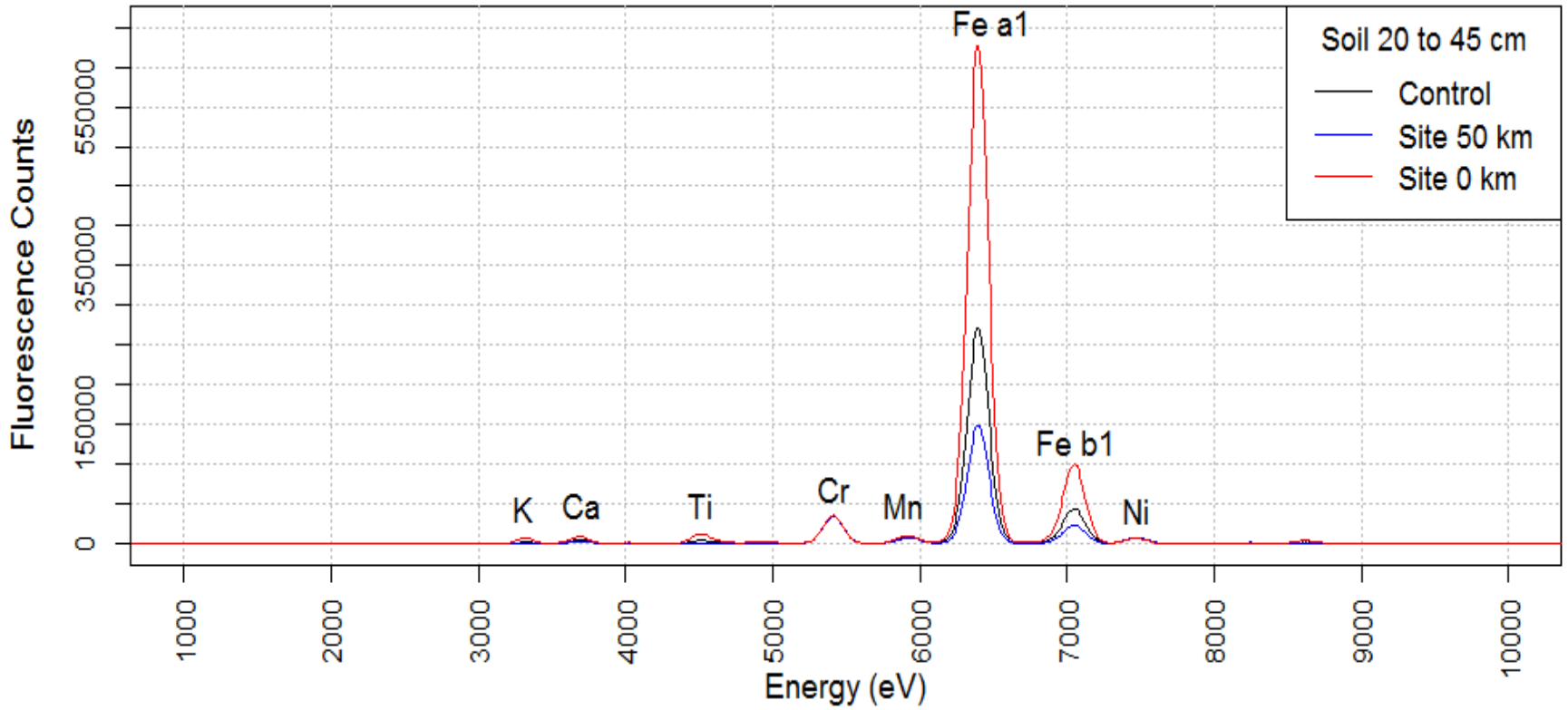

Figure H.19 Normalized fluorescence counts illustrating distinct elements in the soil's 20 to 45 cm depth increment per site.

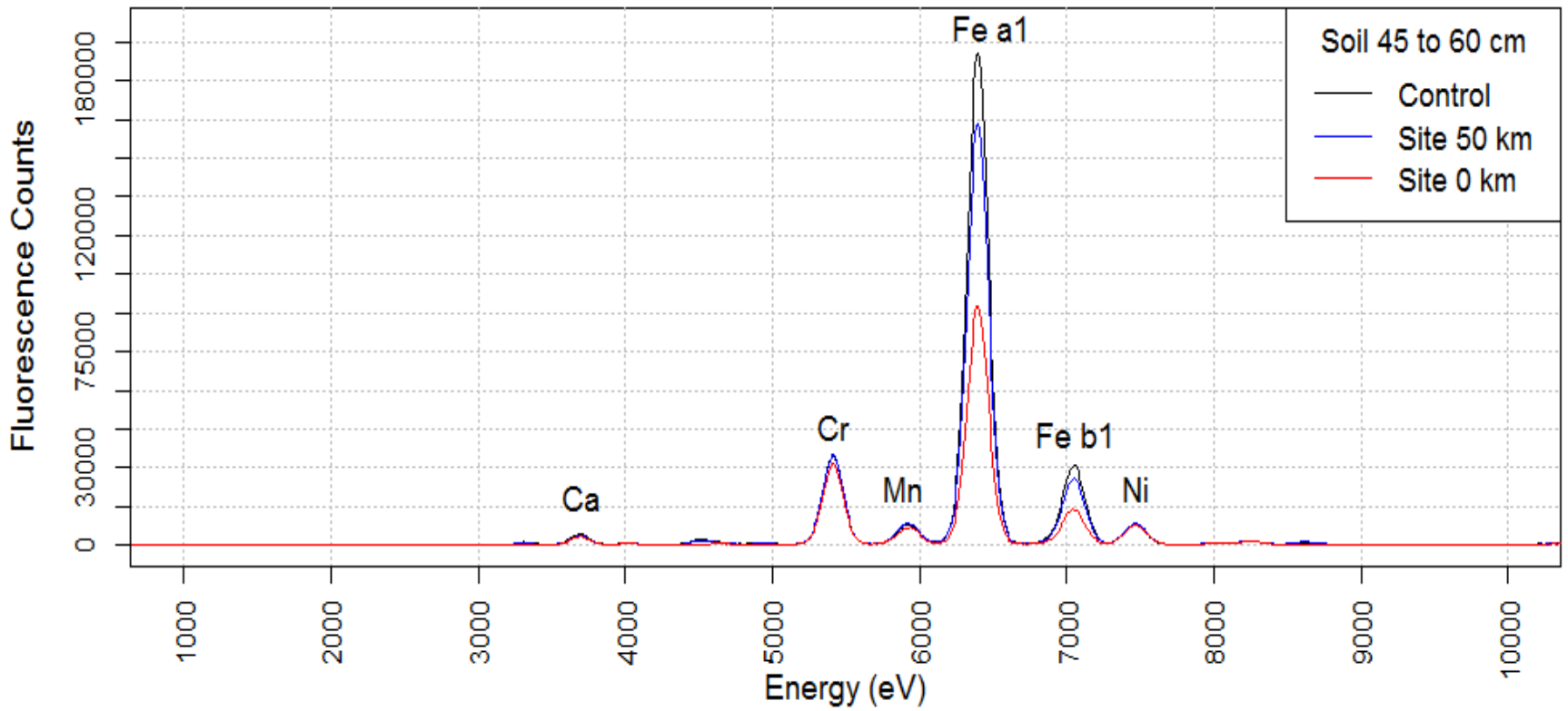

Figure H.20 Normalized fluorescence counts illustrating distinct elements in the soil's 45 to 60 cm depth increment per site.

APPENDIX I:

WHITE SPRUCE AND TREMBLING ASPEN CORE SEGMENTS WITH CORRESPONDING RING YEARS

NOTE: Shortened figure captions were used in this section because all graphs depict the same concepts. Graphs illustrate K-edge Mn plotted over time for white spruce and trembling aspen core (stem wood) segments with standard deviations. A full figure caption is provided below. Italicized words vary per graph.

Figure I. Average normalized fluorescence counts for a duration of 180 s illustrating K-edge Mn plotted over time *for white spruce or trembling aspen at the Control site, Site 50 km, or Site 0 km.* Whiskers represent standard deviations. K-edge Mn corresponds to an electron volt (eV) value of 5898. Fluorescence counts distinguish average relative amounts of Mn per core. Ring years depict the time period present in each core segment. Core segments represent tree rings from pith to bark

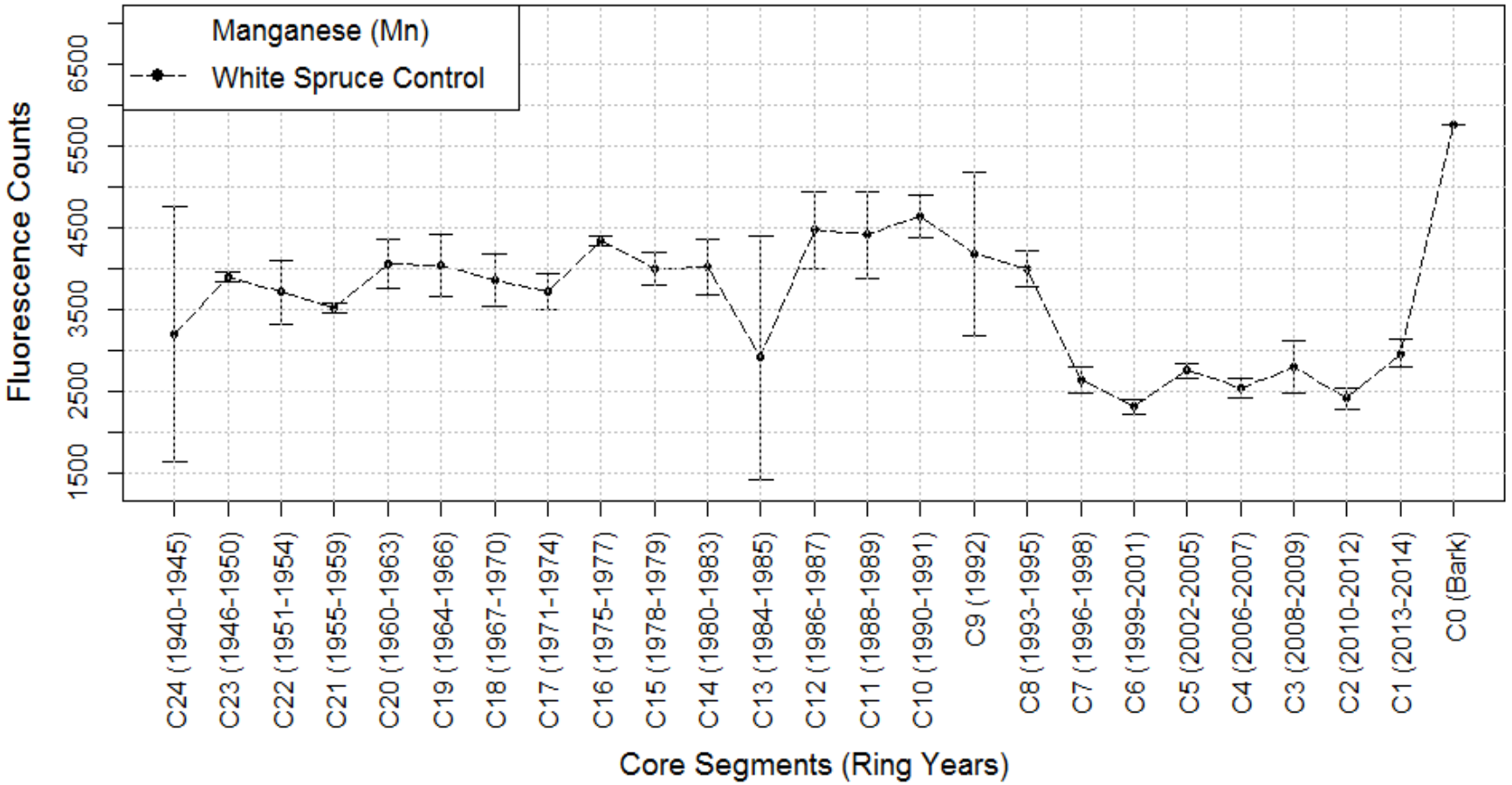

Figure I.1 Average normalized fluorescence counts illustrating K-edge Mn plotted over time for white spruce at the Control site

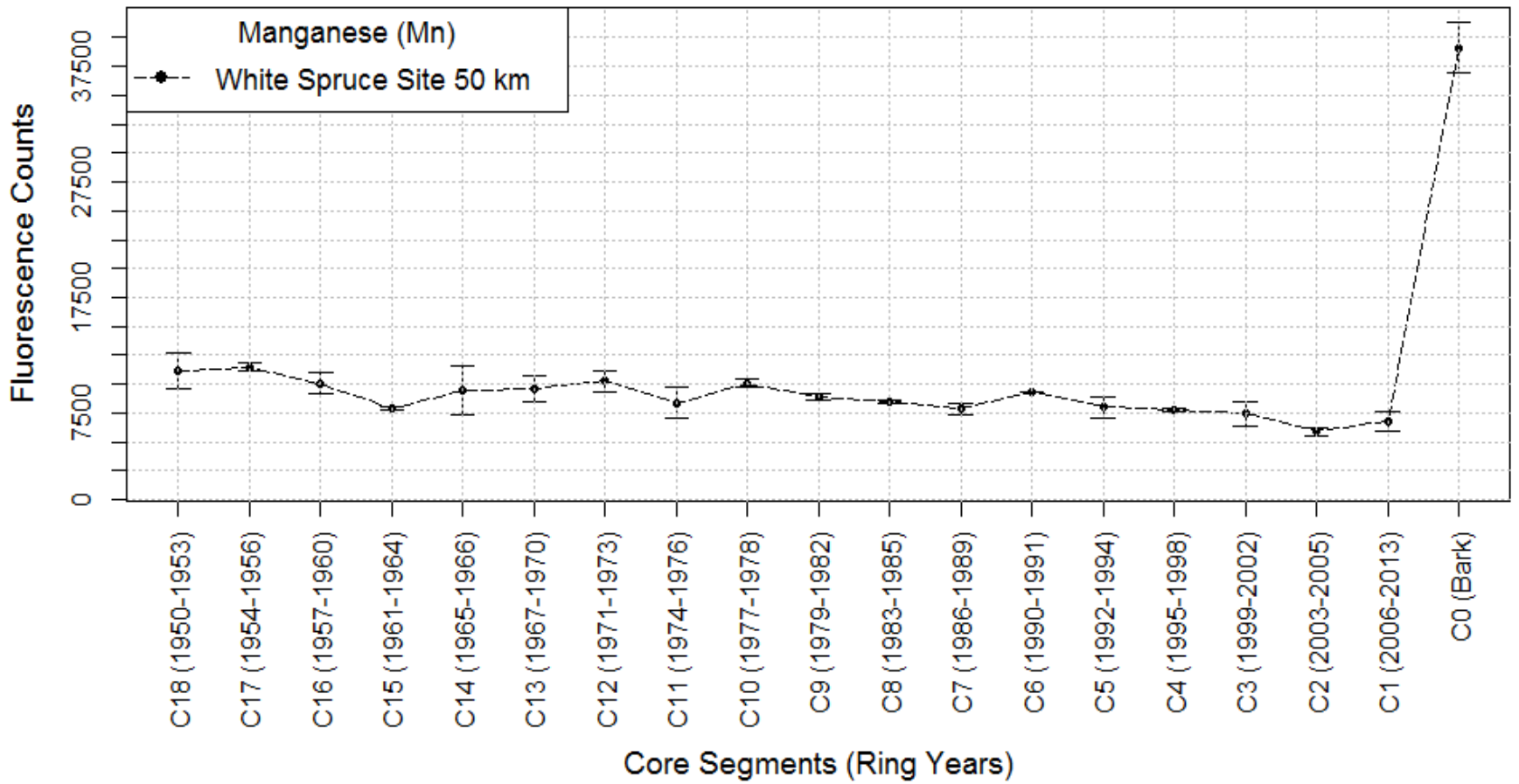

Figure I.2 Average normalized fluorescence counts illustrating K-edge Mn plotted over time for white spruce at Site 50 km.

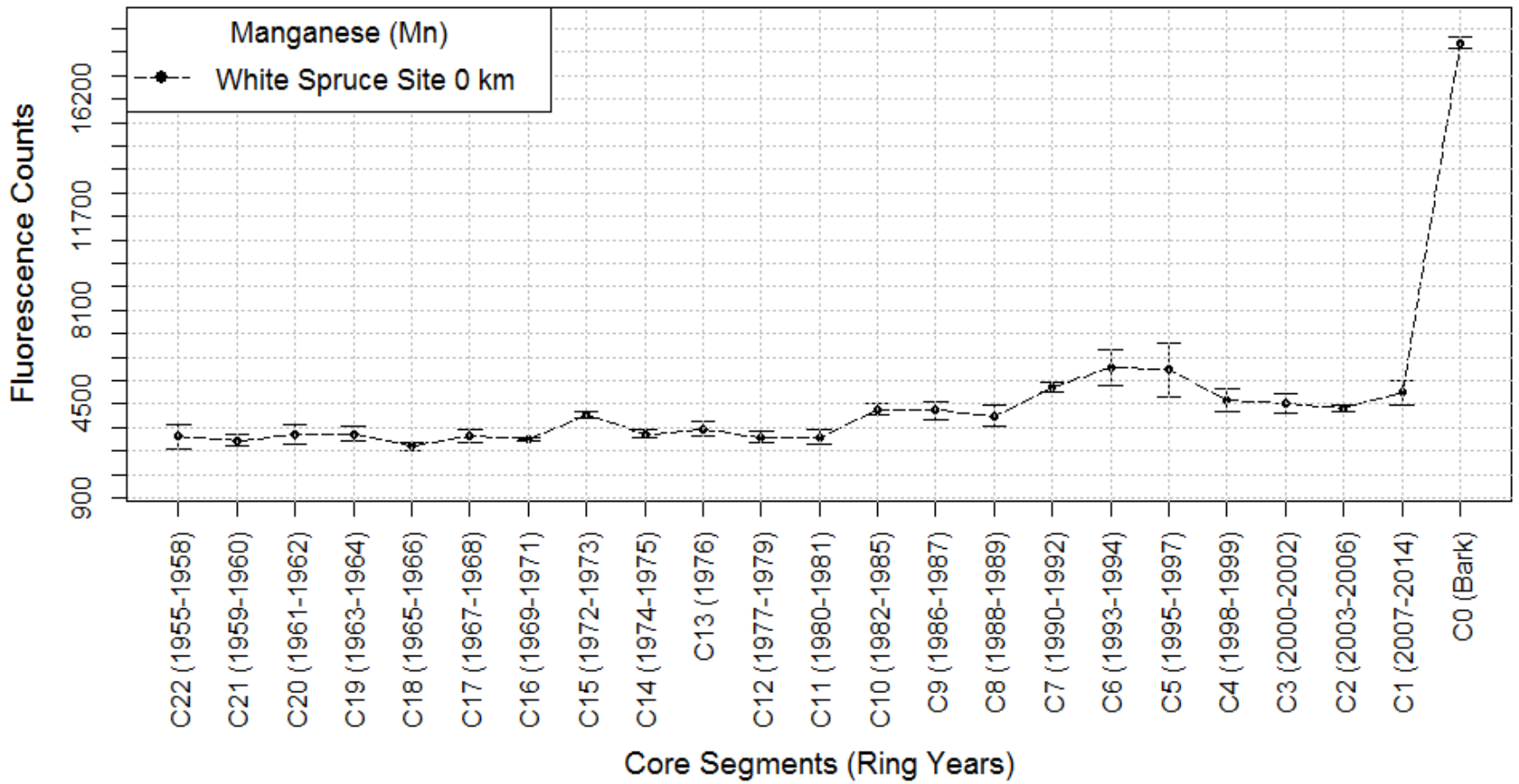

Figure I.3 Average normalized fluorescence counts illustrating K-edge Mn plotted over time for white spruce at Site 0 km.

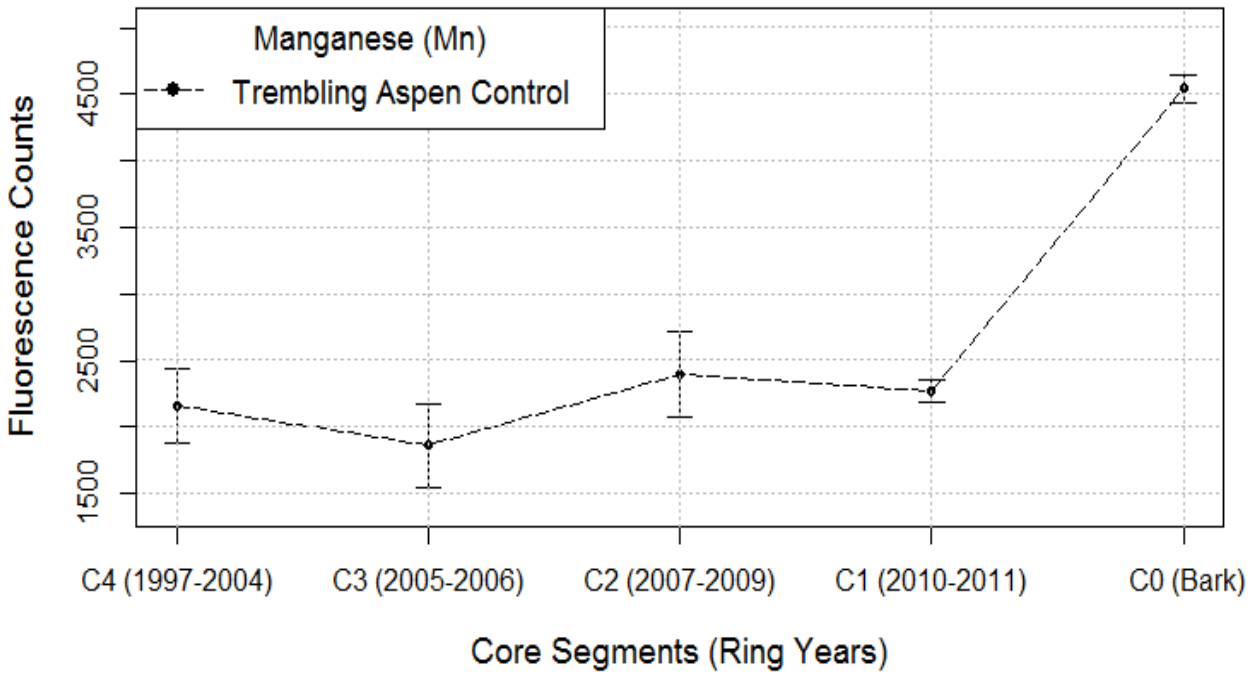

Figure I.4 Average normalized fluorescence counts illustrating K-edge Mn plotted over time for trembling aspen at the Control site.

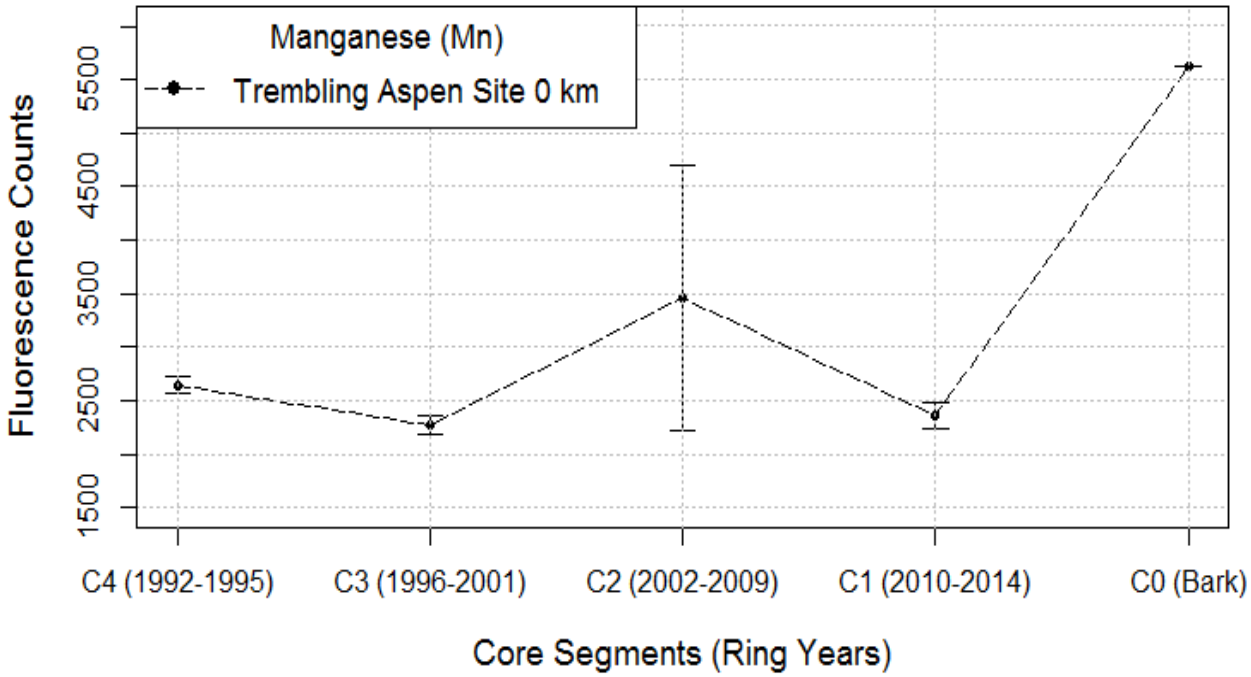

Figure I.5 Average normalized fluorescence counts illustrating K-edge Mn plotted over time for trembling aspen at Site 0 km.